

# ✓ STUDIES IN THE KINETICS OF SOME INDUSTRIALLY IMPORTANT REACTIONS

By

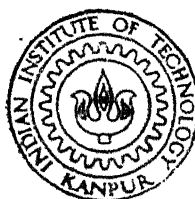
KAPLINGAT NEELAKANTAN

CHE  
1979

TH  
CHE/1979/D  
N292

A65968

D  
NEE  
STU



DEPARTMENT OF CHEMICAL ENGINEERING  
INDIAN INSTITUTE OF TECHNOLOGY, KANPUR  
OCTOBER, 1979

# **STUDIES IN THE KINETICS OF SOME INDUSTRIALLY IMPORTANT REACTIONS**

**A Thesis Submitted  
In Partial Fulfilment of the Requirements  
for the Degree of  
DOCTOR OF PHILOSOPHY**

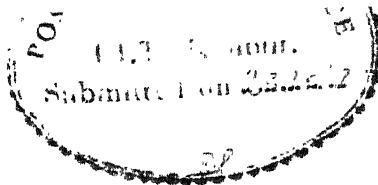
**By  
KAPLINGAT NEELAKANTAN**

**to the  
DEPARTMENT OF CHEMICAL ENGINEERING  
INDIAN INSTITUTE OF TECHNOLOGY, KANPUR  
OCTOBER, 1979**

CHE-1970-D-NES 20

U.S. DEPT. OF JUSTICE  
CENTRAL INTELLIGENCE  
Acc. No. A 65968

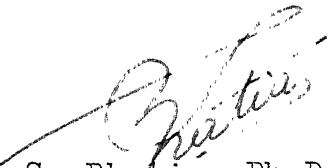
15 MAY 1981



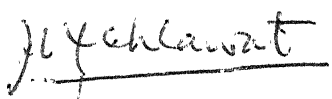
[ii]

CERTIFICATE

This is to certify that the thesis entitled 'STUDIES IN THE KINETICS OF SOME INDUSTRIALLY IMPORTANT REACTIONS' by Kaplingat Neelakantan is a record of work carried out under our supervision and that this has not been submitted elsewhere for a degree.

  
S. Bhatia, Ph.D.  
Assistant Professor  
Department of Chemical Engg.  
Indian Institute of Technology  
Kanpur-208016, India

October 22, 1979

  
J.K. Gehlawat, Ph.D.  
Professor  
Department of Chemical Engg.  
Indian Institute of Technology  
Kanpur-208016, India

October 22, 1979



### ACKNOWLEDGEMENTS

The author feels a deep sense of gratitude and indebtedness to Professor J.K. Gehlawat for his keen interest and valuable guidance and constant encouragement during the period of this investigation. He wishes to thank Dr. S. Bhatia for his valuable suggestions and guidance.

The author is very much grateful to Professor P.C. Nigam of the Department of Chemistry for helpful suggestions in data interpretation for the reaction mechanism.

Thanks are also due to the laboratory, workshop and office staff of the Department. The assistance of Sri R.L. Tripathi deserves special mention. The prompt services rendered by the Glass Blowing Shop are thankfully acknowledged.

Special thanks are due to several of my friends for their valuable help during the course of this work.

The author wishes to express his thanks to Mr. B.S. Pandey for his neat typing, to Mr. D.S. Panesar for making the necessary drawings and to Mr. Hari Ram for very neat work in stencil rolling.

The author is grateful to the Government of Kerala, Quality Improvement Programme and Indian Institute of Technology, Kanpur for an award of a scholarship which enabled this work to be carried out.

Author

CONTENTS

List of Figures	...	vi
List of Tables	...	ix
Nomenclature	...	xiii
Synopsis	...	xv

## CHAPTER

SECTION I: KINETICS OF ABSORPTION OF  
OXYGEN IN AQUEOUS SOLUTIONS  
OF AMMONIUM SULFITE

1	INTRODUCTION AND LITERATURE REVIEW	1
2	THEORY OF ABSORPTION ACCOMPANIED BY CHEMICAL REACTION	...
		4
3	EXPERIMENTAL	...
		10
4	RESULTS AND DISCUSSION	...
		19

SECTION II: KINETICS OF THE REACTION  
BETWEEN BUTADIENE AND  
NAPHTHOQUINONE

5	INTRODUCTION AND LITERATURE REVIEW	45
6	EXPERIMENTAL	...
		49
7	RESULTS AND DISCUSSION	...
		57

SECTION III: DETERMINATION OF EFFECTIVE  
INTERFACIAL AREA AND PHYSICAL  
MASS TRANSFER COEFFICIENT IN  
GAS LIQUID CONTACTORS

8	INTRODUCTION AND LITERATURE REVIEW	83
9	EXPERIMENTAL	...
		87
10	RESULTS AND DISCUSSION	...
		93
11	CONCLUSIONS	...
		107
	REFERENCES	...
		109
	APPENDIX-APPLICATION TO DESIGN	
		114

LIST OF FIGURESFIGURE  
NUMBER

## PAGE

SECTION I: KINETICS OF ABSORPTION OF  
OXYGEN IN AQUEOUS SOLUTIONS OF  
AMMONIUM SULFITE

1	Concentration profiles of reactant [B] and dissolved solute A for a fast reaction conforming to pseudo-nth order mechanism	7
2	Diagram of stirred cell	12
3	Flow diagram for a stirred cell	13
4	The laminar jet apparatus	15
5	Experimental set up for a laminar jet apparatus	17
6	Effect of interfacial area on the specific rate of absorption in stirred cells at 30°C	21
7	Effect of volume of reactant on the specific rate of absorption in a stirred cell at 30°C	22
8	Effect of catalyst concentration on the specific rate of absorption in a stirred cell at 30°C	25
9	Effect of speed of agitation on the specific rate of absorption in a stirred cell at 30°C	26
10	Effect of contact time on the specific rate of absorption in a laminar jet apparatus at 30°C	30
11	Effect of partial pressure of oxygen on the specific rate of absorption in a stirred cell at 30°C	31

FIGURE NUMBER		PAGE
12	Effect of partial pressure of oxygen on the specific rate of absorption at 30°C, analytical method	32
13	Effect of ammonium sulfite concentration on the specific rate of absorption at 30°C	35
14	Plot of $\log [B]$ vs $\log \left( \frac{-R}{[A]} \right)^2$	36
15	Arrhenius plot for the reaction between oxygen and ammonium sulfite	44
SECTION II: KINETICS OF THE REACTION BETWEEN BUTADIENE AND NAPHTHOQUINONE		
16	Calibration curves for Spectronic-20 (Spectrophotometer)	51
17	Calibration curves for Spectronic-20 (Spectrophotometer)	52
18	A schematic diagram of the experimental set up for butadiene naphthoquinone system	55
19	Effect of temperature on the solubility of butadiene in organic solvents	59
20	Effect of temperature on the solubility of naphthoquinone in organic solvents	60
21	Computation of pseudo-first order rate constants at 35°C	64
22	Effect of naphthoquinone on the rate of reaction	67
23	Effect of butadiene concentration on the rate of reaction at 35°C	68
24	Arrhenius plot for the reaction between butadiene and naphthoquinone	74

FIGURE NUMBER		PAGE
25	Effect of dielectric constant (D) on the specific rate constant at 30°C ..	77
26	Plot of reciprocal of dielectric constant vs log of reaction rate constant	78
27	Proposed mechanism for the reaction between 1,3 butadiene and 1,4 naphthoquinone in organic solvents	81
	SECTION III: DETERMINATION OF PHYSICAL MASS TRANSFER COEFFICIENT AND EFFECTIVE INTERFACIAL AREA IN GAS-LIQUID CONTACTORS	
28	Experimental set up for a packed column	88
29	A typical chromatogram for analysis of a butadiene stream <i>liquid</i>	92
30	Effect of superficial/velocity on the effective interfacial area in packed columns <i>gas</i>	96
31	Effect of superficial/velocity on the effective interfacial area in bubble columns	102

---

LIST OF TABLES

TABLE		PAGE
	<u>SECTION I</u>	
1	Major dimensions of stirred cells	10
2	Absorption of oxygen in aqueous solutions of ammonium sulfite in stirred cells.- Effect of interfacial area on the specific rate of absorption ...	20
3	Absorption of oxygen in aqueous solutions of ammonium sulfite in a stirred cell - Effect of volume of reactant on the specific rate of absorption ...	20
4	Absorption of oxygen in aqueous solutions of ammonium sulfite in a stirred cell - Effect of catalyst concentration on the specific rate of absorption	24
5	Absorption of oxygen in aqueous solutions of ammonium sulfite in a stirred cell - Effect of speed of agitation on specific rate of absorption ...	24
6	Absorption of oxygen in aqueous solutions of ammonium sulfite in a laminar jet apparatus - Effect of contact time on specific rate of absorption	28
7	Absorption of oxygen in aqueous solutions of ammonium sulfite in a stirred cell - Effect of partial pressure of oxygen on the specific rate of absorption, volumetric uptake method ...	28
8	Absorption of oxygen in aqueous solutions of ammonium sulfite in a stirred cell - Effect of partial pressure of oxygen, analytical technique ...	29
9	Absorption of oxygen in aqueous solutions of ammonium sulfite in a stirred cell - Effect of concentration of ammonium sulfite on the specific rate of absorption	34

TABLE		PAGE
10	Absorption of oxygen in aqueous solutions of ammonium sulfite in a stirred cell - Calculated values of $(R/[A])^2$ for various values of [B]	34
11	pH of aqueous solutions of ammonium sulfite ...	38
12	Absorption of oxygen in aqueous solutions of ammonium sulfite in a stirred cell - Effect of pH ...	38
13	Solubility of oxygen in aqueous solutions of ammonium sulfite	40
14	Diffusivity of oxygen in aqueous solutions of ammonium sulfite	40
15	Values of true mass transfer coefficient for the absorption of oxygen in aqueous solutions of ammonium sulfite	43
16	Reaction rate constants for the reaction between oxygen and ammonium sulfite	43
<u>SECTION II</u>		
17	Calibration of spectrophotometer (Spectronic-20) for different levels of naphthoquinone content in benzene solution ...	50
18	Physical solubility of butadiene in various organic solvents at 1 atm.	58
19	Physical solubility of 1,4 naphthoquinone in various organic solvents	58
20	Heat of solution of butadiene and naphthoquinone in various organic solvents	63
21	Data for the pseudo-first order rate constant for the reaction between butadiene and naphthoquinone in benzene solution ...	63



TABLE		PAGE
22	Effect of concentration of naphtho-quinone on the rate of reaction	66
23	Effect of butadiene concentration on the rate of reaction ...	66
24	Data for the pseudo-first order rate constant for the reaction between butadiene and naphthoquinone in benzene solution ...	70
25	Data for the pseudo-first order rate constant for the reaction between butadiene and naphthoquinone in benzene solution ...	70
26	Data for the pseudo-first order rate constant for the reaction between butadiene and naphthoquinone in benzene solution ...	71
27	Data for the pseudo-first order rate constant for the reaction between butadiene and naphthoquinone in benzene solution ...	71
28	Reaction rate constants for the reaction between butadiene and naphthoquinone	72
29	A comparison of second order rate constants for different systems in benzene solution ...	73
30	Effect of solvent on the reaction rate constant at 30°C for the reaction between butadiene and naphthoquinone	76
31	Activation parameters in different solvents ...	80
<u>SECTION III</u>		
32	Effective interfacial in packed columns	95
33	Effective interfacial area in bubble columns - batch operation	98

TABLE		PAGE
34	Effective interfacial area in bubble columns - batch operation	99
35	Effective interfacial area in bubble column - countercurrent operation	100
36	Effect of superficial gas velocity on physical mass transfer coefficient in bubble columns for the system Butadiene-Maleic anhydride ...	105
37	Typical values of mass transfer coefficient for aqueous systems from literature ...	106

---

NOMENCLATURE

A	Cross sectional area of bubble column, $\text{cm}^2$ Frequency factor, $1/\text{gmol sec.}$
[A]	Solubility of the solute gas (oxygen) in aqueous solutions of ammonium sulfite, $\text{gmol}/\text{cm}^3$ Concentration of naphthoquinone, $\text{gmol}/\text{l}$
[A <sub>0</sub> ]	Initial concentration of naphthoquinone, $\text{gmol}/\text{l}$
a	Effective gas liquid interfacial area, $\text{cm}^2$
[B]	Concentration of ammonium sulfite, $\text{gmol}/\text{cm}^3$ Concentration of butadiene, $\text{gmol}/\text{l}$
D	Dielectric constant
D <sub>A</sub>	Liquid phase diffusivity of the solute gas (oxygen) in aqueous solutions of ammonium sulfite, $\text{cm}^2/\text{sec.}$
G <sub>i</sub>	Molal flow rate of the inert gas, $\text{gmol}/\text{sec.}$
H	Henry's constant, $\text{gmol}/\text{cm}^3 \text{ atm.}$
I	Ionic strength of electrolyte solution, $\text{g ion}/\text{l}$
i	Contribution due to various species, $1/\text{g ion}$
K	Equilibrium constant in equation (29) and Figure 27
k <sub>m,n</sub>	Reaction rate constant $(\frac{\text{cm}^3}{\text{gmol}})^{m+n-1} \text{ sec}^{-1}$
k <sub>1</sub>	Pseudo-first order rate constant, $\text{sec}^{-1}$
k <sub>2</sub>	Second order reaction rate constant, $\frac{1}{\text{gmol sec}}$
k <sub>3</sub>	Third order reaction rate constant $(\frac{1}{\text{g mol}})^2 \text{ sec}^{-1}$
k <sub>II</sub>	Constant in equation (29)
k <sub>L</sub>	True liquid side mass transfer coefficient, $\text{cm}/\text{sec}$
L	Dispersed height in the bubble column, $\text{cm}$
m	Order of reaction with respect to A Mole ratio of butadiene to inert gas in equation (32)

n	Order of reaction with respect to B
P	Pressure, atm
R	Specific rate of absorption of gas A, $\text{gmol/cm}^2 \text{ sec}$
$r_A$	Rate of reaction between butadiene and naphthoquinone, $\text{gmol/l sec}$
T	Temperature of solution, $^{\circ}\text{K}$
t	Time, min
Z	Stoichiometric coefficient for the reaction between A and B
z	Height from the top of the bubble column in equation (32), cm.

#### Greek Letters

$\delta$	Film thickness, cm
$\mu$	Viscosity of solution, cp
$\rho$	Density, $\text{gm/cm}^3$

#### Subscripts

i	Inlet
o	Outlet
disp	Dispersion

## SYNOPSIS

'STUDIES IN THE KINETICS OF SOME INDUSTRIALLY IMPORTANT REACTIONS' A thesis submitted in partial fulfilment of the requirements for the degree of Doctor of Philosophy by Kaplingat Neelakantan to the Department of Chemical Engineering, Indian Institute of Technology, Kanpur in October 1979.

Aqueous solutions of ammonia are used to absorb the lean mixtures of waste sulfur dioxide to control atmospheric pollution in several fertilizer plants producing sulfur dioxide and ammonia. Ammonium sulfite is thus obtained as a by-product. It may be easily oxidized to ammonium sulfate which is used as a fertilizer. Thus, oxidation of ammonium sulfite is industrially important.

Tetrahydroanthraquinone is the starting material for the manufacture of anthraquinone which is an important intermediate for the manufacture of dyes. It is obtained by the reaction between butadiene and naphthoquinone. Both butadiene and naphthoquinone are obtainable as by-products from petrochemical complexes. They may be economically reacted to produce tetrahydroanthraquinone which on oxidation produces anthraquinone. Recently Gharda<sup>1</sup> proposed that this process for the manufacture of anthraquinone may prove to be economical under Indian conditions.

Very limited information is available in the literature on the kinetics of the above industrially important reactions. This work was therefore undertaken to make a systematic study of the kinetics of these reactions. Further the physical mass transfer coefficients and effective interfacial area are of practical importance for the design of gas-liquid contactors. Chemically reactive systems of known kinetics can be advantageously used for the determination of these important design parameters.

The main study has been divided into three sections. Section I deals with the kinetics of the absorption of oxygen in aqueous solutions of ammonium sulfite. Section II deals with the homogeneous kinetics of the reaction between dissolved butadiene and naphthoquinone. The data on physical mass transfer coefficients and the effective interfacial area in gas-liquid contactors alongwith an illustrative design problem have been discussed in Section III and Appendix respectively.

The kinetics of the absorption of oxygen in aqueous solutions of ammonium sulfite was studied in stirred cells and in a laminar jet apparatus where the interface geometry is well defined. Cobaltous sulfate was used as a soluble catalyst. The absorption of oxygen in ammonium sulfite solutions conformed to fast pseudo-nth order mechanism. In the range of reactant concentrations of 0.045 to 0.45 gmol/l,

the reaction was found to be first order with respect to oxygen and second order with respect to ammonium sulfite. The overall third order reaction rate constant<sup>2</sup> at 30°C was found to be  $2.70 \times 10^4 \text{ (l/gmol)}^2 \text{sec}^{-1}$  with an activation energy of 14.5 kcal/gmol.

The kinetics of the reaction between dissolved butadiene and naphthoquinone in different solvents was studied in a batch reactor. The physical solubility of butadiene in organic solvents is reasonably large (2.82 - 4.45 gmol/l at 30°C) to enable the kinetics of the reaction between dissolved butadiene and naphthoquinone to be determined in the homogeneous phase. The solubility of butadiene and naphthoquinone in various organic solvents was determined experimentally. The dielectric constant of solvents was found to affect the rate of reaction. The reaction was found to be first order with respect to both butadiene and naphthoquinone. The overall second order reaction rate constant<sup>3</sup> at 30°C was found to be  $4.21 \times 10^{-6} \text{ l/gmol sec}$  and the energy of activation was found to be 22.2 kcal/g mol. A reaction mechanism has been proposed.

The data on the kinetics of the fast reaction between oxygen and ammonium sulfite were utilized for the determination of effective interfacial area in a 5 cm i.d. packed column and 2.2 cm and 5 cm i.d. bubble columns. The results

are in good agreement with the published data. The kinetics of the relatively slow reaction between dissolved butadiene and molten maleic anhydride<sup>4</sup> were utilized to determine the physical mass transfer coefficient,  $k_{La}$ , in bubble columns of different dimensions. The results obtained in this study for the molten system are comparable with the reported data for aqueous systems.<sup>5</sup>

Bubble columns may be used as industrial reactors for the gas-liquid reactions with some advantages. Mashelkar<sup>6</sup> discussed the relevant features of the bubble column reactors. A bubble column reactor may be a better choice for the recovery of butadiene from the lean mixtures of C<sub>4</sub>-fraction by its selective reaction with maleic anhydride. A worked out design problem for the absorption of butadiene in molten maleic anhydride illustrates the design procedure for bubble column reactors.<sup>5</sup>

The data obtained in this study are likely to be useful in providing a rational basis for the design of industrial reactors.



SECTION I

KINETICS OF ABSORPTION OF OXYGEN IN AQUEOUS  
SOLUTIONS OF AMMONIUM SULFITE

CHAPTER 1

INTRODUCTION AND LITERATURE REVIEW

Aqueous solutions of ammonia are used to absorb sulfur dioxide to minimize atmospheric pollution in several fertilizer plants producing sulfur dioxide and ammonia. Ammonium sulfite is obtained as a by-product. This can be easily oxidized to ammonium sulfate<sup>7-11</sup> which is used as a fertilizer. Hence the absorption of oxygen into aqueous solutions of ammonium sulfite is an industrially important operation.

#### Literature Review:

In the chemical engineering literature the problem of oxidation of sodium sulfite has been studied extensively. Yagi and Inoue<sup>12</sup> studied the kinetics of the absorption of oxygen in sodium sulfite solution using bubblers. They found the reaction to be first order both with respect to oxygen and sulfite. Barron and O'Hern<sup>13</sup> conducted investigative measurements of homogeneous reaction of sodium sulfite and oxygen by the Hatridge and Roughton method of rapid mixing. The reaction was found to be of zero order with respect to oxygen and  $3/2$  order with respect to sulfite. De Waal and Okeson<sup>14</sup> studied the oxidation of concentrated aqueous solutions of sodium sulfite with gaseous oxygen in the presence of cobaltous sulfate as catalyst. They did not verify it experimentally but assumed that the reaction was first order in oxygen. The rate of reaction was found

to be dependent on pH. At constant pH the reaction was independent of sulfite concentration. Wesselnigh<sup>15</sup> observed from his experiments that the rate of absorption of oxygen was found to decrease with increase in the concentration of sulfite. Linek<sup>16</sup> attributed this decrease due to some inhibitting impurities present in the sulfite used and concluded that the reaction does not depend on sulfite concentration at all. Linek and Mayroferova<sup>17</sup> calculated the kinetic data for the reaction of oxygen with sodium sulfite from the absorption rate of oxygen in mechanically agitated sulfite solutions. They reported that the reaction order in oxygen was found to depend on the oxygen concentration in the liquid phase at the interface. The reaction was first order in oxygen for oxygen concentration higher than approximately  $6 \times 10^{-4}$  M at the interface and second order for lower oxygen concentration. Yasunishi<sup>18</sup> investigated the homogeneous liquid phase oxidation of sodium sulfite catalysed by cupric ions by the rapid mixing flow method at 25°C. The reaction was found to be 1/2 order with respect to oxygen, first order with respect to sulfite and 1/4 order with respect to cupric ions. It is apparent that although extensive studies have been made, the picture regarding the true kinetics of oxidation of sodium sulfite is still not very clear.

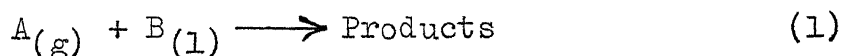
The oxidation of ammonium sulfite on the other hand, has received very little attention. Some preliminary studies on oxidation of ammonium sulfite have been reported by Young<sup>19</sup>, Vorlander and Lainau<sup>20</sup> and Hori<sup>8,9</sup>. Girigoryan<sup>21</sup> investigated the oxidation of ammonium sulfite by atmospheric oxygen in the presence of nitrogen oxides. Matsuura, Harida, Akihata and Shirai<sup>22</sup> studied this reaction in a batch reactor without catalysts. Recently Mishra and Srivastava<sup>23, 24</sup> conducted a study for the liquid phase oxidation of ammonium sulfite. A mechanism of the reaction was proposed.

It may be noted that information on the kinetics of the industrially important heterogeneous reaction between oxygen and ammonium sulfite under conditions of practical importance is not available in the literature. It may be erroneous to infer anything about the kinetics of oxidation of ammonium sulfite based on the controversial information available on sodium sulfite-oxygen system. An independent study is needed. The present work was therefore undertaken to make a systematic study of the kinetics of reaction between dissolved oxygen and ammonium sulfite. According to the theory of absorption with chemical reaction this system is likely to conform to fast reaction regime.

CHAPTER 2

THEORY OF ABSORPTION ACCOMPANIED BY CHEMICAL REACTION

The theory of absorption accompanied by chemical reaction has been discussed by several authors<sup>25-27</sup>. However, a brief description of the relevant theory pertaining to this work is presented here. Consider the reaction



The reaction is irreversible. It is mth order with respect to A and nth order with respect to B. It is assumed that reactant B and the reaction products are nonvolatile. In this heterogeneous gas liquid reaction, the transfer of the solute A and its subsequent reaction with the reactant B in the liquid phase may conform to one of the following regimes:

1. Very slow reaction
2. Slow reaction
3. Fast reaction
4. Instantaneous reaction

#### Very Slow Reaction:

In this case, the reaction between dissolved A and B is very much lower than the rate of transfer of A from the gas phase to the liquid phase. Consequently the liquid phase (B) in which the reaction occurs will be saturated with the solute A at any moment and the overall process will be controlled by the homogeneous reaction between A and

B. The diffusional factors are unimportant and the transfer rate of A,  $R'$  (gmol/sec cm<sup>3</sup>) will be given as:

$$R' = k_{m,n} [A]^m [B]^n \quad (2)$$

where  $k_{m,n}$  = rate constant for the reaction between A and B ( $\frac{\text{cm}^3}{\text{gmol}}$ ) sec<sup>-1</sup>

$[A]$  = solubility of solute gas A in the liquid, gmol/cm<sup>3</sup>

$[B]$  = concentration of reactant B, gmol/cm<sup>3</sup>

The necessary condition to be satisfied for the occurrence of the above mechanism is

$$k_L a [A] > 1 k_{m,n} [A]^m [B]^n \quad (3)$$

where  $k_L$  = true liquid side mass transfer coefficient, cm/sec

$a$  = gas liquid interfacial area, cm<sup>2</sup>/cm<sup>3</sup> of effective contactor volume

$1$  = fractional gas hold up

### Slow Reaction:

Under certain conditions when the reaction is not very slow, it occurs in the bulk of the liquid but the overall reaction rate is controlled by the rate of physical transport of the dissolved gas from the gas liquid interface to the bulk of the liquid. The concentration of the



dissolved gas in the bulk of the liquid is zero since it is completely consumed by the reaction. The overall rate of absorption is then given by the following expression

$$R_a = k_L a [A] \quad (4)$$

The physical condition to be satisfied for the above equation to be applicable is given by the following expression

$$1/k_{m,n} [A]^m [B]^n > k_L a [A] \quad (5)$$

It may be noted from the rate expression (4) that the rate of reaction is independent of the concentration of the reactant B. It is virtually a case of physical absorption.

#### Fast Reaction:

For a fast reaction, the reaction between dissolved solute gas A and the reactant B occurs entirely in the film. Under certain conditions, the concentration of the reactant B in the neighbourhood of the gas liquid interface is very little different from that in the bulk of the liquid. Further, if the numerical value of concentration of B is much larger than the concentration of dissolved gas A, the concentration of the reactant does not drop appreciably in the film. Under these conditions the solute gas A undergoes a pseudo-nth order reaction mechanism. Figure 1 shows the concentration profiles for a pseudo-nth order reaction.

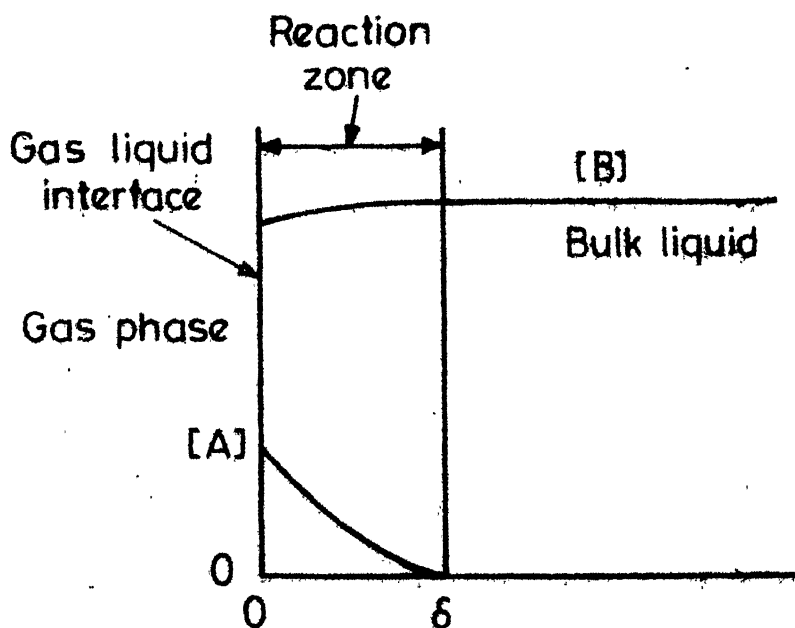


Fig.1 -Concentration profiles of reactant  $[B]$  and dissolved solute  $[A]$  for a fast reaction conforming to pseudo-nth order mechanism. The film thickness is  $\delta$ .

Brian<sup>25</sup> has discussed the appropriate theory. The following equation for the specific rate of absorption was derived on the basis of the penetration theory.

$$R = [A] \sqrt{\frac{2}{m+1} D_A k_{m,n} [B]^n [A]^{m-1}} \quad (6)$$

$D_A$  = diffusivity of solute gas (species A) in liquid,  $\text{cm}^2/\text{sec}$ .

The necessary physical conditions to be satisfied for the occurrence of the above mechanism are:

$$\text{and } \frac{\sqrt{\frac{2}{m+1} D_A k_{m,n} [A]^{m-1} [B]^n}}{k_L} = \frac{-k}{[A] k_L} > 3 \quad (7)$$

$$\frac{\sqrt{\frac{2}{m+1} D_A k_{m,n} [A]^{m-1} [B]^n}}{k_L} = \frac{-R}{[A] k_L} \ll \frac{[B]}{Z[A]} \quad (8)$$

where Z is the number of moles of the reactant B reacting with one mole of A.

#### Instantaneous Reaction:

In this case the reaction is potentially so fast that the reaction plane is starved of both of the reactants. The reaction between the dissolved solute and the reactant could be treated as instantaneous and the controlling step would be the diffusion of the reactants to a reaction zone close to the interface where the concentration of both is zero.

The condition for occurrence for this mechanism is given by

$$\sqrt{\frac{(2/m+1) D_A k_{m,n} [A]^{m-1} [B]^n}{k_L}} \gg \frac{[B]}{z[A]} \quad (9)$$

when the value of  $\frac{[B]}{z[A]} > 3$ , the rate of transfer,  $R$ , is approximately given by

$$R = k_L [A] \sqrt{\frac{D_A}{D_B}} \left(1 + \frac{D_B}{D_A} \frac{[B]}{[A]}\right) \quad (10)$$

Further, if  $[B]$  is considerably greater than  $[A]$  the equation (10), reduces to

$$R = k_L [B] \sqrt{\frac{D_B}{D_A}} \quad (11)$$

when  $D_A$  and  $D_B$  are of the same order of magnitude, then,

$$R = k_L [B] \quad (12)$$

The rate of mass transfer is then governed by the rate of diffusion of reactant B to the surface and is independent of the concentration of solute A, that is, it is independent of the partial pressure of solute A.

CHAPTER 3

EXPERIMENTAL

The design of stirred cells and laminar jet apparatus provides a well-defined interfacial geometry. They have been used for discerning the kinetics of relatively fast gas-liquid reactions. According to Danckwerts<sup>26</sup> model laboratory experiments may be carried out in apparatus of such design to obtain meaningful results useful for the design and simulation of the performance of industrial gas-liquid contactors. In the present case stirred cells and laminar jet apparatus have been used for studying the kinetics of absorption of oxygen in aqueous solutions of ammonium sulfite.

#### Stirred Cells:

Absorption experiments were carried out in stirred cells of different dimensions. The design features of the stirred cells were similar to that employed by Sharma and Danckwerts<sup>28</sup>, Gehlawat and Sharma<sup>29,30</sup> and Jhaveri and Sharma.<sup>31</sup> Table 1 gives the major dimensions of the stirred cells used in this study.

TABLE 1  
MAJOR DIMENSIONS OF STIRRED CELLS

No.	I.D. of stirred cell, cm.	Effective inter-facial area, cm <sup>2</sup>	Material of construction
1	5.5	22	glass
2	10.0	79	glass
3	15.0	177	perspex

Figure 2 shows the main features of the apparatus. Most of the experiments were carried out in stirred cell No.2 where the top part was provided with one B-24 and two B-14 joints. The stirrer shaft passed through a mercury seal through the central B-24 joint. The glass stirrer had flat vertical blades intersecting the plane of the surface. The gas phase in the stirred cell was also agitated by another stirrer kept at about 0.5 cm above the gas liquid interface. The speed of agitation could be kept constant in the range of 20-120 revolutions per minute. The apparatus was suitably fixed in a constant temperature bath where the temperature could be maintained constant within  $\pm 0.2^{\circ}\text{C}$  in the range of  $30-80^{\circ}\text{C}$ .

A known amount of solution was introduced in the stirred cell which was maintained at a constant temperature. The absorption of oxygen was measured by the volumetric uptake method employed by Gehlawat and Sharma<sup>29,30</sup> and the analytical method described by Jhaveri and Sharma.<sup>31</sup>

In the volumetric uptake method, pure oxygen was taken in a balloon which was connected to the stirred cell. The volumetric uptake of oxygen was measured by a soap film meter. The schematic diagram of the experimental set up for the above method is shown in Figure 3.

In a few experiments (carried out in stirred cell No.2) the partial pressure of oxygen was varied from 12.5 per

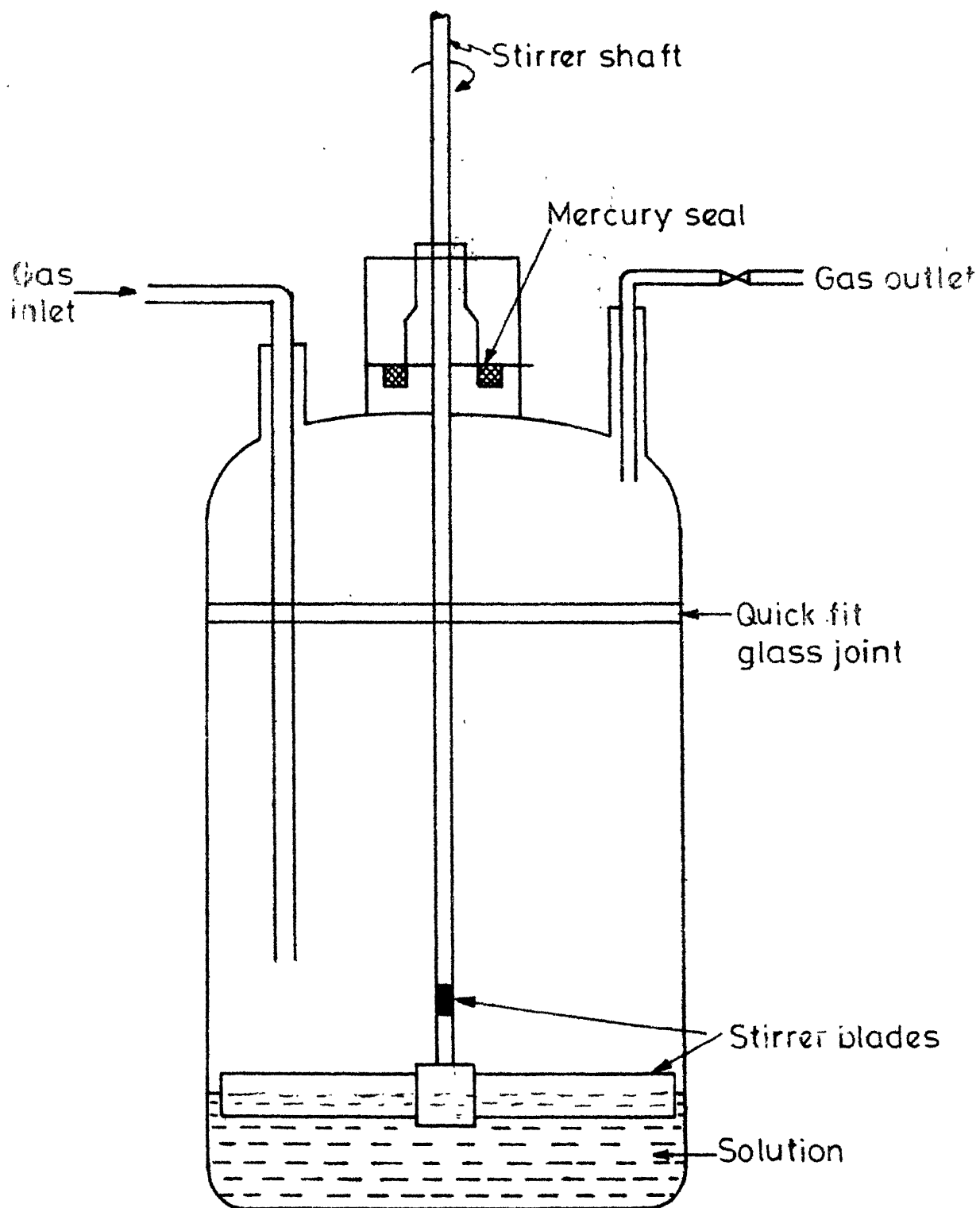
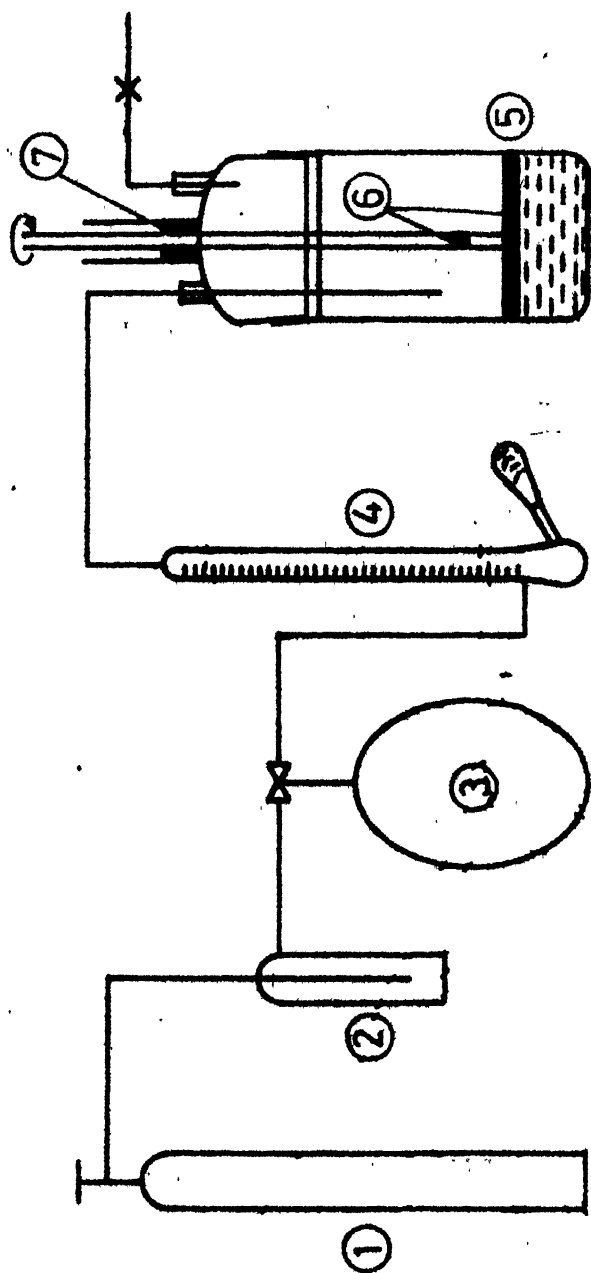


Fig. 2 - Diagram of stirred cell.





- |                 |                    |                   |                 |
|-----------------|--------------------|-------------------|-----------------|
| 1. Gas cylinder | 3. Balloon         | 5. Stirred cell   | 7. Mercury seal |
| 2. Bubbler      | 4. Soap film meter | 6. Stirrer blades |                 |

Fig.3 - Flow diagram for a stirred cell.

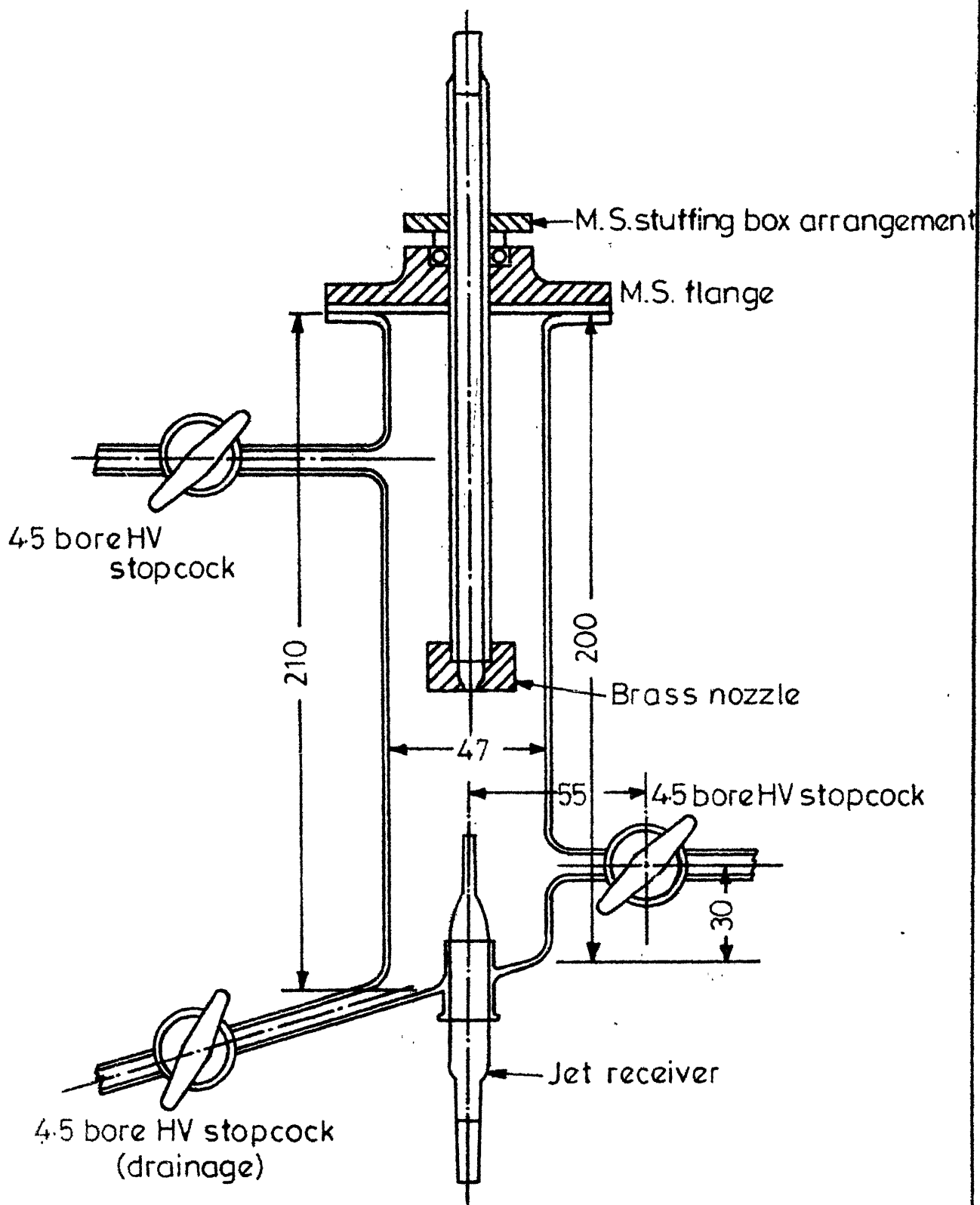
cent to 99 per cent using nitrogen as the diluent. The mixture of oxygen and nitrogen in the desired proportion was passed through the apparatus for sufficient time so that the partial pressure of oxygen was the same as that in the incoming stream. A known amount of solution of prefixed concentration was then introduced in the cell, the gas flow was stopped and the unit was connected to a balloon containing pure oxygen at essentially atmospheric pressure. After a couple of minutes the volumetric uptake of oxygen was noted.

In the analytical technique oxygen or a mixture of oxygen and nitrogen was passed through the apparatus containing a known amount of solution of prefixed concentration for a known period of time. The progress of reaction was determined by analysing the solution for the sulfite content before and at the end of the run.

The ammonium sulfite was analysed according to the method suggested by Vogel.<sup>32</sup> A known amount of ammonium sulfite solution was titrated against standard iodine-iodide solution using starch as indicator.

#### Laminar Jet Apparatus:

The principal design features of the apparatus were akin to those employed by Sharma and Danckwerts<sup>28</sup> and Gehalwat and Sharma.<sup>29,30</sup> The pertinent details have been shown in Figure 4. The apparatus consists of a glass



Dimensions in mm

Fig. 4 -The laminar jet apparatus.

chamber of 47 mm I.D. flattened and ground at the top. The nozzle was mounted on the end of a slide tube which passed through an O ring seal in the mild steel cover plate used to seal the top of the glass chamber. The cover plate was polished to a fine finish so that a gas tight seal allowing sliding motion was possible with the aid of stopcock grease. The jet length was adjusted by raising or lowering the slide tube. The jet chamber was provided with a gas inlet, a gas outlet and a drain. The jet nozzle, made of good quality brass was carefully turned to a shape shown in the Figure 4 and the profile of the covering section was made as smooth as possible. The throat and face surfaces were polished to a smooth finish. A jet of liquid flowed downward from the nozzle through an atmosphere of oxygen into a glass receiver of diameter slightly more than that of the jet. The receiver was connected to an overflow vessel for the adjustment of liquid level in the receiver.

Figure 5 gives the flow diagram of the experimental set-up for the laminar jet apparatus. Aqueous solutions of ammonium sulfite of known concentration were stored in overhead aspirator bottles. The liquid from the overhead bottles was supplied to the laminar jet apparatus through a needle control valve. The dimensions of the liquid jet

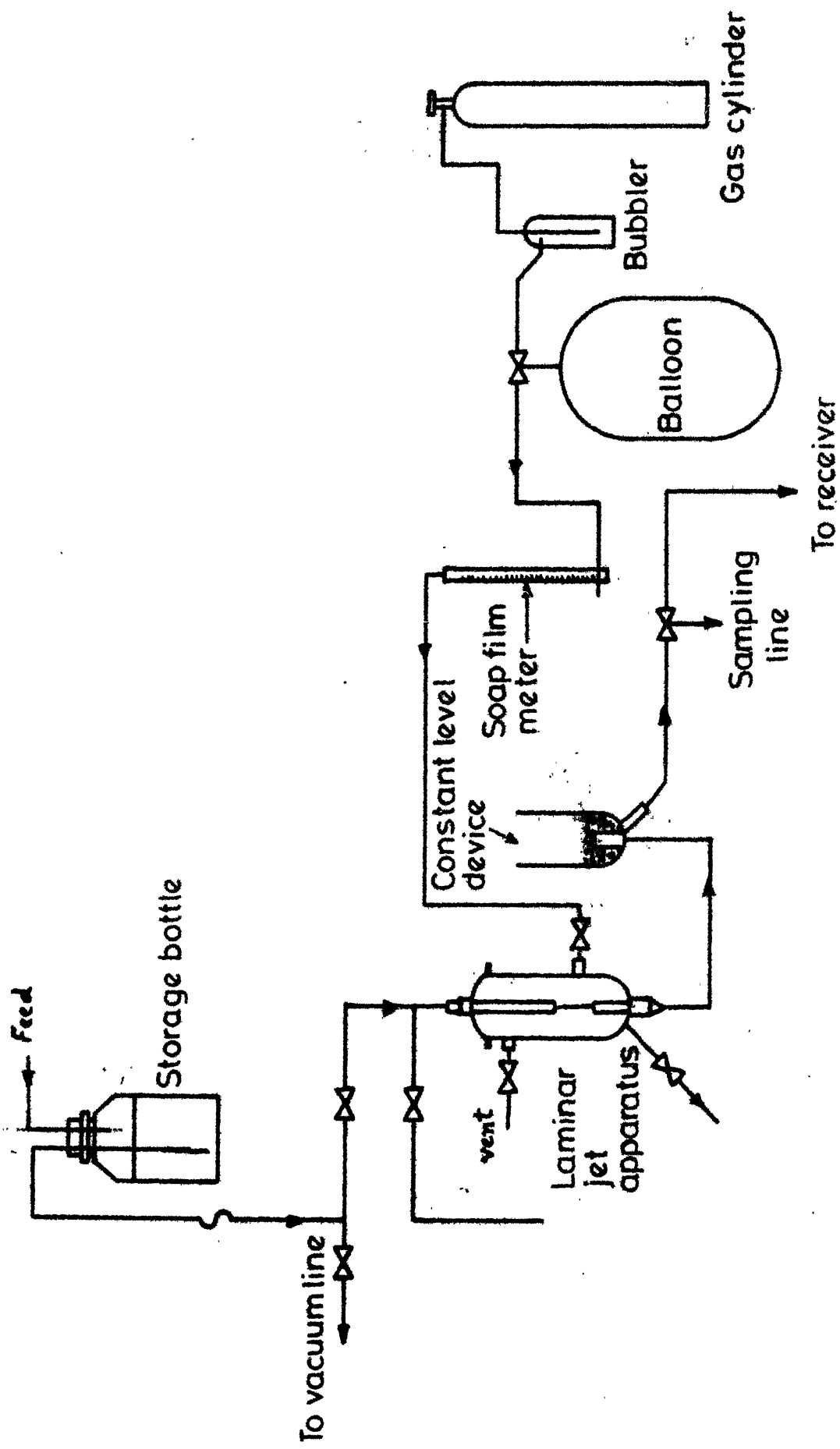


Fig. 5 - Experimental set-up for laminar jet apparatus.

thus formed were determined by using a travelling microscope. Oxygen was collected and stored in a balloon which was essentially at atmospheric pressure. The rate of absorption was measured using a soap film meter. A change in the flow rate of liquid and the jet dimensions enabled the contact time of gas and liquid to be varied from 0.016 to 0.09 sec. Results obtained using the above apparatus are discussed in the next chapter.

## CHAPTER 4

### RESULTS AND DISCUSSION

### Absorption in Different Stirred Cells:

The data obtained on the absorption of oxygen in aqueous solutions of ammonium sulfite in different stirred cells using cobalt sulfate as the catalyst are reported in Table 2, and are also shown graphically in Figure 6. It is noted that the specific rate of absorption,  $R$  ( $\text{gmol}/\text{cm}^2\text{sec}$ ) is the same for an eight fold variation in the interfacial area. Further the specific rate of absorption of oxygen in ammonium sulfite solutions was noted at different volume of the reactant taken in the same stirred cell. The results are given in Table 3 and also shown in Figure 7. It is observed that for about three fold variation in the volume of the reactant the specific rate of absorption was independent of the volume of the reactant. This means that the reaction is fast and takes place at interface.

### Effect of Catalyst Concentration:

The absorption of oxygen in aqueous solutions of ammonium sulfite was carried out using different concentration of cobaltous sulfate as catalyst. The results are reported in Table 4. Figure 8 shows the effect of catalyst concentration on the specific rate of absorption. It is observed that the specific rate of absorption increased with an increase of catalyst concentration upto about  $4.70 \times 10^{-3}$   $\text{gmol}/\text{l}$ , thereafter it tended to level off



TABLE 2ABSORPTION OF OXYGEN IN AQUEOUS SOLUTIONS OF  
AMMONIUM SULFITE IN STIRRED CELLS

Speed of agitation = 54 R.P.M.

Catalyst concentration =  $2.0 \times 10^{-3}$  gmol/l

Temperature = 30°C

Concentration of ammonium sulfite [B], gmol/l	Specific Rate of Absorption, $R \times 10^7$ , gmol/cm <sup>2</sup> sec		
	Stirred cell No.1 Effective interfacial area = 22 cm <sup>2</sup>	Stirred cell No.2 Effective interfacial area, a = 79 cm <sup>2</sup>	Stirred cell No. 3 Effective interfacial area, a = 177 cm <sup>2</sup>
0.080	0.562	0.620	0.568
0.180	1.519	1.530	1.470
0.400	1.925	1.960	1.980

TABLE 3ABSORPTION OF OXYGEN IN AQUEOUS SOLUTIONS  
OF AMMONIUM SULFITE IN STIRRED CELLS

Speed of agitation = 54 R.P.M.

Catalyst concentration =  $2 \times 10^{-3}$  gmol/l

Concentration of ammonium sulfite = 0.16 gmol/l

Temperature = 30°C

Volume of Reactant, ml	Absorption rate, $R \times 10^7$ , gmol/cm <sup>2</sup> sec
130	1.39
210	1.43
300	1.46

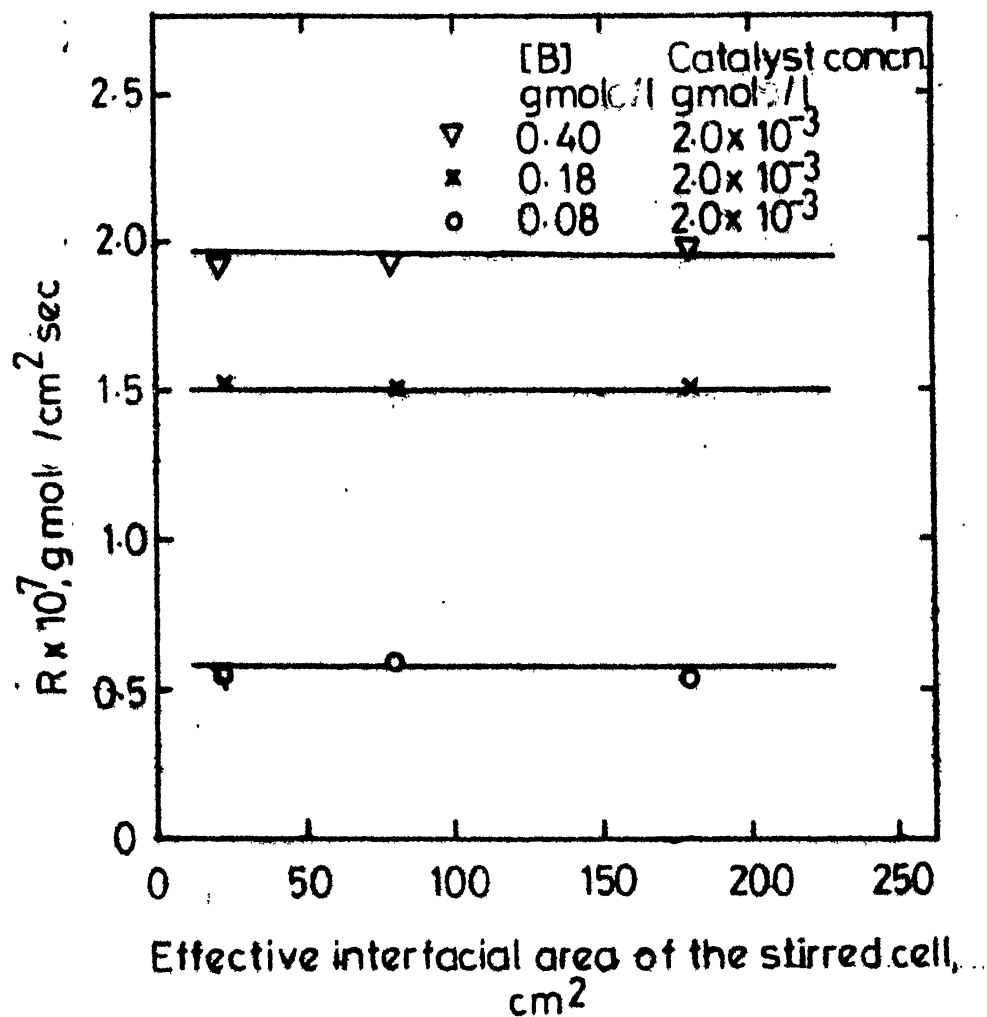


Fig.6 - Effect of interfacial area on the specific rate of absorption in stirred cells at 30°C.

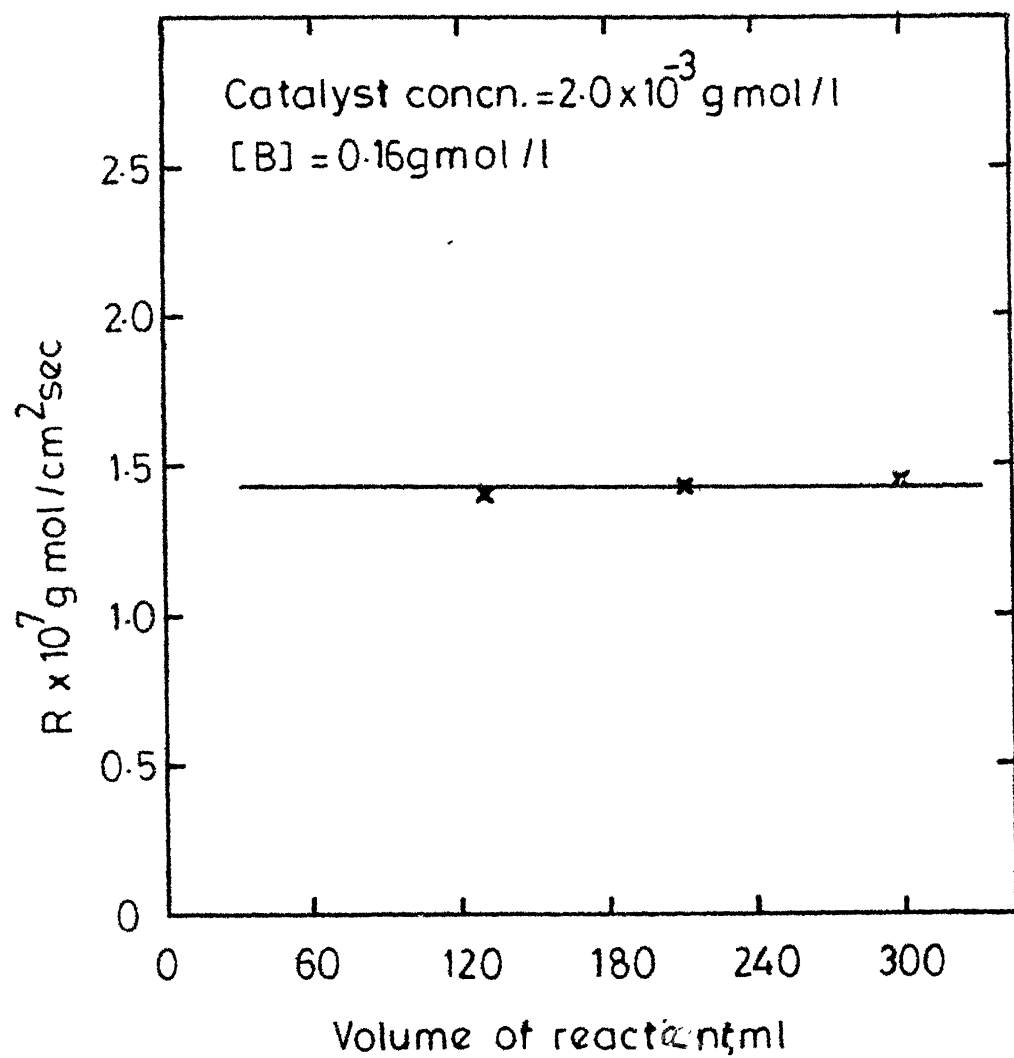


Fig. 7 -Effect of volume of reactant on the rate of absorption in stirred cells at 30°C.

with the catalyst concentration. Thus the order of reaction with respect to catalyst becomes zero at concentrations above  $4.70 \times 10^{-3}$  gmol/l. Hence additional experiments were carried out at this optimum catalyst concentration.

#### Effect of Speed of Agitation:

The absorption of oxygen in aqueous solutions of ammonium sulfite was carried out at different speeds of agitation and the results are shown in Table 5. Figure 9 shows a plot of speed of agitation versus the specific rate of absorption. It may be noted that the rate does not vary with the speed of agitation. Hence the hydrodynamic factors are unimportant in the speed range used in this study.

#### Absorption in the Jet Apparatus:

A few runs for the absorption of oxygen in ammonium sulfite solutions were carried out in a laminar jet apparatus. The results are given in Table 6. The data are also shown graphically in Figure 10. It is noted that specific rate of absorption remained practically constant when the time of contact was varied from 0.016 to 0.090 sec.

This confirms that the hydrodynamic factors are unimportant under the conditions of this study.

TABLE 4

ABSORPTION OF OXYGEN IN AQUEOUS SOLUTIONS OF  
AMMONIUM SULFITE - EFFECT OF CATALYST CONCENTRATION

Concentration of ammonium sulfite solution = 0.430 gmol/l

Speed of agitation = 54 R.P.M.

Temperature = 30°C

Run No.	Concentration of cobaltous sulfate catalyst, gmol/l $\times 10^3$	Specific rate of absorption, R, (gmol/cm <sup>2</sup> sec) $\times 10^7$
1	1.079	0.979
2	2.080	2.150
3	3.078	2.600
4	4.128	3.110
5	5.125	3.400

TABLE 5

ABSORPTION OF OXYGEN IN AQUEOUS SOLUTIONS OF AMMONIUM  
SULFITE IN STIRRED CELLS: EFFECT OF SPEED OF AGITATION

Concentration of ammonium sulfite = 0.43 gmol/l

Catalyst concentration =  $4.70 \times 10^{-3}$  gmol/l

Temperature = 30°C

Run No.	Speed of agitation rev/min	Specific rate of absorption, R, (gmol/cm <sup>2</sup> sec) $\times 10^7$
1	30	3.10
2	44	3.10
3	54	3.20
4	67	3.20
5	88	3.28

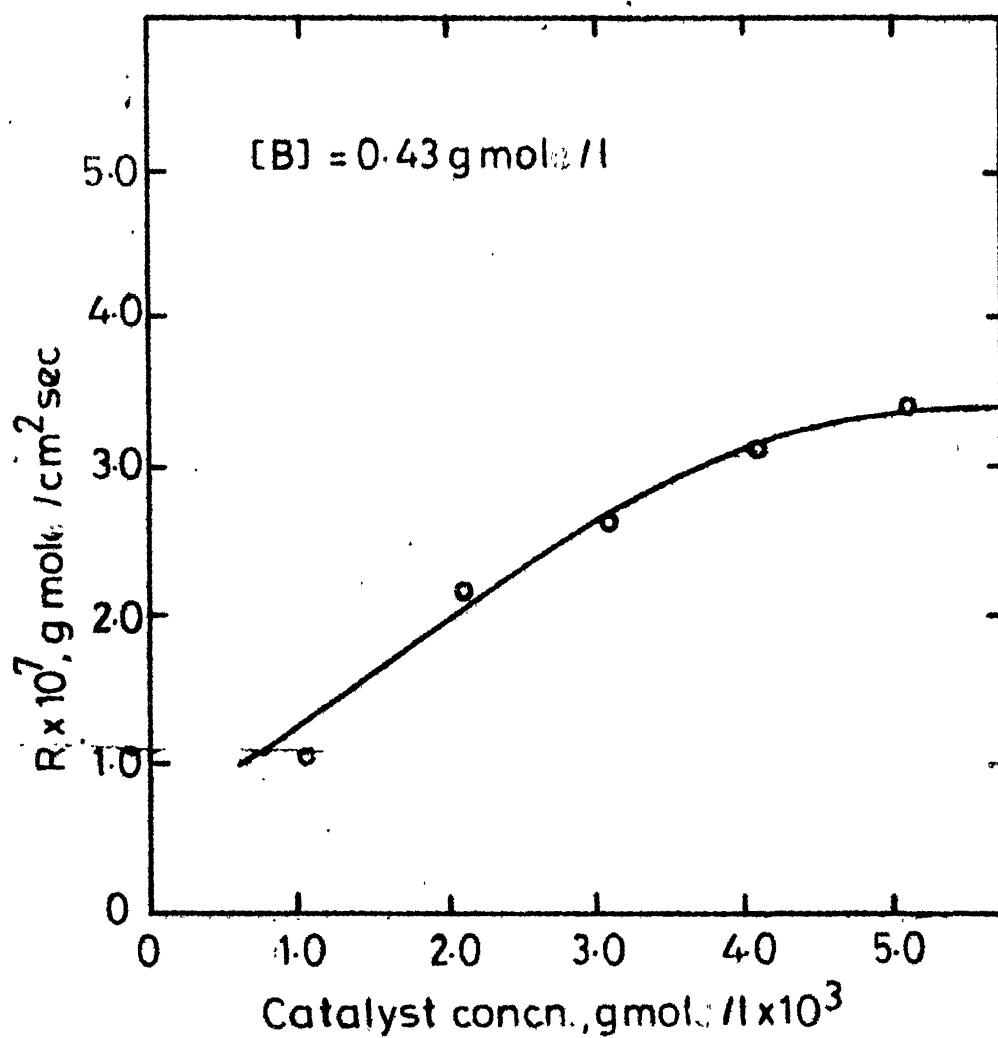


Fig.8 - Effect of catalyst concentration on the specific rate of absorption in a stirred cell at  $30^\circ\text{C}$ .

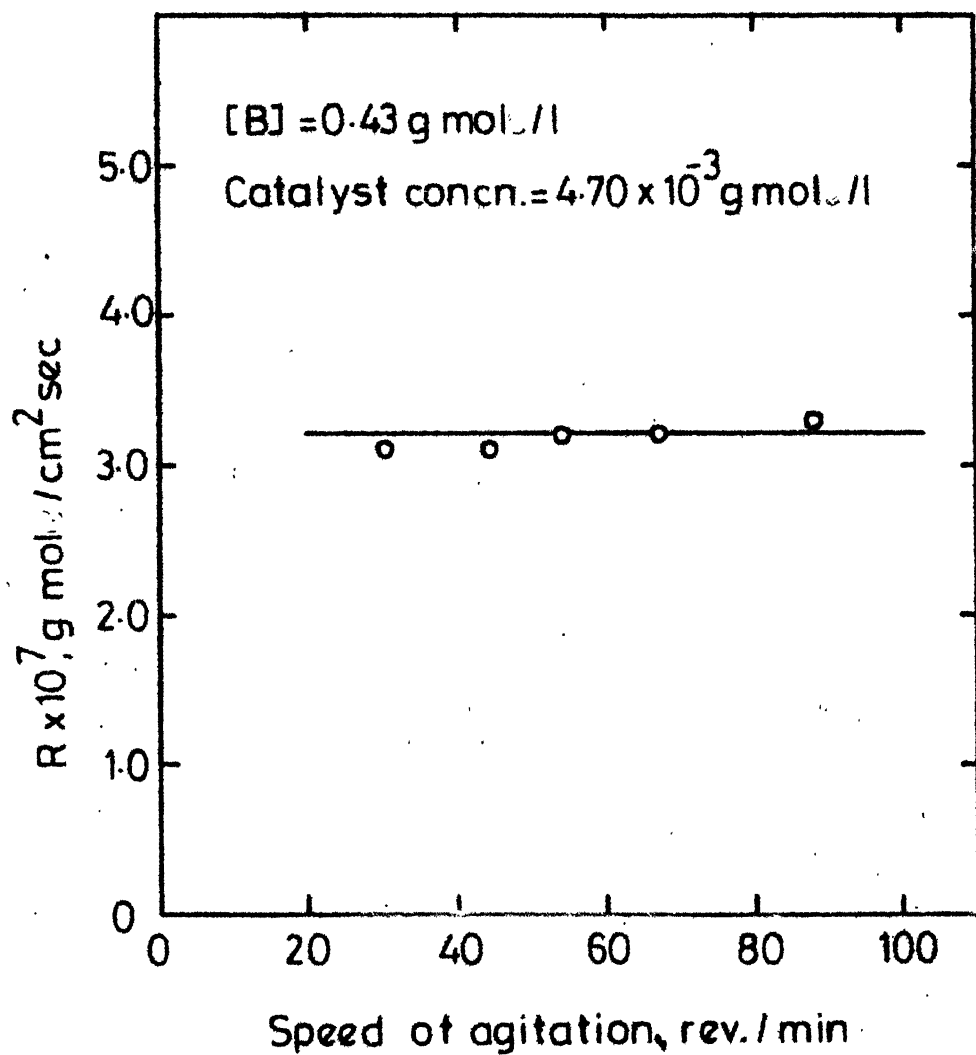


Fig. 9 - Effect of speed of agitation on the specific rate of absorption in a stirred cell at 30°C.

### Effect of Partial Pressure of Oxygen:

The effect of partial pressure of oxygen on the absorption of oxygen in aqueous solutions of ammonium sulfite was studied by the volumetric uptake method as well as the analytical method. The results are given in Tables 7 and 8 respectively. Figure 11 shows a plot of partial pressure of oxygen versus specific rate of absorption for the volumetric uptake method. Figure 12 shows a plot partial pressure of oxygen versus  $R/[B]_{\text{average}}$ . The specific rate of absorption is found to vary linearly with partial pressure of oxygen, which shows that the reaction is first order with respect to oxygen. This is in agreement with the observation of Mishra and Srivastava.<sup>24</sup>

### Effect of Concentration of Ammonium Sulfite:

The reactant concentration  $[B]$  was varied from 0.045 to 0.45 gmol/l. The absorption data are given in Table 9 and also plotted in Figure 13. It is observed that the rate of absorption increased linearly with reactant concentration. According to equation(6) this observation indicates that the reaction is second order with respect to ammonium sulfite.

Alternatively, as already noted, the reaction is first order with respect to oxygen. Thus, with the value



TABLE 6

ABSORPTION OF OXYGEN IN AQUEOUS SOLUTIONS OF  
AMMONIUM SULFITE IN LAMINAR JET APPARATUS:  
EFFECT OF CONTACT TIME

Concentration of ammonium sulfite = 0.420 gmol/l

Concentration of cobaltous sulfate =  $4.70 \times 10^{-3}$  gmol/l

Temperature = 30°C

No.	Contact time, sec.	Specific rate of absorption,
		$R \times 10^7$ , gmol/cm <sup>2</sup> sec
1	0.016	3.16
2	0.019	3.14
3	0.024	3.12
4	0.038	3.14
5	0.053	3.18
6	0.065	3.12
7	0.090	3.18

TABLE 7

ABSORPTION OF OXYGEN IN AQUEOUS SOLUTIONS OF AMMONIUM  
SULFITE IN STIRRED CELL: EFFECT OF PARTIAL PRESSURE  
OF OXYGEN, VOLUMETRIC UPTAKE METHOD

Concentration of ammonium sulfite = 0.45 gmol/l

Catalyst concentration =  $4.70 \times 10^{-3}$  gmol/l

Temperature = 30°C

Run No.	Partial pressure of oxygen, per cent	Specific rate of absorption, $R \times 10^7$ , gmol/cm <sup>2</sup> sec
1	12.5	0.44
2	27.2	0.88
3	43.8	1.50
4	60.8	1.92
5	80.5	2.20
6	99.0	3.10

TABLE 8

ABSORPTION OF OXYGEN IN AQUEOUS SOLUTIONS OF AMMONIUM  
SULFITE IN STIRRED CELLS: EFFECT OF PARTIAL PRESSURE

OF OXYGEN: ANALYTICAL METHOD

Catalyst concentration =  $4.70 \times 10^{-3}$  gmol/l

Temperature =  $30^{\circ}\text{C}$

Run No.	Partial pressure of oxygen, per cent	Initial conc <sup>n</sup> of ammonium sulfite gmol/l	Conc <sup>n</sup> of ammonium sulfite after 10 min. of reaction gmol/l	Average conc <sup>n</sup> of ammonium sulfite, [B] <sub>a</sub> , gmol/l	Specific rate of absorption, $\frac{R}{[B]_a} \times 10^7$ Rx10 <sup>7</sup> gmol/cm <sup>2</sup> sec.
1	16.6	0.426	0.398	0.412	0.59
2	27.2	0.426	0.378	0.402	1.01
3	46.0	0.426	0.345	0.386	1.71
4	62.2	0.426	0.322	0.374	2.20
5	86.5	0.426	0.296	0.361	2.74
6	99.0	0.426	0.274	0.350	3.20

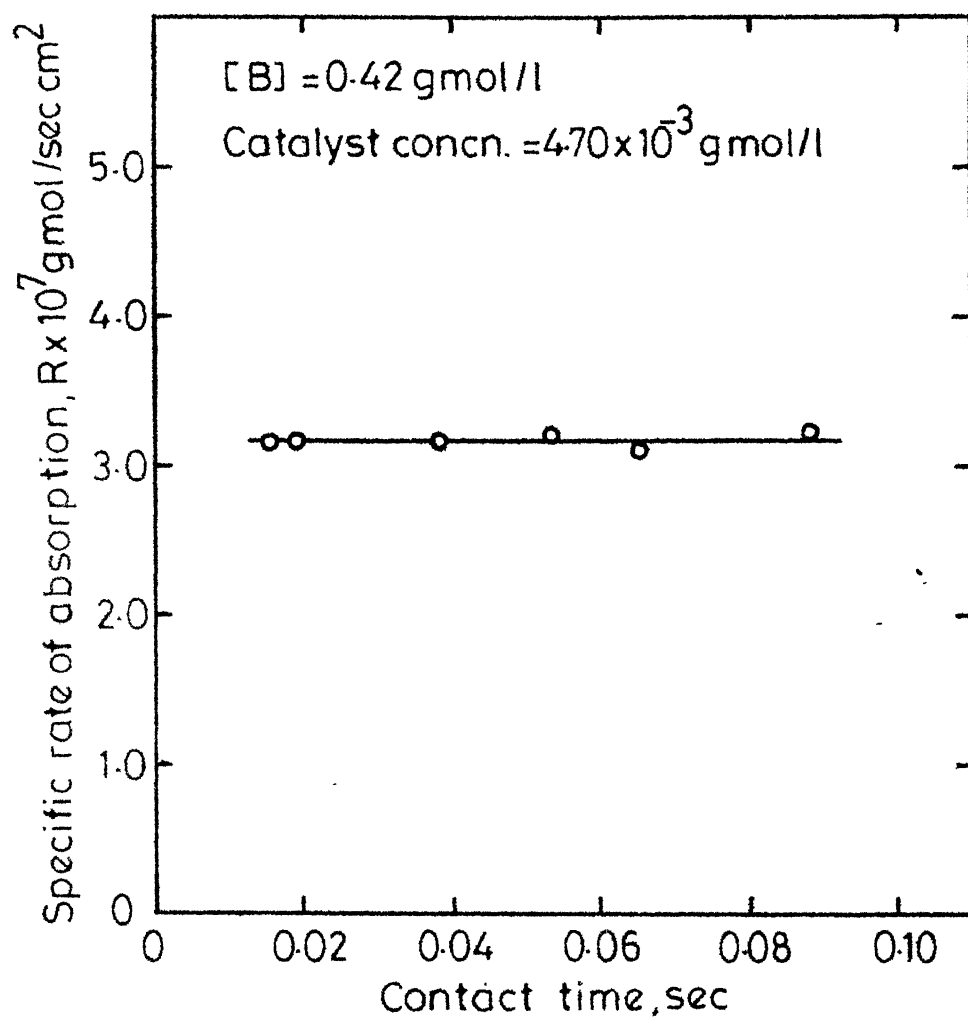


Fig. 10 - Effect of contact time on the specific rate of absorption in a laminar jet apparatus at 30°C.

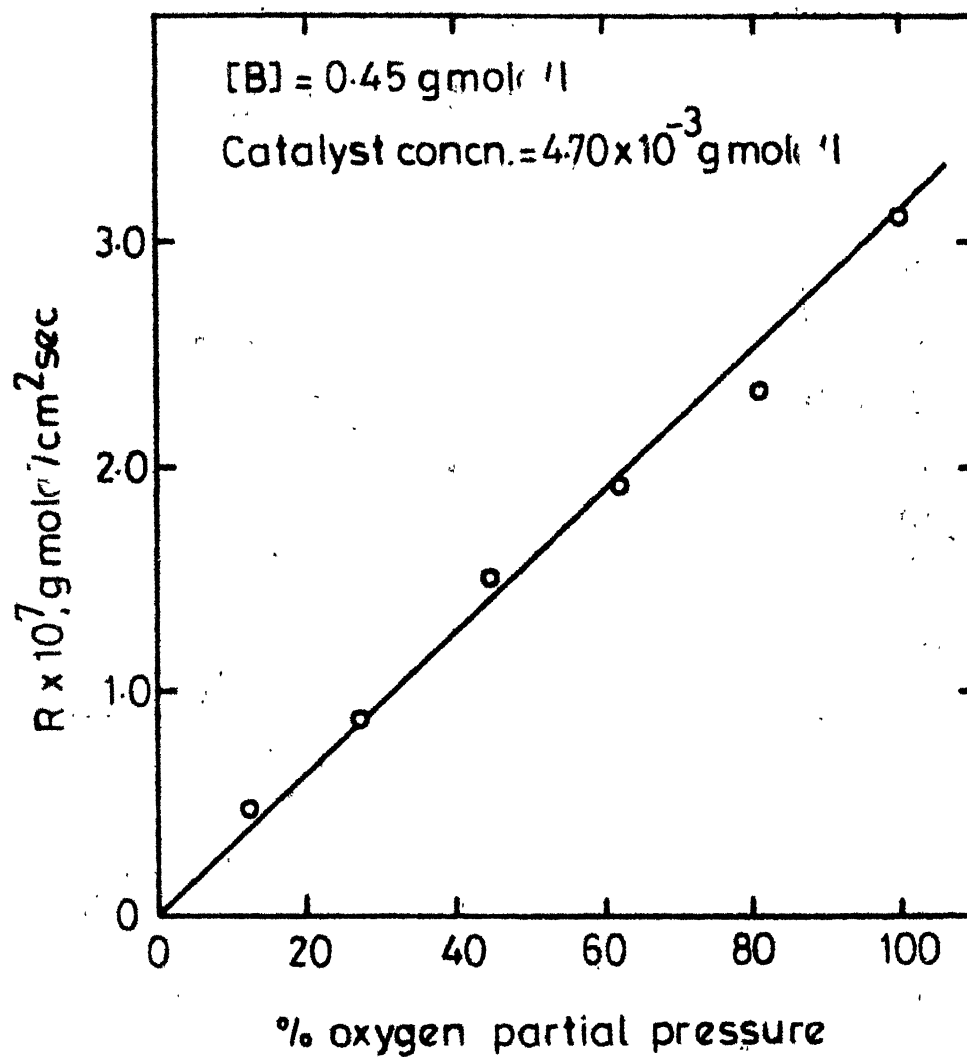


Fig.11 - Effect of partial pressure of oxygen on the specific rate of absorption at 30°C.

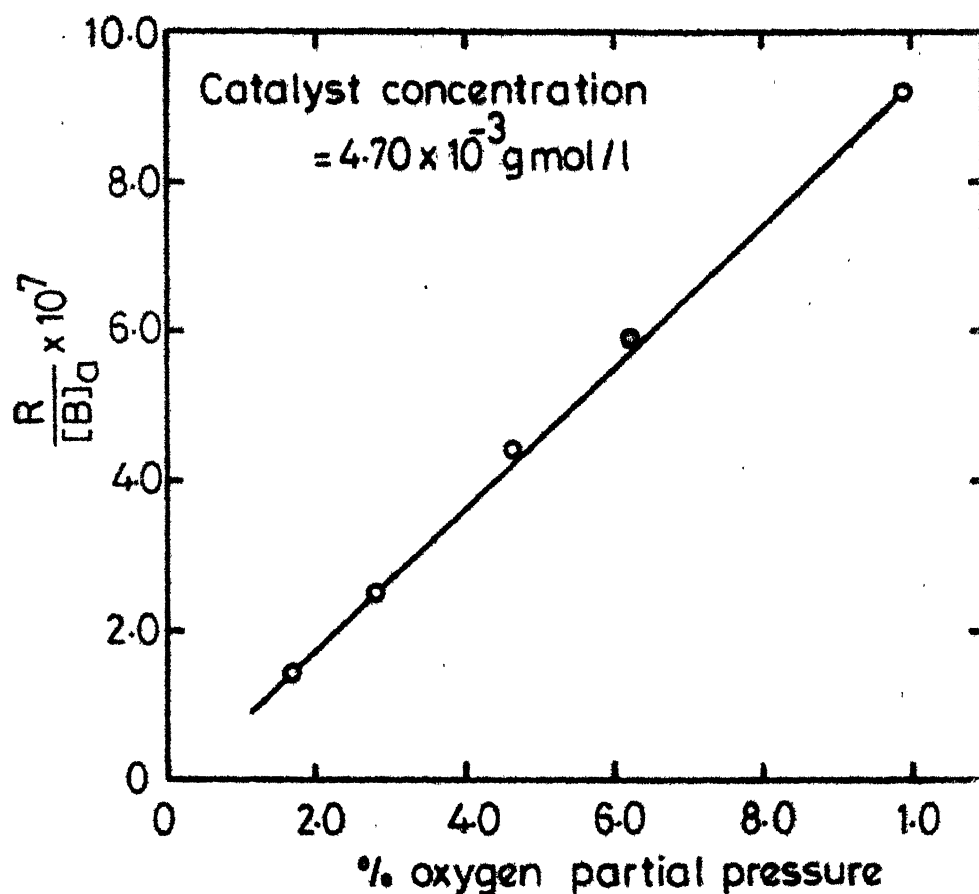


Fig. 12 -Effect of partial pressure of oxygen on the specific rate of absorption in stirred cell at 30°C -analytical method.

of  $m=1$  in equation (6), it reduced to

$$R = [A] \sqrt{D_A k_{m,n} [B]^n} \quad (13)$$

or

$$\left(\frac{R}{[A]}\right)^2 = D_A k_{m,n} [B]^n \quad (14)$$

or

$$\log\left(\frac{R}{[A]}\right)^2 = \log D_A k_{m,n} + n \log [B]$$

Thus plot of  $\log [B]$  versus  $\log \left(\frac{R}{[A]}\right)^2$  may be used to determine the order with respect to the reactant B. (Table 10 gives the calculated values of  $\left(\frac{R}{[A]}\right)^2$  for various values of  $[B]$ ). Figure 15 shows such a plot. The slope of the straight line of Figure 13 is found to be equal to 2. It confirms that the reaction is second order with respect to ammonium sulfite.

#### Effect of pH:

The pH of the aqueous solutions of sodium sulfite has been found to influence the rate of absorption of oxygen.<sup>14,33</sup> A similar influence may be present in the case of ammonium sulfite also. Hence the pH of the aqueous solutions of ammonium sulfite was determined. The data are given in Table 11. The variation of pH of the ammonium sulfite solution of different concentrations is negligibly small. The rate of absorption of oxygen under the conditions used in the present study is unlikely to be

TABLE 9

ABSORPTION OF OXYGEN IN AQUEOUS SOLUTIONS OF  
AMMONIUM SULFITE IN STIRRED CELLS: EFFECT OF  
CONCENTRATION OF AMMONIUM SULFITE [B]

Concentration of catalyst =  $4.70 \times 10^{-3}$  gmol/l  
 Temperature = 30°C

Run No.	Concentration of ammonium sulfite, [B], gmol/l	Specific rate of absorption, $R \times 10^7$ gmol/cm <sup>2</sup> sec
1	0.045	0.350
2	0.093	0.670
3	0.158	1.140
4	0.195	1.430
5	0.273	1.900
6	0.414	3.030

TABLE 10

ABSORPTION OF OXYGEN IN AQUEOUS SOLUTIONS OF AMMONIUM  
SULFITE IN STIRRED CELLS: CALCULATED VALUES OF  $(R/[A])^2$   
FOR VARIOUS VALUES OF [B]

Run No.	[B], gmol/cm <sup>3</sup>	$R \times 10^7$ gmol/cm <sup>2</sup> sec	[A] $\times 10^6$ gmol/cm <sup>3</sup>	$(R/[A])^2$
1	0.000045	0.35	1.12	0.00092
2	0.000093	0.67	1.09	0.00362
3	0.000158	1.14	1.05	0.01000
4	0.001950	1.43	1.04	0.01560
5	0.000273	1.90	1.01	0.02770
6	0.000414	3.03	0.94	0.07700

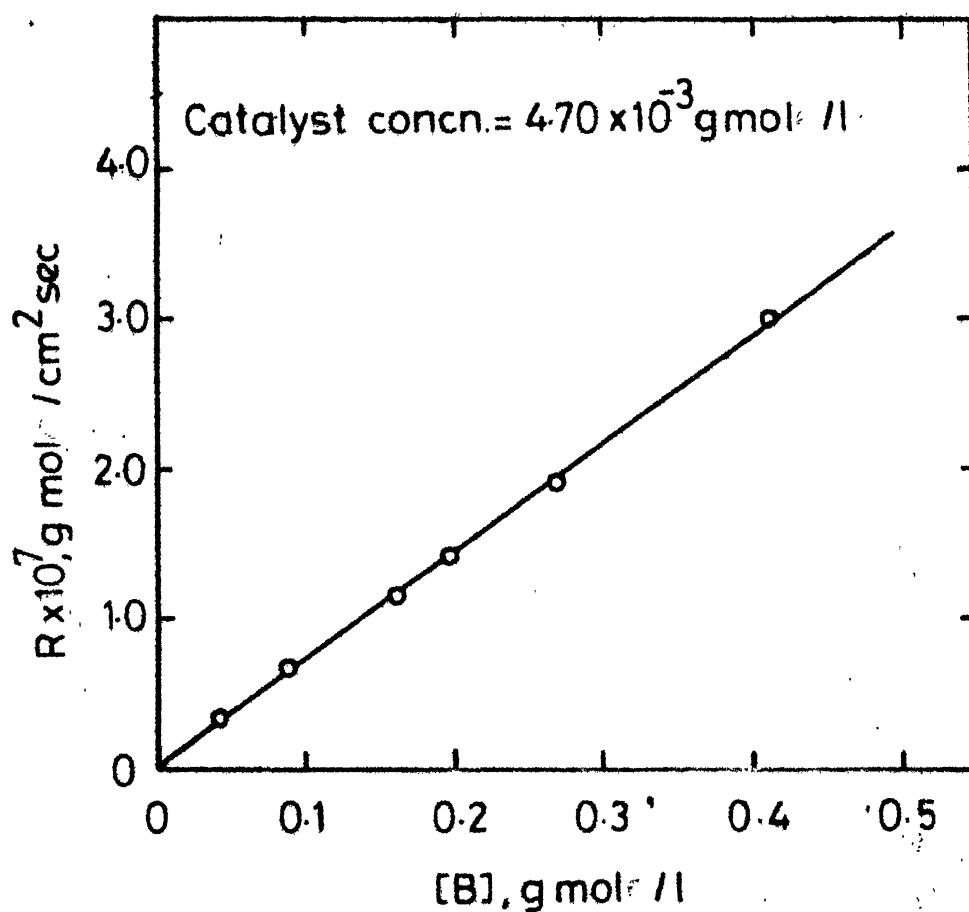


Fig.13 - Effect of ammonium sulfite concentration on the specific rate of absorption at 30°C.



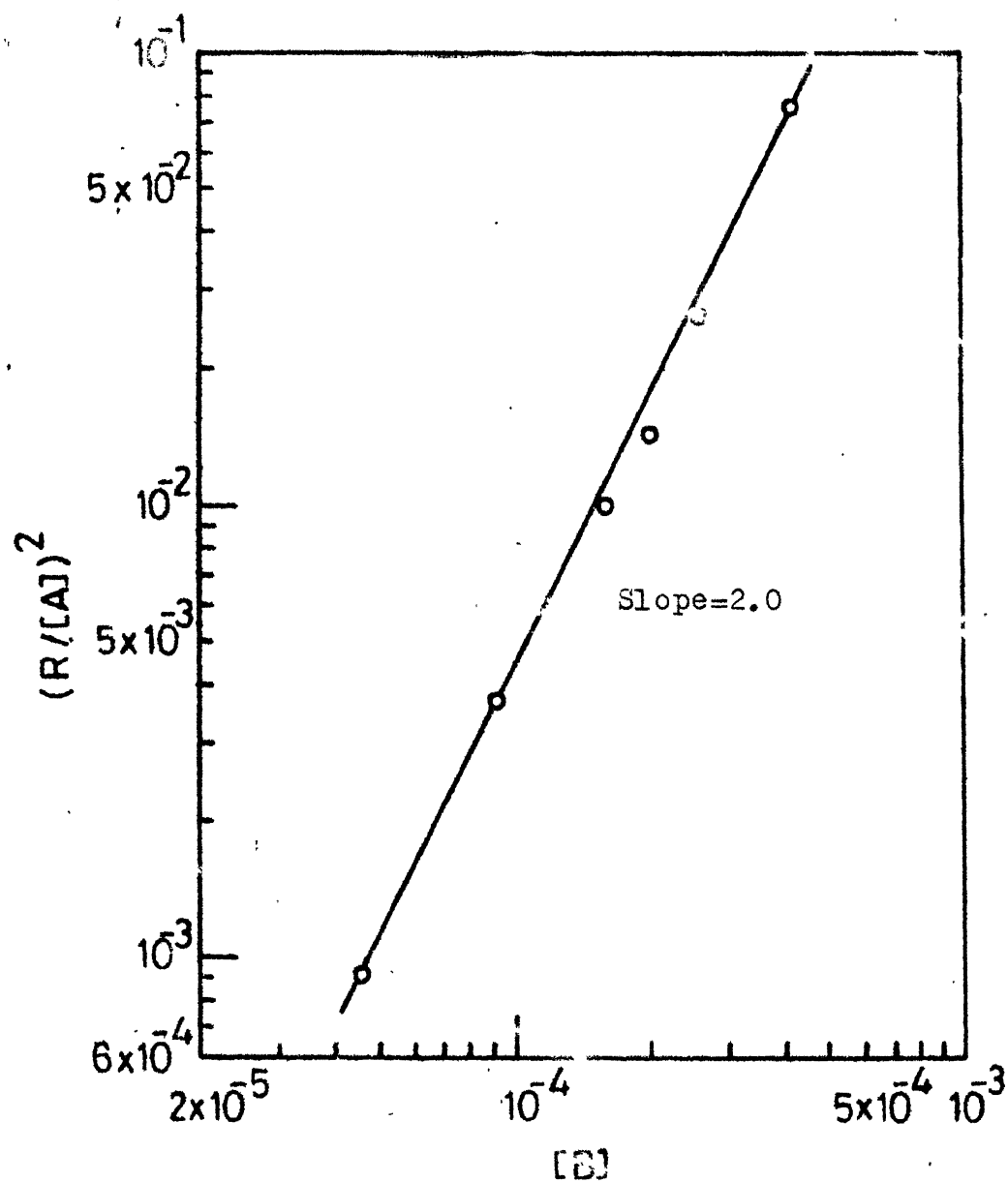


Fig.14 - Plot of  $\log [B]$  vs.  $\log (R/[A])^2$ .

affected by pH. However, a few runs were carried out after artificially adjusting the pH of the solutions at different levels. The data are reported in Table 12. It is noted from the data given in Table 12 that the rate of absorption of oxygen was unaffected by an artificially introduced change in the pH.

#### PHYSICOCHEMICAL DATA:

The values of the solubility and diffusivity of oxygen in aqueous solutions of ammonium sulfite have to be computed for determining the true value of the reaction rate constant.

#### Solubility of Oxygen in Aqueous Solutions of Ammonium Sulfite:

The solubility of oxygen in water has been reported by Morrison and Billet.<sup>34</sup> Its solubility in the reactant solution was estimated by using the expression

$$\log_{10} \frac{[A]}{[A_w]} = K_s I \quad (15)$$

where  $[A]$  = solubility of oxygen in aqueous ammonium sulfite solutions,  $\text{gmol/cm}^3$

$[A_w]$  = solubility of oxygen in water,  $\text{gmol/cm}^3$

$$K_s = i_+ + i_- + i_g$$

$i$  = contribution due to various species, l/g ion

$I$  = ionic strength of solution, l/g ion

TABLE 11pH OF AQUEOUS SOLUTIONS OF AMMONIUM SULFITEConcentration of catalyst =  $4.70 \times 10^{-3}$  gmol/lTemperature =  $30^{\circ}\text{C}$ 

No.	Concentration of ammonium-sulfite solution [B], gmol/l	pH of Aqueous Solutions	
		Without Catalyst	With Catalyst
1	0.0605	8.10	8.00
2	0.1070	8.10	8.00
3	0.2360	8.15	8.05
4	0.3670	8.15	8.05
5	0.4510	8.10	8.00

TABLE 12ABSORPTION OF OXYGEN IN AQUEOUS SOLUTIONS OF AMMONIUM SULFITE IN STIRRED CELLS: EFFECT OF pH

Concentration of ammonium sulfite [B] = 0.43 gmol/l

Concentration of catalyst =  $4.70 \times 10^{-3}$  gmol/lTemperature =  $30^{\circ}\text{C}$ 

Run No.	pH	Specific rate of absorption,
		$R \times 10^7$ gmol/cm <sup>2</sup> sec
1	7.0	3.10
2	7.45	3.10
3	8.00	3.20

Van Krevelen and Hoftizer<sup>35</sup> have given the values of  $i$  for various ions and gases. The values of solubility of oxygen in aqueous solutions of ammonium sulfite computed by the equation 15 and used in this study at various temperatures are given in Table 13.

#### Diffusivity of Oxygen in Aqueous Solutions of Ammonium Sulfite:

The values of diffusivity of oxygen in water have been reported by Himmelblau.<sup>36</sup> The values of diffusivity of oxygen in various reactant solutions were estimated by the expression

$$\frac{D_A}{\mu T} = \text{constant} \quad (16)$$

where  $D_A$  = diffusivity of oxygen in solution,  $\text{cm}^2/\text{sec}$

$\mu$  = viscosity of solution, cp

$T$  = temperature,  $^{\circ}\text{K}$

Table 14 gives the values of diffusivity computed by using equation 16 for oxygen-ammonium sulfite system at various temperature.

#### Physical Mass Transfer Coefficient:

The values of true mass transfer coefficient are required to check the conditions given by the expressions 7 and 8. The values of physical mass transfer coefficient for

TABLE 13SOLUBILITY OF OXYGEN IN AQUEOUS SOLUTIONS OF AMMONIUM SULFITE

No.	Concentration of ammonium sulfite solution [B], g/mol/l	[A] x 10 <sup>6</sup> , g/mol/cm <sup>3</sup>			
		20°C	30°C	40°C	46°C
1	0.000	1.30	1.19	1.05	1.01
2	0.045	1.28	1.12	1.04	0.99
3	0.093	1.20	1.09	1.02	0.98
4	0.158	1.18	1.05	1.01	0.95
5	0.195	1.10	1.04	0.96	0.94
6	0.273	1.05	1.01	0.92	0.90
7	0.414	1.02	0.94	0.94	0.87

TABLE 14DIFFUSIVITY OF OXYGEN IN AQUEOUS SOLUTIONS OF AMMONIUM SULFITE

No.	Temperature, °C	Diffusivity, D <sub>A</sub> x 10 <sup>5</sup> , cm <sup>2</sup> /sec
1	20	2.01
2	25	2.12
3	30	2.22
4	35	2.23
5	40	2.27
6	46	2.30

sulphur dioxide-water system at different speeds of agitation have been reported by Gehlawat<sup>30</sup> for the same stirred cell. They have been corrected for the diffusivity and viscosity effects by the following expression

$$k_L = k_{L_{\text{SO}_2-\text{H}_2\text{O}}} \left( \frac{\mu_{\text{water}}}{\mu_{\text{solution}}} \cdot \frac{D_{\text{O}_2-\text{H}_2\text{O}}}{D_{\text{SO}_2-\text{H}_2\text{O}}} \right)^{0.5} \quad (17)$$

Table 16 gives the values of physical mass transfer coefficient at various speeds of agitation.

#### Test for Physical Conditions:

For a typical run for the ammonium sulfite concentration of 0.41 gmol/l, the specific rate of absorption was  $R = 3.03 \times 10^{-7}$  gmol/sec.cm<sup>2</sup>. The solubility of oxygen,  $[A] = 9.4 \times 10^{-7}$  gmol/cm<sup>3</sup> and the physical mass transfer coefficient  $k_L = 3.12 \times 10^{-3}$  cm/sec. Thus

$$\frac{R}{[A] k_L} = 100.$$

which satisfied the condition given by expression (7).

Further, the value of  $[B]/Z[A]$  is 213 indicating that the condition given by expression (8) was also satisfied.

Hence the reaction is found to conform to fast pseudo-nth order regime with values of  $n=1$  and  $n=2$ . Equation (6) may be used for the determination of the values of the reaction rate constant.

### Reaction Rate Constant:

For the present system, the equation (6) reduces to

$$R = [A] \sqrt{D_A k_3 [B]^2} \quad (18)$$

$$\text{from which } k_3 = \left(\frac{-R}{[A]}\right)^2 \cdot \left(\frac{1}{D_A [B]^2}\right) \quad (19)$$

Equation(19) has been used to calculate the values of the third order reaction rate constant,  $k_3$ . The effect of temperature on reaction rate constant was studied. Figure 14 shows the Arrhenius plot. The apparent energy of activation is found to be 14.5 kcal/gmol. Table 16 gives the data on reaction rate constant along with the original values of the specific rates of absorption. The data obtained are likely to be useful for a rational design of industrial reactors.

TABLE 15

VALUES OF TRUE MASS TRANSFER COEFFICIENTS FOR THE  
ABSORPTION OF OXYGEN IN AQUEOUS SOLUTIONS OF AMMO-  
NIUM SULFITE IN STIRRED CELL

Effective interfacial area of stirred cell =  $79 \text{ cm}^2$

Temperature =  $30^\circ\text{C}$

No.	Speed of agitation rev/min.	Physical mass transfer <sup>50</sup> coefficient for $\text{SO}_2\text{-H}_2\text{O}$ system, $k_L \times 10^3 \text{ cm/sec}$	Physical mass transfer coefficient for $\text{O}_2\text{-}$ $(\text{NH}_4)_2\text{SO}_3$ system, $k_L \times 10^3, \text{cm/sec}$
1	30	1.85	2.22
2	42	2.30	2.76
3	54	2.60	3.12
4	65	2.85	3.42
5	88	3.50	4.20

TABLE 16

REACTION RATE CONSTANTS FOR THE REACTION BETWEEN OXYGEN AND  
AMMONIUM SULFITE

$\text{CoSO}_4$  catalyst concentration =  $4.70 \times 10^{-3} \text{ gmol/l}$

No.	Tempera- ture, $^\circ\text{C}$	Specific rate of absorption, $R \times 10^7 \text{ gmol/cm}^2\text{sec}$	Reaction rate constant, $k_3 \times 10^{-4} (\text{l/gmol})^2 \text{sec}^{-1}$
1	20	2.05	1.05
2	30	3.11	2.70
3	40	4.15	4.95
4	46	5.30	8.15



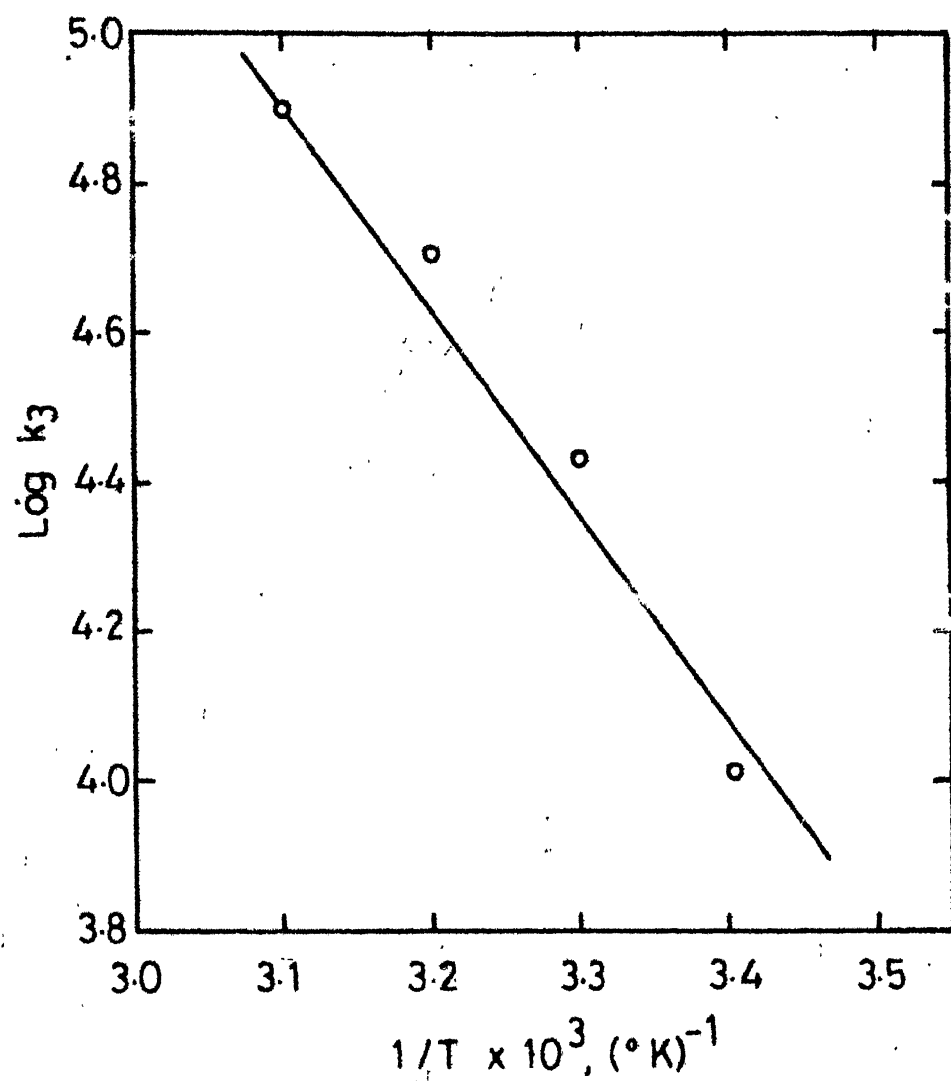


Fig.15 -Arrhenius plot for the reaction between oxygen and ammonium sulfite.

## SECTION II

KINETICS OF THE REACTION BETWEEN BUTADIENE AND NAPHTHOQUINONE

## CHAPTER 5

### INTRODUCTION AND LITERATURE REVIEW

Tetrahydroanthraquinone is obtained by the reaction between butadiene and naphthoquinone. It is the starting material for the manufacture of anthraquinone which is an important intermediate for the manufacture of dyes. Three different processes are used for the commercial manufacture of anthraquinone. They are:

1. Oxidation of anthracene derived from coal tar
2. Friedel craft condensation of phthalic anhydride with benzene in the presence of anhydrous aluminium chloride and the ring closure of the orthobenzoyl benzoic acid so formed to anthraquinone with concentrated sulfuric acid.
3. Diels-Alder reaction between butadiene and either benzoquinone or naphthoquinone followed by the oxidation of the adduct, tetrahydroanthraquinone in the presence of an alkali.

Recently Gharda<sup>1</sup> has made an economic evaluation of the above three processes with specific reference to Indian conditions. It was concluded that the third process would prove more economical than the existing process (second one) under certain favourable conditions. Naphthoquinone is formed as a by-product during the vapour phase oxidation of naphthalene to phthalic anhydride upto an extent of 15 per cent. Thus large amounts of naphthoquinone may be available as by-product. Similarly butadiene may

be available as a co-product during the production of ethylene from a naphtha cracker. In India, at a particular location two neighbouring plants produce both naphthoquinone and butadiene as the by-products. They may be economically reacted for the ultimate conversion to anthraquinone. It may be noted that the reaction between naphthoquinone and butadiene is very selective. Therefore, it may be used for the selective reaction of butadiene from the  $C_4$ -fraction since other members do not react with naphthoquinone. Similarly crude naphthoquinone may be selectively reacted with butadiene and recovered from the reaction mixture as tetrahydroanthraquinone. Hence the reaction between butadiene and naphthoquinone is of great industrial importance.

#### LITERATURE REVIEW

Very limited information is available in the literature about the reaction between butadiene and naphthoquinone. A few studies have been reported in the literature regarding the kinetics of some closely related Diels-Alder reactions. Wassermann<sup>37</sup> studied the kinetics of the reaction between cyclopentadiene and naphthoquinone and between cyclopentadiene and benzoquinone in benzene solution. He found the reaction to be first order with respect to benzoquinone and naphthoquinone and also with

respect to butadiene. At low temperatures the reaction products were analysed by the colourimetric method. A vapour pressure technique was employed to study the reaction at higher temperatures. The kinetics of the reaction between butadiene and benzoquinone was studied by Eisler and Wassermann<sup>38</sup> using benzene as solvent. In this case also, the reaction was found to be first order with respect to both butadiene and benzoquinone.

Some information about the general process conditions and purification steps for the production of anthraquinone through the butadiene-naphthoquinone route are given in a few patents.<sup>39-42</sup> Practically no information is available in the literature about the kinetics of the reaction between butadiene and naphthoquinone. Butadiene is a gas and naphthoquinone is a solid at ambient conditions. Naphthoquinone sublimes at its melting point. Therefore, it is not possible to carry out this reaction under molten conditions as was done by Gehlawat<sup>4</sup> for the butadiene-maleic anhydride system. Benzene has been used as a solvent by other investigators for similar Diels-Alder reactions. The reaction between butadiene and naphthoquinone may be carried out using a solvent. A comparative study may be conducted to select a proper solvent for this purpose. The solubilities of butadiene and naphthoquinone in various

organic solvents are not reported in the literature. An experimental determination of physical solubility of butadiene and naphthoquinone in different solvents is needed. The present work was therefore undertaken to make a systematic study of the kinetics of this industrially important reaction using organic solvents.

CHAPTER 6

EXPERIMENTAL



## MATERIALS

A butadiene cylinder was obtained from M/S Synthetics and Chemicals, Bareilly. The purity of the gas was reported to be 99 per cent. Naphthoquinone, solvents and other chemicals used in the present study were of high purity. They were obtained from firms of repute.

## METHODS OF ANALYSIS

(a) Butadiene: The physical solubility of butadiene in various organic solvents was determined by preparing saturated solutions of known amounts of solvents at specified temperatures. The amount of butadiene was determined by an increase of weight as well as by the bromate-bromide method.<sup>43-45</sup>

### Bromate-Bromide Method for the Determination of Butadiene:

10 ml of 0.05 N bromate-bromide solution (prepared by weighing 1.392 gm of potassium bromate and dissolving it in one litre of water containing potassium bromide) was pippetted out into a conical flask. Following the addition of 5 ml of 6 N sulfuric acid, a known amount of solution containing butadiene was introduced into the conical flask. The flask was shaken frequently for ten minutes. 15 ml of freshly prepared 2N potassium iodide solution was then added. The liberated iodine was determined by titration with 0.02N sodium thiosulfate.

A blank run was made under identical conditions and necessary correction was applied for determining the amount of butadiene dissolved in the solution.

(b) Naphthoquinone: The solubility of naphthoquinone in various organic solvents was determined by preparing its saturated solutions at a given temperature. The amount of dissolved naphthoquinone could be determined by noting the amount of residual naphthoquinone. It could also be determined colorimetrically using Bausch and Lomb Spectrophotometer (Spectronic-20).

Table 17 gives the data for the calibration of Spectronic 20. The calibration charts for the solubility of naphthoquinone in various solvents are given in Figures 16 and 17. They were used for the determinations of naphthoquinone content in kinetic runs.

TABLE 17

CALIBRATION OF SPECTROPHOTOMETER (SPECTRONIC-20) FOR DIFFERENT LEVELS OF NAPHTHOQUINONE CONTENT IN BENZENE SOLUTION

WAVELENGTH USED = 700 millimicrons

No.	Concentration of naphthoquinone, gmol /l	Per cent Transmittance
1	0.0000	88.0
2	0.0245	75.0
3	0.0490	67.5
4	0.0980	45.0
5	0.1960	13.0

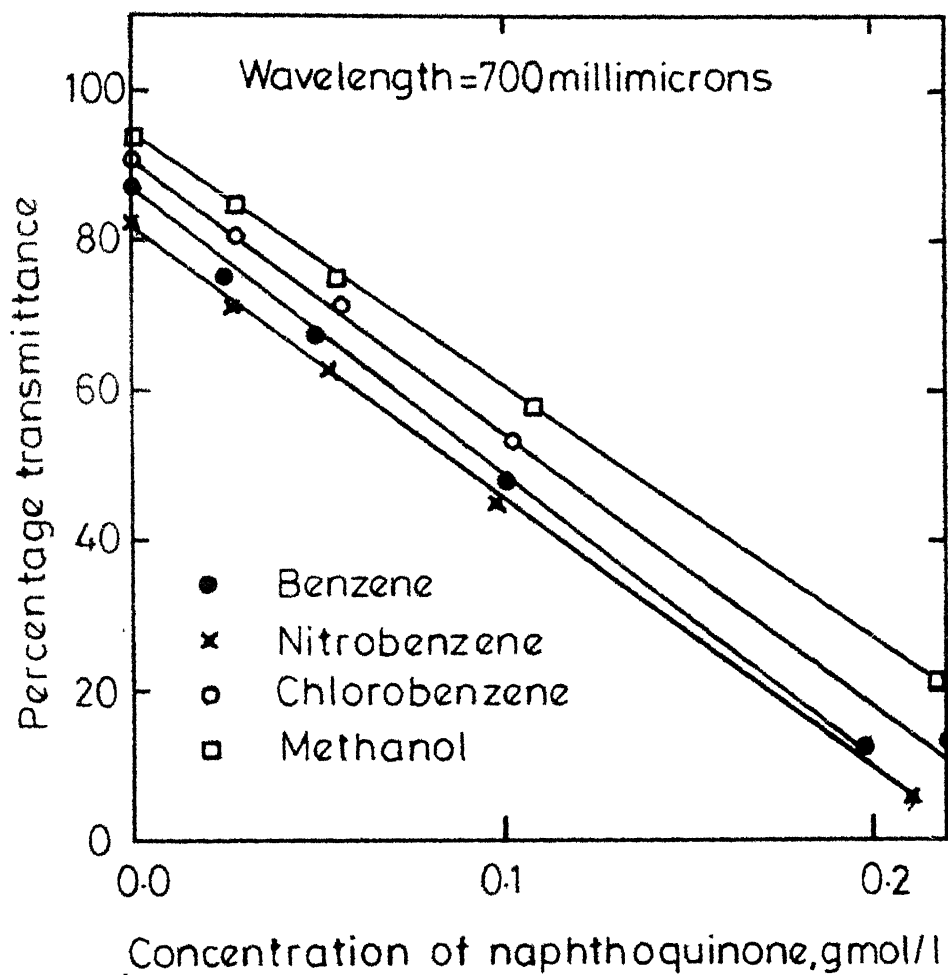


Fig. 16 -Calibration curves for Spectronic-20.  
(Spectrophotometer)

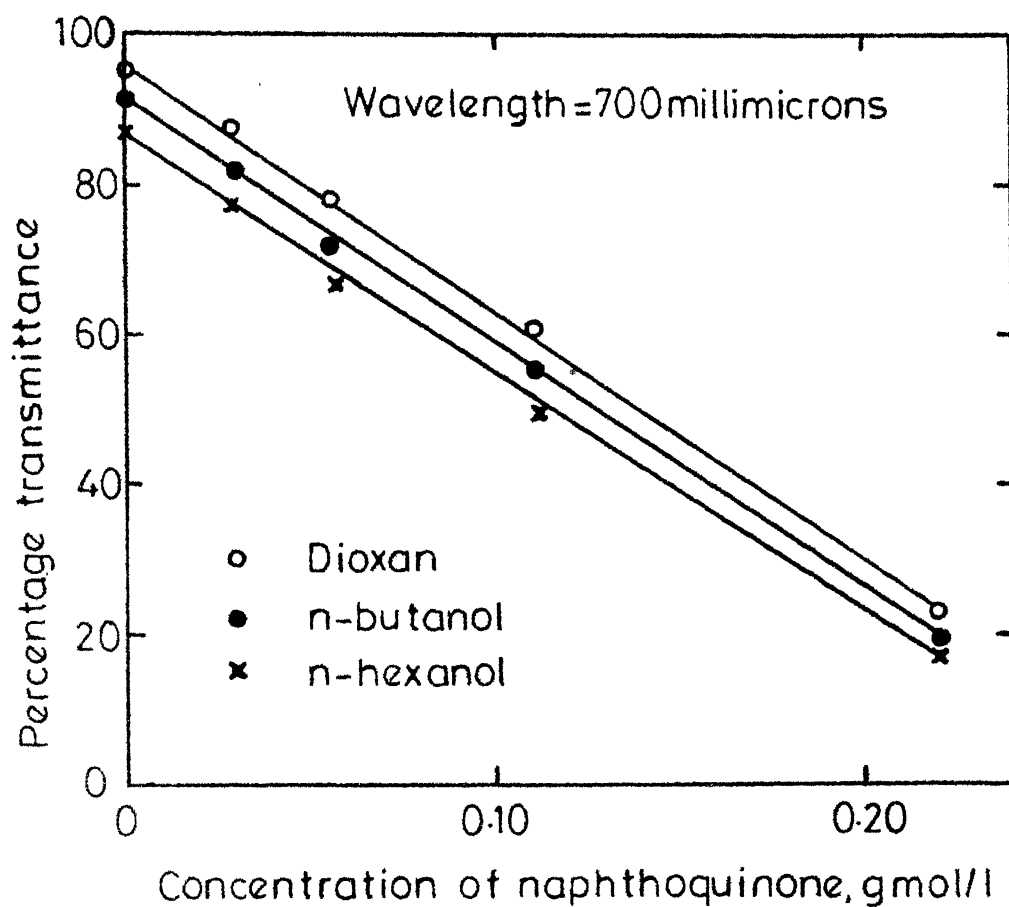


Fig. 17 - Calibration curves for Spectronic-20.  
(Spectrophotometer)

### Determination of Physical Solubility:

A 100 ml size glass bubbler provided with a quickfit standard glass joint with inlet and outlet connections for gas was used for the determination of physical solubility of butadiene in various organic solvents. The bubbler was placed in a constant temperature bath. The temperature of the bath could be controlled within  $\pm 0.2^{\circ}\text{C}$ . Another bubbler containing the solvent was installed in the same bath in series with the main bubbler. A known amount of solvent (50 ml) was taken in each bubbler. Butadiene gas was bubbled through the solvent at a slow rate until saturation was attained. The difference in initial and final weights gave the amount of butadiene present i.e. solubility of butadiene. As a countercheck, the above saturated solution was also analysed for its butadiene content using bromate-bromide method. The two methods gave results which were in close agreement.

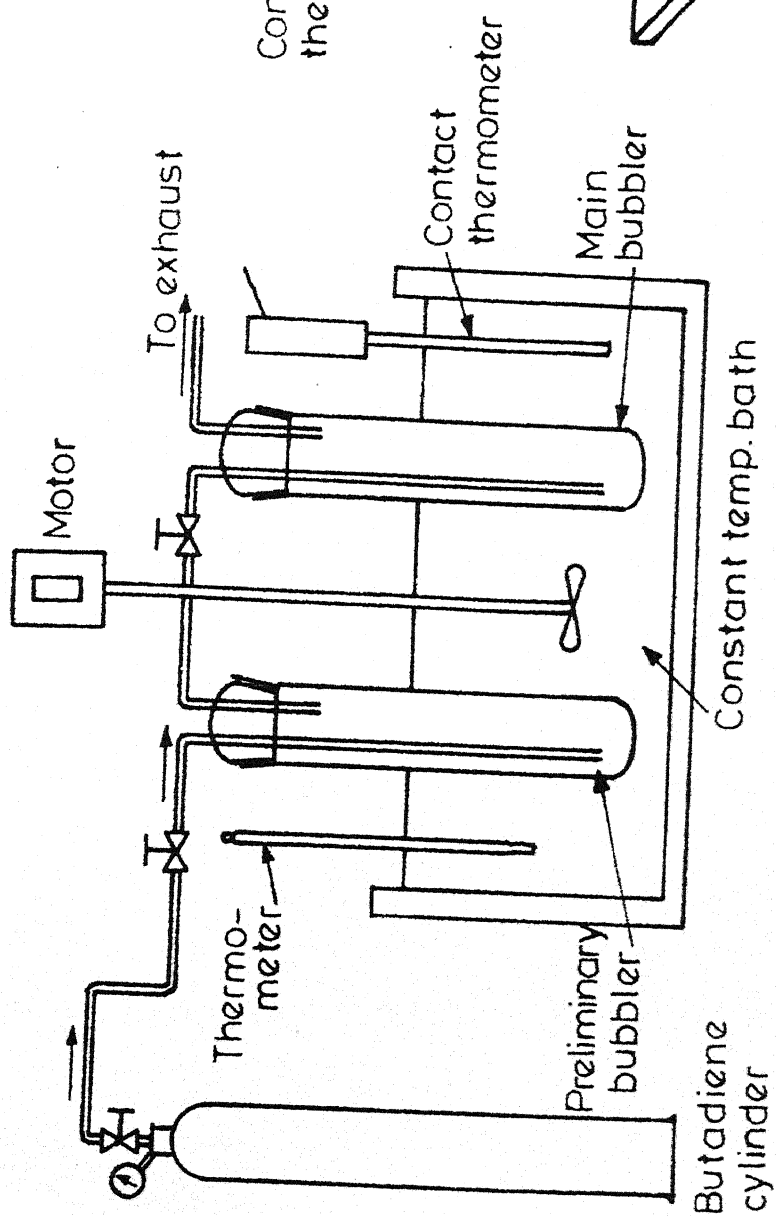
A 100 ml conical flask provided with a stopper and containing the solvent was used for the determination of physical solubility of naphthoquinone. It was placed in the constant temperature bath. A known amount of naphthoquinone was added to the flask containing the solvent. The contents were stirred manually using a glass rod until no more of naphthoquinone was dissolved. That is, a

saturated solution of naphthoquinone was obtained at the given temperature. The excess undissolved naphthoquinone was recovered by filtration and its weight was noted. A spectrophotometer (Spectronic-20) was used to determine the amount of the dissolved naphthoquinone.

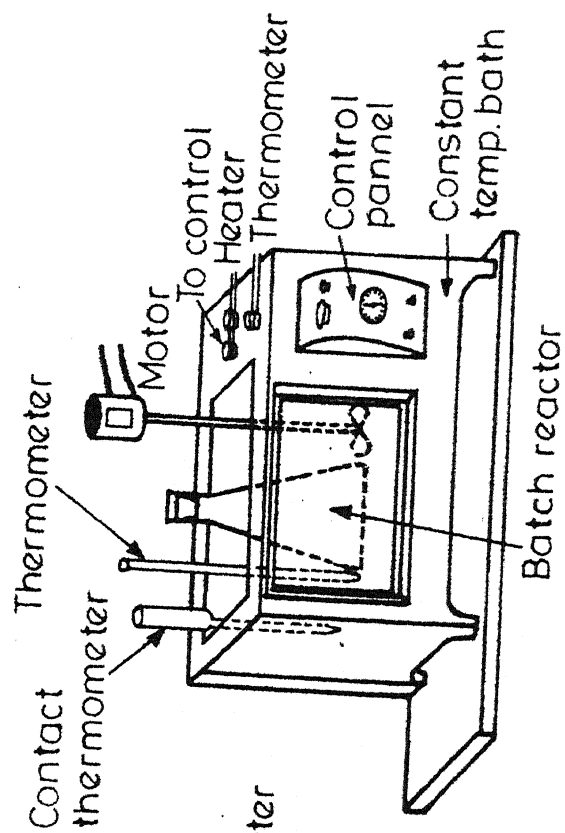
#### Kinetic Runs:

The kinetic runs were carried out in a 500 ml Erlenmeyer flask which served as a batch reactor. The reactor was placed in a constant temperature bath equipped with a stirrer and arrangements for temperature control within  $\pm 0.2^{\circ}\text{C}$ . The apparatus and the general procedure were similar to those employed by Kumar and Gehlawat<sup>45</sup> for the homogeneous kinetic studies between dissolved chlorine and acetic acid. Figure 18 gives the schematic diagram of the experimental set up.

In a typical run, the reactor containing a known amount of naphthoquinone dissolved in the solvent and a bubbler containing the pure solvent to dissolve butadiene were installed in the constant temperature bath. After the attainment of the steady state temperature, butadiene gas was bubbled through the solvent until saturation. A known amount of the saturated butadiene solution thus prepared and it was transferred to the batch reactor containing the naphthoquinone solution. This was taken as



A. Apparatus for solubility determination.



B. Apparatus for kinetic runs.

Fig. 18 - A schematic diagram of the experimental set-up for butadiene naphthoquinone system.

the zero reactions time. At various intervals of time, 10 ml of the reaction mixture were withdrawn. The reaction was followed by noting the drop in concentration of naphthoquinone with respect to time. The change in naphthoquinone concentration was noted with the help of Spectronic-20. Experiments were conducted using benzene, nitro-benzene, chloro-benzene, n-hexanol, n-butanol and dioxane as solvents over the temperature range of 25-50°C.



## CHAPTER 7

### RESULTS AND DISCUSSION.

### Solubility Data:

The solubility data of butadiene and naphthoquinone in various organic solvents determined experimentally are given in Tables 18 and 19. For an ideal gas at constant pressure the following equation holds:

$$\frac{d \ln C}{dt} = \frac{\Delta H}{RT^2} \quad (20)$$

where  $C$  is the concentration in gmol /l of solute in the liquid phase and  $\Delta H$  is the heat of dissolution. If  $\Delta H$  is assumed to be independent of temperature, an integration of equation (20) would give

$$\ln \frac{C_2}{C_1} = - \frac{\Delta H}{R} \left( \frac{1}{T_2} - \frac{1}{T_1} \right) \quad (21)$$

Equation (21) may be used for the determination of heat of dissolution. Figures 19 and 20 show the plot of reciprocal of absolute temperature versus logarithm of solubility. The slopes of the straight line enables the determination of the heat of dissolution. The data for heats of dissolution are given in Table 20. It may be noted that the heats of dissolution for gases carry negative sign since the solubility of gases decreases with temperature. It carries a positive sign for solids since their solubility increases with temperature in general.

TABLE 18

PHYSICAL SOLUBILITY OF BUTADIENE IN ORGANIC SOLVENTS  
AT 1 ATM

No.	Temp., °C	Physical Solubility of Butadiene, gmol /l					
		Benzene	Nitroben- zene	Chloro- benzene	Dioxane	n-buta- nol	n- hexanol
1	25	3.00	-	-	3.53	-	-
2	30	2.82	2.88	4.45	3.16	3.15	3.25
3	40	2.60	2.64	4.02	3.04	-	-
4	50	2.20	-	-	2.85	-	-
5	60	2.05	1.90	3.33	2.39	-	-
6	70	-	1.79	2.96	2.32	-	-

TABLE 19

PHYSICAL SOLUBILITY OF 1,4 NAPHTHOQUINONE IN VARIOUS  
ORGANIC SOLVENTS

No.	Temp., °C	Physical Solubility, gmol /l				
		Benzene	Chloro- benzene	Nitro- benzene	Dioxane	Methanol
1	20	0.700	0.44	0.40	-	0.850
2	25	0.805	-	-	0.86	0.900
3	30	0.852	0.600	0.52	0.91	0.960
4	40	1.000	0.710	0.60	1.05	1.150
5	50	1.100	0.840	0.74	1.15	1.210
6	60	-	1.000	0.84	1.25	-
7	70	-	1.100	0.96	-	-

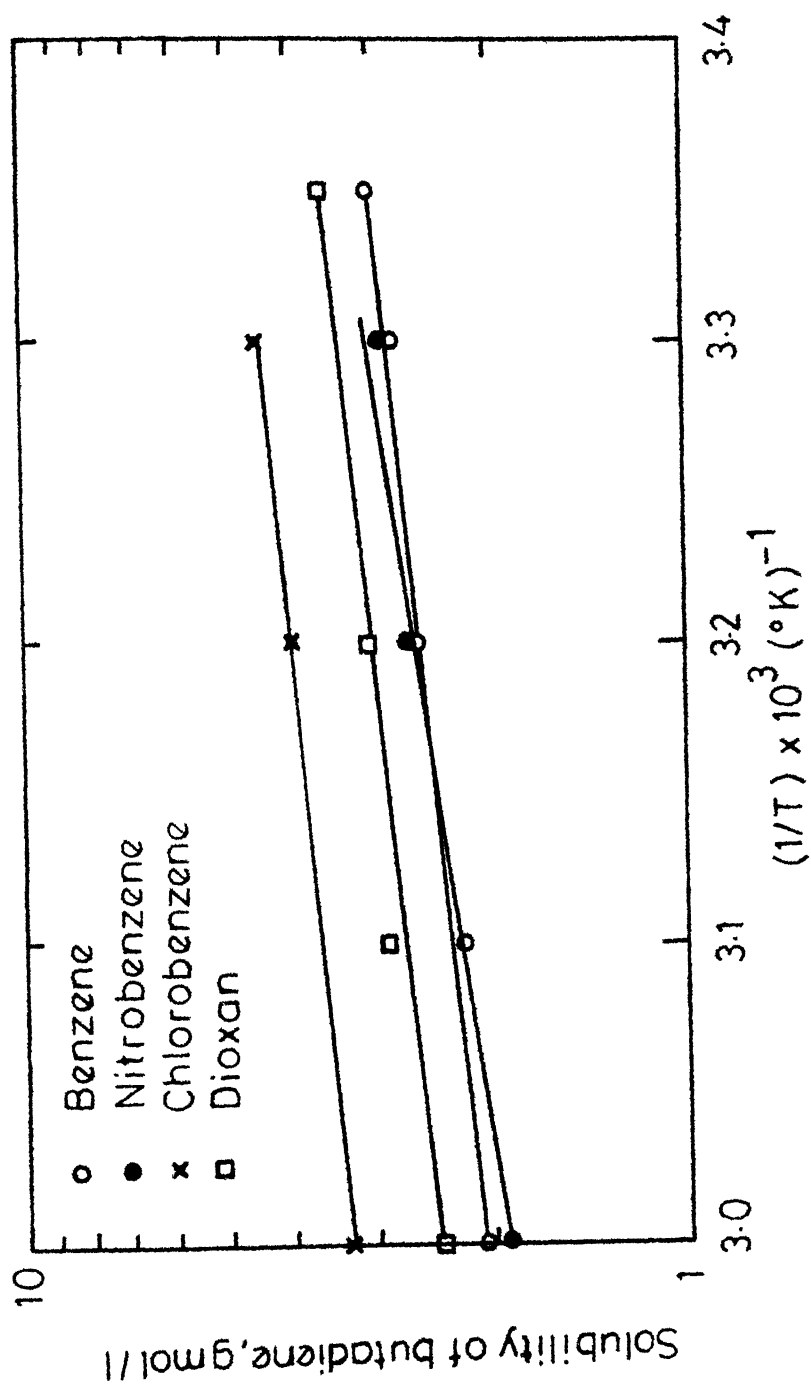


Fig. 19 - Effect of temperature on the solubility of butadiene.

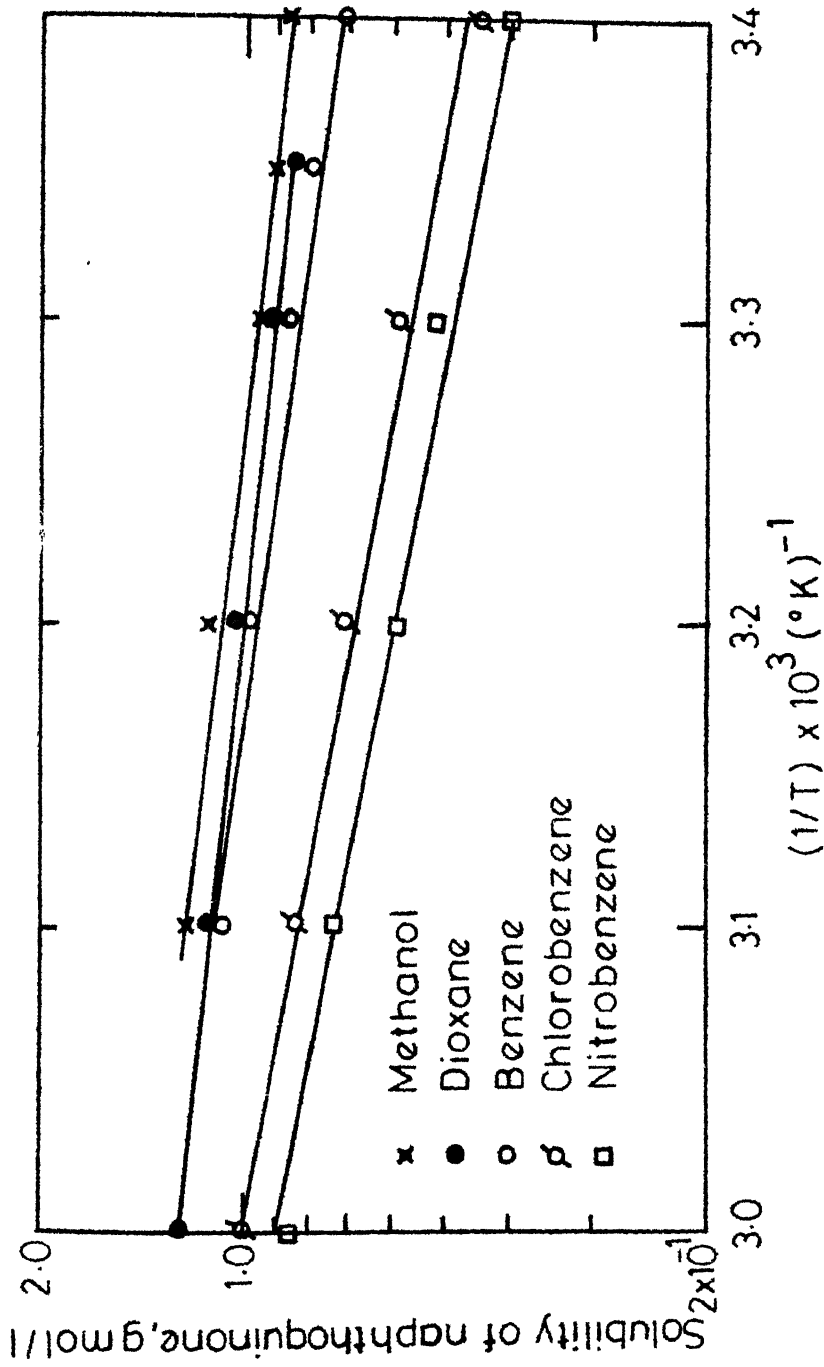
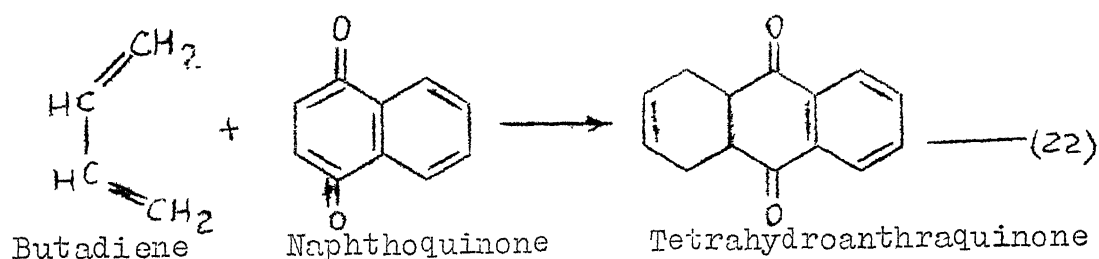


Fig. 20 - Effect of temperature on the solubility of naphthoquinone.

### Kinetics of the Reaction Between Dissolved Butadiene and Naphthoquinone:

The physical solubility of butadiene in organic solvents is reasonably large to enable the kinetics of the reaction between dissolved butadiene and naphthoquinone to be determined in the homogeneous phase.

The homogeneous irreversible reaction between the dissolved butadiene and naphthoquinone is given by the equation (22).



The rate of reaction,  $r_A$ , in gmol /l sec is given by

$$r_A = -\frac{d[A]}{dt} = k_{m,n} [A]^m [B]^n \quad (23)$$

where  $[A]$  = concentration of naphthoquinone, gmol /l

$[B]$  = concentration of butadiene, gmol /l

$m$  = order of reaction with respect to reactant A

$n$  = order of reaction with respect to reactant B

$k_{m,n}$  = specific rate constant  $(\text{l/gmol})^{m+n-1} \text{ sec}^{-1}$ .

### Pseudo-First Order Runs:

When the concentration of reactant B is very much

larger as compared to the concentration of reactant A the concentration of reactant B would remain virtually constant as A is reacted. Pseudo-first order mechanism would prevail under these conditions. In some experimental runs the concentration of naphthoquinone was maintained relatively low at 0.05 gmol /l as compared to the concentration of butadiene which was higher at 1.1 to 1.40 gmol /l. Therefore the concentration of butadiene was very large (22 to 28 times higher) as compared to the concentration of naphthoquinone. As the reaction between butadiene and naphthoquinone progressed, the butadiene concentration remained practically constant throughout the reaction period. Consequently a pseudo-first order behaviour of the reaction was prevalent. Under these conditions the equation (23) reduces to

$$r_A = - \frac{d[A]}{dt} = k_1 [A] \quad (24)$$

Integration of equation (24) gives

$$-\ln \frac{[A]}{[A_0]} = k_1 t \quad (25)$$

Thus, a plot of reaction time 't' versus  $-\ln \frac{[A]}{[A_0]}$  would give a straight line the slope of which will give the value of  $k_1$ . The results obtained for a set of runs conducted at 35°C under pseudo first order conditions are given in Table 21. Figure 21 shows the plot 't' versus

TABLE 20

HEAT OF DISSOLUTION OF BUTADIENE AND NAPHTHOQUINONE  
IN ORGANIC SOLVENTS

No.	Solvent	Heat of solution, kcal/gmol	
		Naphthoquinone	Butadiene
1	1,4 Dioxane	2.56	-2.16
2	Methanol	2.68	-
3	Benzene	2.80	-2.48
4	Chlorobenzene	3.66	-1.82
5	Nitrobenzene	3.94	-2.10

TABLE 21

DATA FOR PSEUDO-FIRST ORDER RATE CONSTANT FOR THE REACTION  
BETWEEN BUTADIENE AND NAPHTHOQUINONE IN BENZENE SOLUTION

Temperature = 35°C

Concentration of Butadiene = 1.35 gmol /l

No.	Time, 't', min.	Per cent Transmi- ttance	Concentration of naphthoquinone [A], gmol /l	$-\ln \frac{[A]}{[A_0]}$	$k_1^a$ , sec <sup>-1</sup>
1	0	65.0	0.0560	0.000	
2	20	65.5	0.0550	0.0150	
3	40	66.0	0.0540	0.0240	1.06x10 <sup>-5</sup>
4	60	66.5	0.0535	0.0420	
5	80	67.0	0.0530	0.0510	
6	100	67.5	0.0525	0.0640	

<sup>a</sup> Value computed from the slope of the straight line relationship between 't' versus  $-\ln \frac{[A]}{[A_0]}$ .



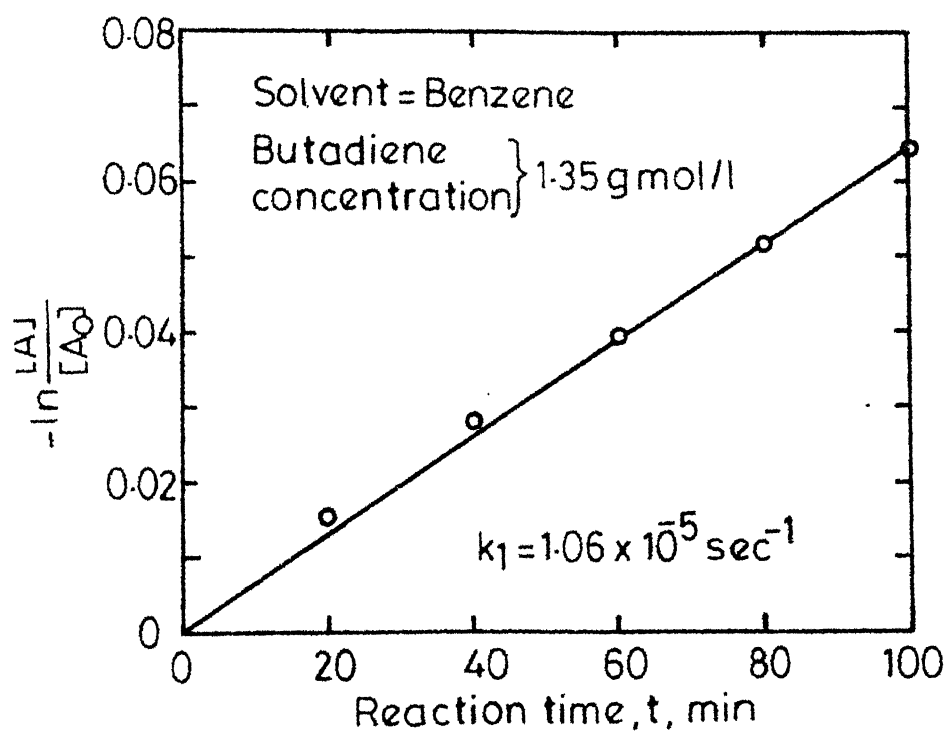


Fig. 21 - Computation of pseudo first order rate constant at 35°C.

$-\ln \frac{[A]}{[A]_0}$  for the above runs. A straight line relationship confirms the pseudo-first order behaviour of the reaction.

#### Effect of Concentration of Naphthoquinone:

A few runs were carried out at  $35^{\circ}\text{C}$  in which the concentration of naphthoquinone was varied from 0.05 to 0.30 gmol /l keeping the concentration of butadiene constant at 1.35 gmol /l. The results are given in Table 22. Figure 22 shows a plot of concentration of naphthoquinone versus the rate of reaction. All data points lie on a straight line passing through the origin. It can be inferred from Figure 22 that the reaction is first order with respect to naphthoquinone. This was further confirmed by plotting the concentration of naphthoquinone versus rate of reaction on a log log plot. The slope of the straight line obtained was unity.

#### Effect of Concentration of Butadiene:

In order to find the order of reaction with respect to butadiene, experiments were carried out at  $35^{\circ}\text{C}$  in which the concentration of butadiene was varied from 0.05 to 0.4 gmol /l maintaining the concentration of naphthoquinone constant at 0.5 gmol /l. The results are given in Table 23. Figure 23 shows a plot of butadiene concentration versus rate of reaction. It is clear from Figure 23 that the reaction is first order with respect to butadiene. Further

TABLE 22

EFFECT OF CONCENTRATION OF NAPHTHOQUINONE ON THE RATE OF REACTION

Solvent : Benzene

Concentration of butadiene = 1.35 gmole/l

Temperature = 35°C

Run No.	Concentration of Naphthoquinone gmol /l	Rate of reaction $\times r_A \times 10^7$ , gmol/(1.sec)
1	0.050	5.80
2	0.104	11.50
3	0.152	16.67
4	0.200	23.00
5	0.250	27.00
6	0.306	33.00

TABLE 23

EFFECT OF BUTADIENE CONCENTRATION ON THE RATE OF REACTION

Solvent : Benzene

Temperature = 35°C

Concentration of Naphthoquinone = 0.5 gmole/l

Run No.	Concentration of butadiene, gmol /l	Rate of reaction, $r_A \times 10^7$ , gmol / (1. sec)
1	0.050	1.02
2	0.076	1.60
3	0.096	2.30
4	0.200	5.10
5	0.400	9.30

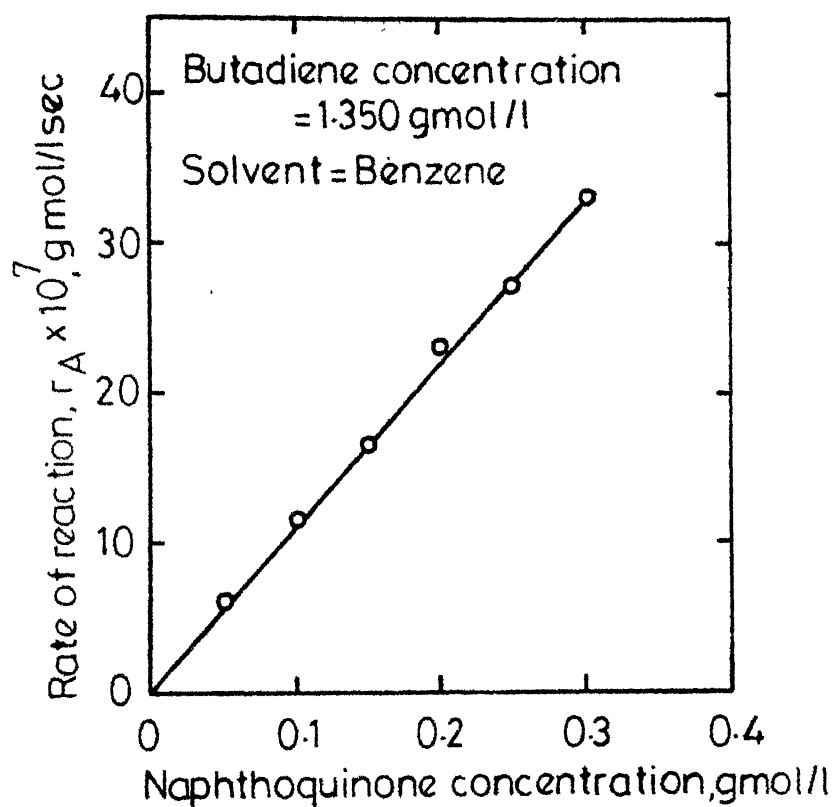


Fig. 22 - Effect of naphthoquinone concentration on rate of reaction at 35°C.

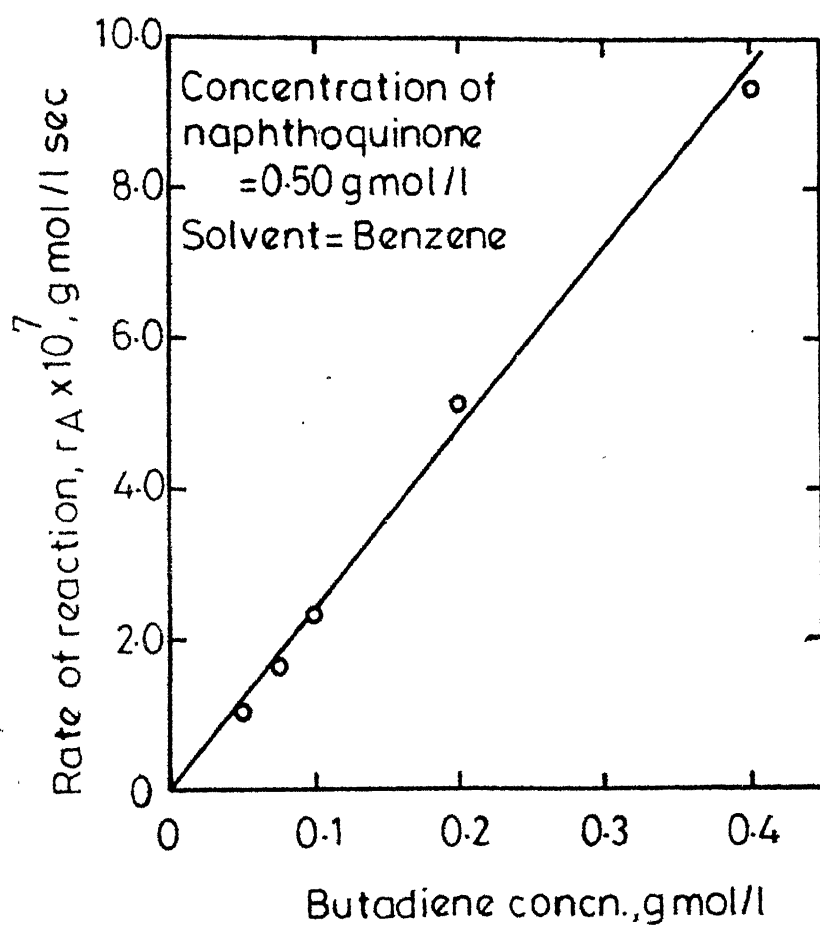


Fig. 23 - Effect of butadiene concentration on rate of reaction at 35°C.

a log-log plot of concentration of butadiene and the rate of reaction gave a straight line whose slope is unity. This confirms that reaction is first order with respect to butadiene. Thus, the overall reaction was found to be second order.

#### Reaction Rate Constant:

The overall rate expression (23) reduces to

$$r_A = k_2 [A] [B] \quad (26)$$

A comparison of equations (26) and (24) shows that

$$k_1 = k_2 [B] \quad (27)$$

Tables 24 to 27 give the basic data for different temperatures along with the values of pseudo-first order rate constants computed from the slopes of the straight lines for 't' versus  $-\ln \frac{[A]}{[A]_0}$ . The values of the second order reaction rate constant,  $k_2$ , l/(gmol sec), were obtained by using equation (27). Table 28 gives the value of second order rate constants at different temperatures. Figure 24 shows the Arrhenius plot for the reaction between butadiene and naphthoquinone. The energy of activation was found to be 22.2 kcal /gmol.

The values of the second order reaction rate constants for similar type Diels-Alder reaction systems are given in Table 29. It may be noted that the value of second order

TABLE 24

DATA FOR PSEUDO-FIRST ORDER RATE CONSTANT FOR THE REACTION  
BETWEEN BUTADIENE AND NAPHTHOQUINONE IN BENZENE SOLUTION

Temperature = 25°C

Concentration of butadiene = 1.5 gmol /l

No.	Time, min. 't'	Per cent transmi- ttance	Concentration of naphthoquinone, [A] gmol /l	$-\ln \frac{[A]}{[A_0]}$	$k_1^a, \text{sec}^{-1}$
1	0	65.0	0.0560	0.000	
2	50	65.5	0.0550	0.010	
3	100	66.0	0.0540	0.024	$3.5 \times 10^{-6}$
4	150	66.5	0.0535	0.030	

<sup>a</sup>Value computed from the slope of the straight line relationship between 't' versus  $-\ln \frac{[A]}{[A_0]}$

TABLE 25

DATA FOR PSEUDO-FIRST ORDER RATE CONSTANT FOR THE REACTION  
BETWEEN BUTADIENE AND NAPHTHOQUINONE IN BENZENE SOLUTION

Temperature = 30°C

Concentration of butadiene = 1.4 gmol /l

No.	Time, min. 't'	Per cent Transmitt- ance	Concentration of naphthoqui- none, [A] gmol /l	$-\ln \frac{[A]}{[A_0]}$	$k_1^a, \text{sec}^{-1}$
1	0	65.0	0.0560	0.000	
2	40	65.5	0.0550	0.015	
3	60	66.0	0.0540	0.024	$5.9 \times 10^{-6}$
4	80	66.5	0.0535	0.030	

<sup>a</sup>Value computed from the slope of the straight line relationship between 't' versus  $-\ln \frac{[A]}{[A_0]}$

TABLE 26

DATA FOR PSEUDO-FIRST ORDER RATE CONSTANT FOR THE REACTION  
BETWEEN BUTADIENE AND NAPHTHOQUINONE IN BENZENE SOLUTION

Temperature = 40°C

Concentration of butadiene = 1.30 gmol / l

No.	Time, min. 't'	Per cent Transmi- ttance	Concentration of Naphthoquinone, [A], gmol / l	$-\ln \frac{[A]}{[A_0]}$	$k_1^a, \text{sec}^{-1}$
1	0	65.0	0.0560	0.000	
2	20	66.0	0.0540	0.024	
3	40	66.5	0.0535	0.042	$1.58 \times 10^{-5}$
4	60	67.5	0.0525	0.064	
5	80	68.0	0.0520	0.078	
6	100	68.5	0.5000	0.100	

<sup>a</sup>Value computed from the slope of the straight line relationship  
between 't' versus  $-\ln \frac{[A]}{[A_0]}$

TABLE 27

DATA FOR THE PSEUDO-FIRST ORDER RATE CONSTANT FOR THE REACTION  
BETWEEN BUTADIENE AND NAPHTHOQUINONE IN BENZENE SOLUTION

Temperature = 50°C

Concentration of butadiene = 1.10 gmol / l

No.	Time, min. 't'	Per cent Transmitt- ance	Naphthoquinone concentration, [A] gmol / l	$-\ln \frac{[A]}{[A_0]}$	$k_1^a, \text{sec}^{-1}$
1	0	65.0	0.0560	0.000	
2	20	66.5	0.0535	0.045	
3	40	67.5	0.0505	0.110	$4.1 \times 10^{-5}$
4	60	68.5	0.0490	0.145	
5	80	69.0	0.0470	0.186	
6	100	70.0	0.0440	0.241	

<sup>a</sup>Value computed from the slope of the straight line relation-  
ship between 't' versus  $-\ln \frac{[A]}{[A_0]}$



TABLE 28

REACTION RATE      CONSTANTS FOR THE REACTION BETWEEN  
BUTADIENE AND NAPHTHOQUINONE IN BENZENE SOLUTION

No.	Temperature, °C	Second order reaction rate constant, $k_2 \times 10^6$ l/gmol sec
1	25	2.34
2	30	4.24
3	35	7.85
4	40	12.15
5	50	37.30

reaction rate constant for reaction between butadiene and benzoquinone in benzene solution<sup>38</sup> at 35°C is  $5.83 \times 10^{-6}$  l/gmol sec. This may be compared with the value of second order rate constant for the reaction between butadiene and naphthoquinone of  $7.85 \times 10^{-6}$  l/gmol sec at 35°C. Further the reported value of second order rate constant for the reaction between cyclopentadiene and naphthoquinone<sup>37</sup> in benzene solution at 30°C is  $4.0 \times 10^{-3}$  l/gmol sec. This is about 1000 times higher than the value of the second order rate constant for the reaction between butadiene and naphthoquinone obtained in the present study. Also, the reaction rate constant for

TABLE 29

A COMPARISON OF SECOND ORDER RATE CONSTANTS FOR DIFFERENT SYSTEMS IN BENZENE SOLUTION

Temperature, °C	$k_2$ , l/gmol, sec				
	Present Work	Reported Data			
	Butadiene- Naphthoquinone	Cyclopentadiene <sup>37</sup> Naphthoquinone	Butadiene <sup>38</sup> Benzoquinone	Cyclopenta- diene <sup>37</sup> Benzoquinone	Butadiene <sup>47</sup> Maleic Anhydride
25	$2.34 \times 10^{-6}$	-	-	-	$3.1 \times 10^{-5}$
30	$4.21 \times 10^{-6}$	$4.20 \times 10^{-3}$	-	-	-
35	$7.85 \times 10^{-6}$	-	$5.83 \times 10^{-6}$	$1.67 \times 10^{-2}$	-

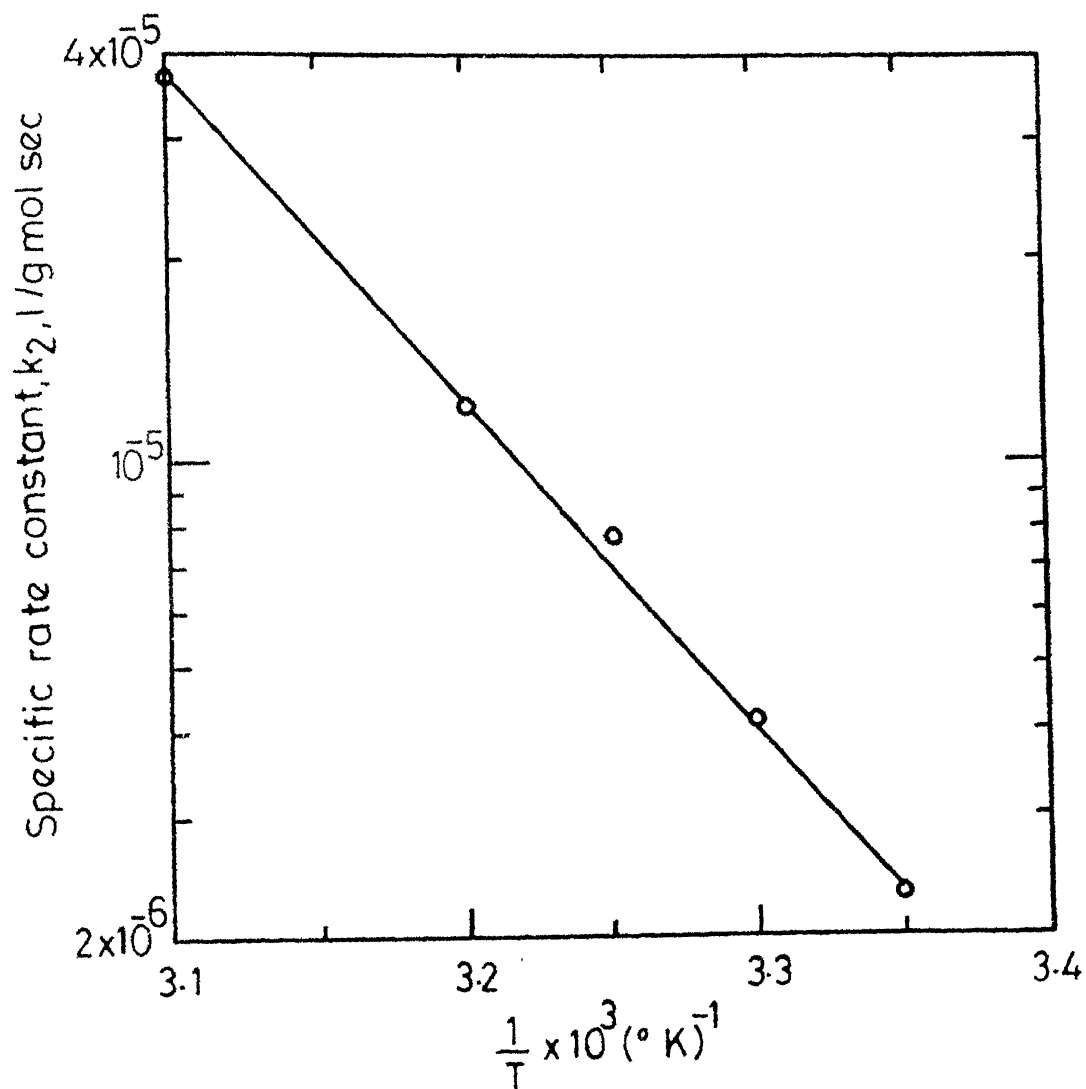


Fig. 24 -Arrhenius plot for the reaction between butadiene and naphthoquinone in benzene solution.

cyclopentadiene and benzoquinone<sup>37</sup> is about 3000 times faster than the reaction rate of butadiene with benzoquinone while it is comparable with butadiene-maleic anhydride reaction.<sup>47</sup> It appears that the more stable transbutadiene must isomerise to a cisoid configuration before a 1,4 addition to a dienophile can take place. Further, the highly strained five member ring structure of cyclopentadiene would make it more reactive than butadiene.

#### Effect of Solvent and Reaction Mechanism

The rate of reaction may be affected by the nature of solvent. To study the effect of solvent on the rate of reaction, different solvents with a wide variation in dielectric constant were used. The data obtained are given in Table 30. Figure 25 shows a plot of dielectric constant versus reaction rate constant at 30°C. It is noted that the reaction rate constant increased with an increase in dielectric constant upto its value of about 20 and then it became virtually constant. In view of higher reaction rates obtainable with nitrobenzene it may be preferred as a solvent for this reaction.

Figure 26 shows a plot of reciprocal of dielectric constant, ( $\frac{1}{D}$ ) versus logarithm of second order rate constant, ( $\log k_2$ ) which is a straight line. Such a relationship is expected if the transition state is more

TABLE 30

EFFECT OF SOLVENT ON THE REACTION RATE CONSTANT AT 30°C FOR  
THE REACTION BETWEEN BUTADIENE AND NAPHTHOQUINONE

No.	Solvent	Dielectric constant <sup>46</sup> 'D'	Reaction Rate Constant, $k_2$ , l/gmole sec $\times 10^6$
1	Benzene	2.20	4.21
2	Dioxane	2.10	4.11
3	Chlorobenzene	5.50	6.20
4	n-butanol	17.30	7.14
5	n-hexanol	13.00	6.90
6	Nitrobenzene	33.80	7.18

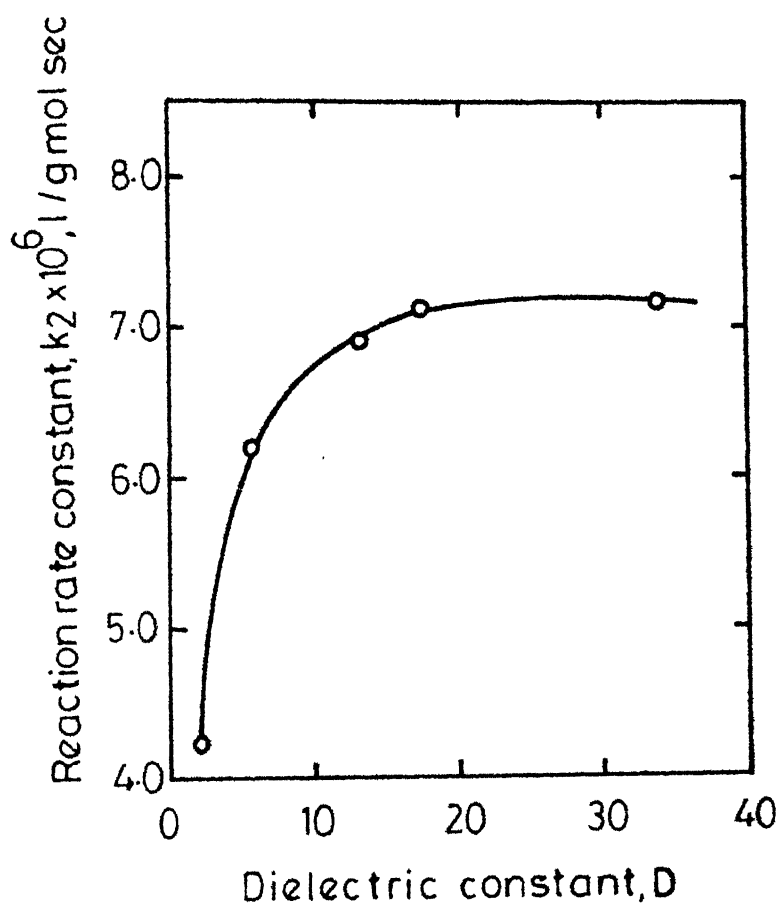


Fig. 25 - Effect of dielectric constant of the solvent on reaction rate constant at 30°C.

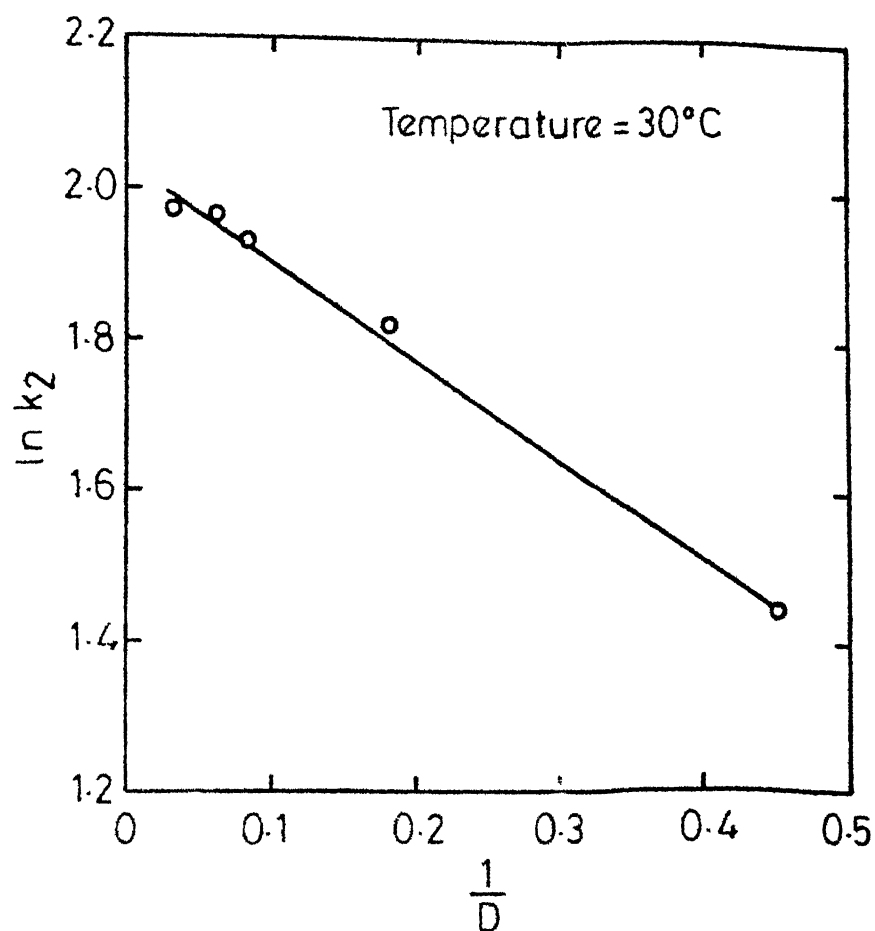
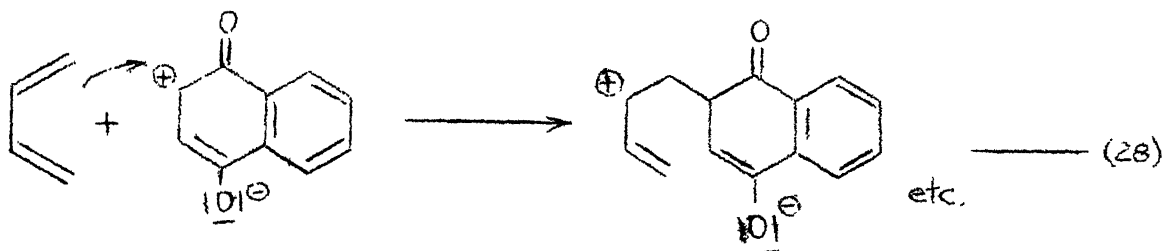


Fig. 26 -Plot of reciprocal of dielectric constant vs.  
log of reaction rate constant.

polar than the reactants when the reaction is carried out in polar solvents.<sup>48</sup>

Table 31 gives the value of activation parameters for different solvents. The activation energy is found to be of the same order for all solvents. It is noted that the value of the frequency factor 'A' increases with an increase in the value of dielectric constant 'D' in a similar manner as the rate of reaction. The overall reaction appears to occur through a transition state. 1,4-Naptho-quinone has a dipole moment of 1.33 D in benzene.<sup>49</sup> This should be sufficient to cause an induced dipole on the incoming butadiene molecule to produce a transition state as shown below:



A solvent of higher dielectric constant enhances the reaction rate because it would stabilise the transition state involving separation of induced charges. The activation parameters for different solvents are of the same order of magnitude. This would disfavour the presence of any other specific solvent effects. Thus, the overall reaction mechanism may be as shown in Figure 27.



TABLE 31

ACTIVATION PARAMETERS IN DIFFERENT SOLVENTS FOR THE  
REACTION BETWEEN BUTADIENE AND NAPHTHOQUINONE

Solvent	Dielectric constant, $\epsilon$ , at 30°C	Reaction Rate constant, $k_2 \times 10^6$ l/gmol sec at 30°C	Frequency factor, $A \times 10^{-10}$ l/gmol sec	Activation Energy, E kcal/gmol	$\Delta S$ kcal/gmol °K
Benzene	2.20	4.20	3.23	22.2	-15.10
Dioxane	2.10	4.10	3.52	22.2	-14.90
Chloro- benzene	5.50	6.20	3.94	21.6	-14.70
n-butanol	17.30	7.14	5.38	21.8	-13.90
Nitro- benzene	33.80	7.18	5.51	22.2	-14.00

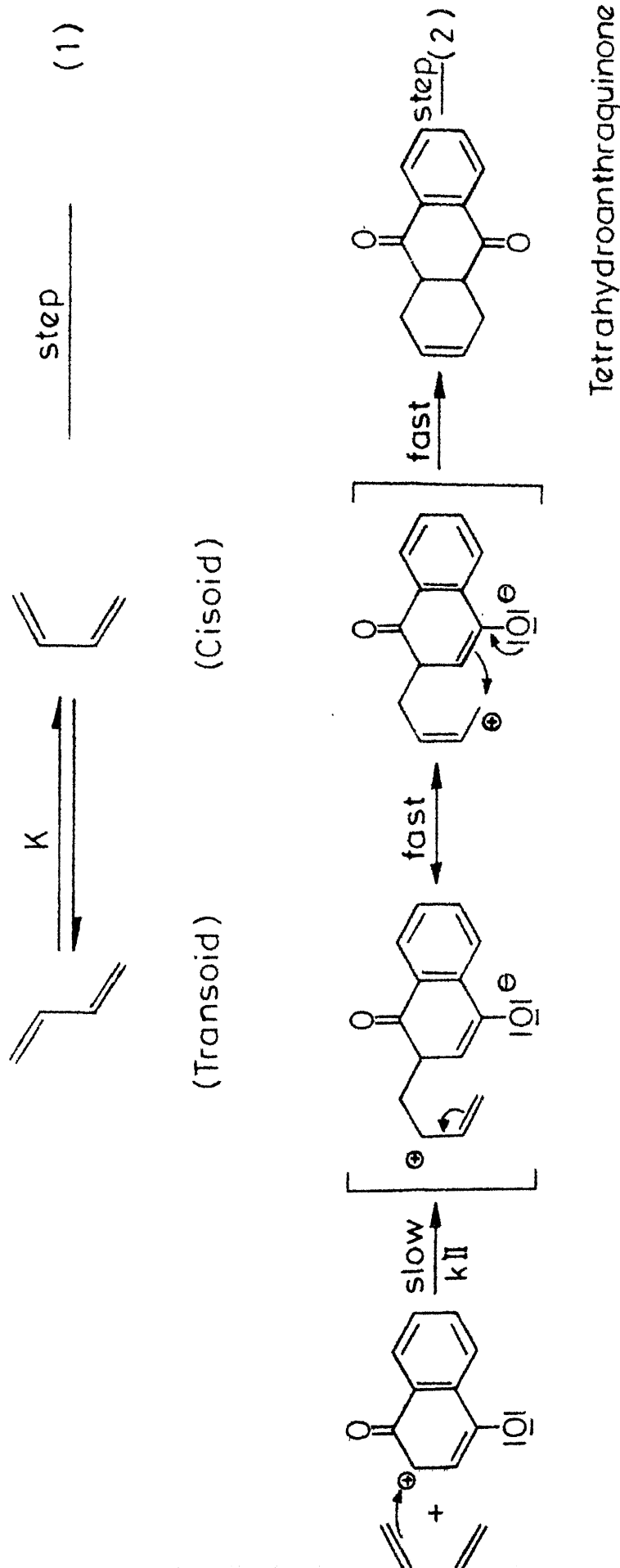


Fig. 27 -Proposed mechanism for the reaction between 1,3-butadiene & 1,4-naphthoquinone in organic solvents.

According to the proposed mechanism of the reaction between butadiene and naphthoquinone the rate expression may be represented as:

$$\text{Rate} = K k_{\text{II}} [\text{Butadiene}][\text{Naphthoquinone}] \quad (29)$$

This rate expression is consistent with the overall rate expression (26) used for correlating the kinetic data. Perhaps the second step of the reaction mechanism shown in Figure 27 may be best described as a two-stage single-step process. That is, the transformations following the attack of butadiene on the dinophile (1,4-naphthoquinone) are quite fast to be considered as a single step process.

The rate data obtained in the present study could be utilized for rational design of reactors.

### SECTION III

DETERMINATION OF EFFECTIVE INTERFACIAL AREA AND MASS  
TRANSFER COEFFICIENTS IN GAS-LIQUID CONTACTORS

## CHAPTER 8

### INTRODUCTION AND LITERATURE REVIEW

The liquid-side mass transfer coefficient and effective interfacial area are two important parameters for designing gas-liquid contactors. Physical methods and chemical methods have been used for determining the effective interfacial area. Among physical methods the following are important:

1. Optical transmittance method<sup>50-52</sup>
2.  $\gamma$ -ray transmittance<sup>53</sup>
3. Photographic technique<sup>54-55</sup>
4. Sedimentation<sup>56</sup>

Danckwerts and Sharma<sup>57</sup> have examined these methods and have shown that the physical methods suffer from considerable disadvantages due to one or more of the following reasons:

1. For a proper study probes have to be inserted into the liquid to a substantial depth which would disturb the system and affect the true area.
2. Photographs taken at the walls of the column give a picture of bubbles which may not be truly representative of the bubbles in the bulk of liquid.
3. Existence of small micron-sized ionic bubbles may not be brought out by these methods. It is very likely that the area measurements

obtained in this way are not necessarily the areas which are effective for mass transfer.

4. When more than two phases are present in the system it probably becomes impossible to find the effective interfacial area by these techniques.

Chemical methods can be advantageously used for the determination of effective interffacial area as well as the liquid side mass transfer coefficients. For example the data on absorption accompanied by pseudo-nth order reaction can be conveniently used for the determination of effective interfacial area  $a$ , in gas liquid contactors. The theory of absorption accompanied by a relatively slow reaction may be used for the determination of liquid side mass transfer coefficients.

#### LITERATURE REVIEW:

A variety of systems obeying different kinetics have been used by various authors for determining the values of effective interfacial area and physical mass transfer coefficients in gas-liquid contactors. Cottmers and Rasc<sup>58</sup> studied the characteristics of single and multiple hole orifice plates as gas-liquid contactors with respect to

plate design, plate spacing and gas liquid flow rates. The reactive system used was catalytic oxidation of aqueous sodium sulfite solution using air. Yoshida and Akita<sup>59</sup> used the same system for determining the volumetric mass transfer coefficient,  $k_L a$ , in bubble columns of various sizes. Braulick, Fair and Lerner<sup>60</sup> carried out a detailed study of bubble contacting columns of 3, 4 and 6 in diameter. Cooper, Fernstrom and Miller<sup>61</sup> presented the above system as a tool for studying the design variables pertinent to agitated gas liquid contactors. Jhaveri and Sharma<sup>62</sup> used the theory of absorption accompanied by a pseudo-nth order reaction to determine the values of effective interfacial area in laboratory packed columns. Oxygen was absorbed in aqueous solution of cuprous chloride and sodium dithionite. Gehlawat<sup>30</sup> used the kinetics of absorption of isobutylene in the aqueous solutions of sulfuric acid for the determination of effective interfacial area in a laboratory packed column and bubble column. Bhargava and Sharma<sup>63</sup> used the **reactive system** of hydrochloric acid gas with terpenes ( $\alpha$ -pinene, myrcene, camphene,  $\Delta^3$ -carene) and isoamylene using chlorobenzene as solvent for determining effective interfacial area and liquid side mass transfer coefficient of mechanically agitated contactor and packed columns. Mashelkar and Sharma<sup>64,65</sup> studied the mass transfer characteristics of bubble columns



operated in semi-batch, continuous, cocurrent and counter-current modes of absorption with chemical reaction. Juvekar and Sharma<sup>66</sup> used the system of oxidation of alkaline solution of sodium dithionate to determine the values of physical mass transfer coefficient and effective interfacial area in the bubble column and mechanically agitated contactors.

Practically no information is available in the literature for the liquid side mass transfer coefficient,  $k_{La}$ , for molten systems. Gehlawat<sup>4</sup> studied the kinetics of absorption of butadiene in molten maleic anhydride. The reaction was found to be relatively slow. It could be conveniently used for the determination of the values of  $k_{La}$  for laboratory bubble columns which can be used as a design parameter for industrial absorbers. The absorption of butadiene into molten maleic anhydride may be carried out to produce tetrahydrophthalic anhydride which is an industrially important product.

The kinetics of absorption of oxygen in aqueous solutions of ammonium sulfite discussed in Section I can be conveniently used for the determination of true mass transfer coefficients in gas-liquid contactors. It is a new system that can be used for this purpose.

CHAPTER 9

EXPERIMENTAL

Packed columns and bubble columns are amongst the most important industrial contactors for gas-liquid systems. They are very simple in construction and can be conveniently used for a large number of industrial applications. The determination of the physical mass transfer coefficients and effective interfacial area was therefore carried out using laboratory sized packed columns and bubble columns.

#### Packed Columns:

Pure oxygen was absorbed in aqueous solutions of ammonium sulfite in a 5 cm i.d. glass packed column randomly packed with 9.5 mm glass Raschig rings. The main features of the column were akin to those used for Jhaveri and Sharma.<sup>62</sup> The rate of absorption was measured by the volumetric method adopted by Jhaveri and Sharma.<sup>62</sup> Pure oxygen was collected in a balloon which was essentially at atmospheric pressure and the rate of absorption of oxygen was measured by using a soap film meter. The liquid flow rate was varied from 2.16 to 7.5 cm<sup>3</sup>/sec. The column was purged with pure oxygen (purity 99.0 per cent) after every run. Figure 28 shows the schematic flow diagram of the apparatus.

#### Bubble Columns:

The absorption of oxygen in aqueous solutions of ammonium sulfite was carried out in bubble columns of

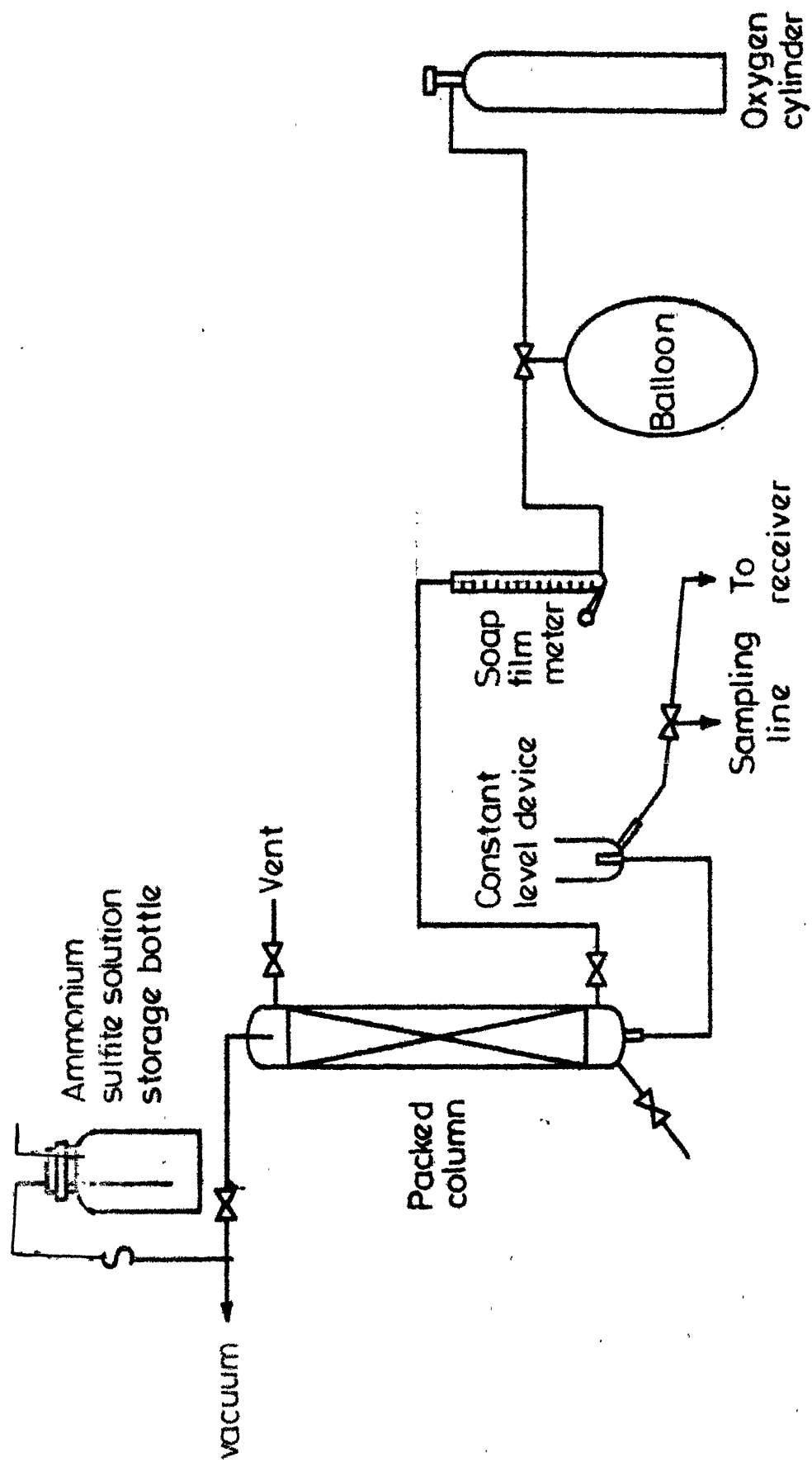


Fig. 228 - Experimental set-up for packed column.

2.2 cm and 5 cm i.d. in a batch as well as in a continuous counter current manner. For batch operations, aqueous solutions of ammonium sulfite in concentration range of 0.4 to 0.45 gmol./l were taken in the bubble column. The concentration of the cobaltous sulphate catalyst was maintained at  $4.70 \times 10^{-3}$  gmol/l. The ratio of height of dispersion to column diameter was kept at about 8.0. Pure oxygen was introduced from the bottom through an inlet tube of 4 mm diameter provided with a non-return valve. The run was carried out for a known time. The rate of reaction,  $R_a$ , gmol/sec.  $\text{cm}^3$  was calculated from the drop in the concentration of ammonium sulfite during this period.

Continuous runs were conducted in the 5 c.m. i.d. bubble column. The concentration of ammonium sulfite in the aqueous solutions was maintained between 0.370 to 0.440 gmol/l. Air was introduced through a bottom inlet tube of 4 mm dia. The inlet and outlet liquid streams were analysed for its ammonium sulfite content. The experiments were conducted at different liquid flow rates for a given gas flow rate. The ratio of height of dispersion to column diameter was kept constant at 10.0 using a constant level device.

#### Jacketted Bubble Columns:

The absorption of butadiene gas in molten maleic anhydride was carried out in jacketted glass bubble columns

of sizes 3.5 cm and 4.6 cm diameter and 65 cm in height. In a typical run a known amount of maleic anhydride was taken in the bubble column. The entire column assembly was weighed. The bubble column was connected to the butadiene gas supply from a cylinder. The purity of the gas was 99.5 per cent. Hot aqueous solution of glycerine was circulated through the column jacket to bring the temperature of molten maleic anhydride to the desired value of  $102 - 105^{\circ}\text{C}$ . Pure butadiene gas was then introduced at the bottom through an inlet tube of 4 mm dia at a known flow rate for a given time. The ratio of dispersion height to column diameter was maintained at about 8.0. The increase in weight of the contents for a known period of time was taken as a measure of the rate of absorption. The reaction time was short (2-10 min) so that the concentration of the reactant (maleic anhydride) decreased marginally from an initial value of 10 gmol/l to about 8 gmol/l in the extreme case.

Some runs were carried out in a 7.5 cm i.d. and 120 cm tall jacketted stainless steel bubble column using an industrial  $\text{C}_4$ -stream from a synthetic rubber plant containing about 35 per cent butadiene. About 2 kg of maleic anhydride was charged into the reactor per batch. It was heated to about  $80^{\circ}\text{C}$  by steam in the jacket and the butadiene stream was introduced at the bottom through an inlet tube of 6 mm dia.

The progress of the reaction was followed by analysing the inlet and outlet gas streams for butadiene content using gas liquid chromatography. A 6 mm dia 8 metre long column packed with dimethyl sulfolane on 60 mesh size chromosorb-W was used with hydrogen as the carrier gas. Figure 29 shows a typical chromatogram of the C<sub>4</sub>-fraction from the butadiene plant.

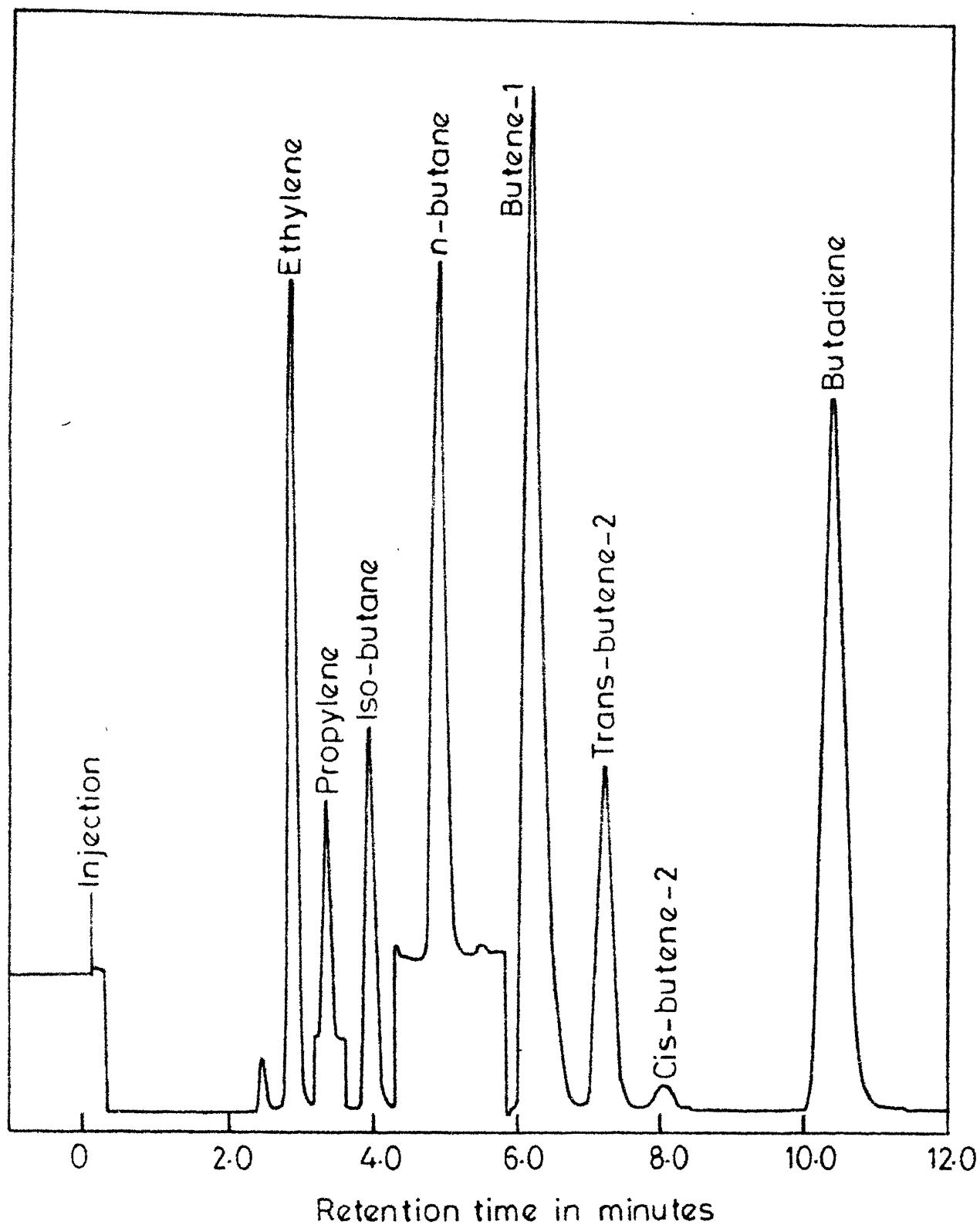


Fig. 29 - A typical chromatogram for the analysis of a butadiene stream.



CHAPTER 10

RESULTS AND DISCUSSION

Absorption of Oxygen in Aqueous Solutions of Ammonium Sulfite in Packed Columns:

As discussed in Section I the system of absorption of oxygen in aqueous solutions of ammonium sulfite conforms to pseudo-nth order mechanism with the values of  $m=1$  and  $n=2$ . The rate of absorption is given by the following equation

$$\underline{R_a} = \underline{a} [\underline{A}] \sqrt{\underline{D_A} k_3 [\underline{B}]^2} \quad (18)$$

where  $\underline{R_a}$  = Rate of absorption in packed column,  $\text{gmol/cm}^3\text{sec}$ .

$[\underline{A}]$  = Solubility of oxygen in aqueous solutions of ammonium sulfite,  $\text{gmol/l}$ .

It is noted that stirred cell may be considered as a model for packed columns<sup>26</sup>. Thus, the values of  $k_L$  obtained experimentally in stirred cells as reported in Table 15 of Section I may be considered to be of the same order of magnitude as obtainable for packed columns in actual practice.

For a typical run for the absorption of pure oxygen in aqueous solutions of ammonium sulfite in a packed column, the following values are applicable

$$\begin{aligned} k_L &= 3 \times 10^{-3} \text{ cm/sec, (from Table 15 of Section I)} \\ [\underline{B}] &= 4 \times 10^{-4} \text{ gmol/cm}^3 \end{aligned}$$

$$[A] = 9.4 \times 10^{-7} \text{ gmol/cm}^3 \text{ (From Table 13 of Section I)}$$

wherefrom

$$\sqrt{\frac{D_A k_3 [B]^2}{k_L}} = 105$$

$$\frac{[B]}{2[A]} = 213$$

Thus, the conditions given by expressions (7) and (8) of Section I are satisfied. Equation (18) can therefore be used to determine the values of effective interfacial area in packed columns.

The values of effective interfacial area obtained for a packed column at different liquid flow rates are given in Table 32 and are also plotted in Figure 30. The data obtained in the present work have been compared with the data reported by Jhaveri and Sharma<sup>62</sup> (last column of Table 32 and 0 data points in Figure 30). It is observed that the values of effective interfacial area obtained by using this system agree reasonably well with those obtained with other reactive systems.

#### Effective Interfacial Area in Bubble Columns:

For a typical run for the absorption of pure oxygen in aqueous solutions of ammonium sulfite in a bubble column, the following data are representative ,

TABLE 32

## EFFECTIVE INTERFACIAL AREA IN PACKED COLUMNS

System: Ammonium sulfite-oxygen ; Temperature = 30°C

Cobaltous sulfate catalyst concentration =  $4.70 \times 10^{-5}$  gmol/l

Inside diameter of column = 5 cm

Packing height = 81 cm

Packing material = 9.5 mm glass Raschig rings

Run No.	Linear velocity cm/sec	Rate of absorption $R_a \times 10^7$ gmol/cm <sup>2</sup> sec.	Average concentration of ammonium sulfite, gmol/l	Specific Rate of absorption, $R \times 10^7$ gmol/cm <sup>2</sup> sec		Effective Interfacial Area	
				from Fig. 13		Present Work Published data <sup>62</sup>	
1	0.110	3.36	0.456	3.30	1.02	1.05	
2	0.160	4.30	0.453	3.25	1.32	1.25	
3	0.256	4.88	0.440	3.20	1.51	1.45	
4	0.384	5.57	0.436	3.20	1.73	1.68	

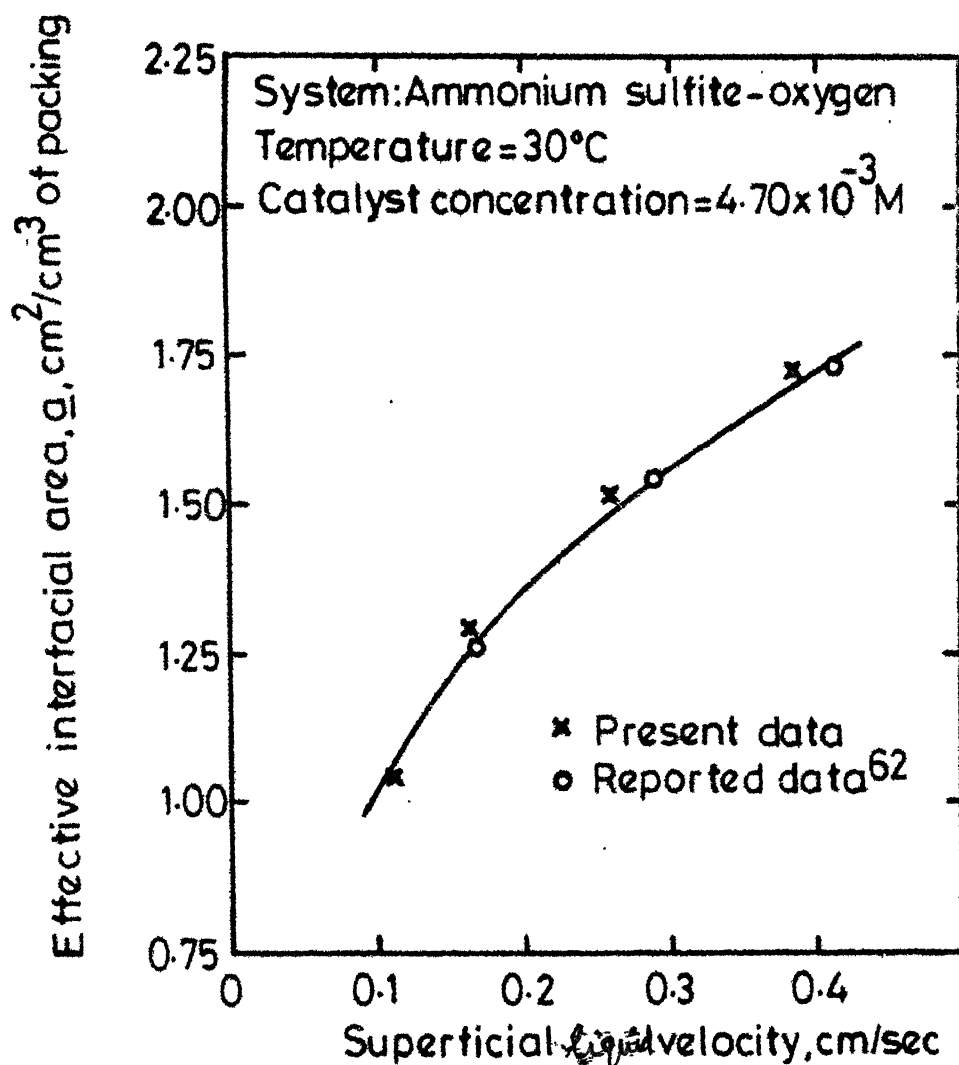


Fig. 30 - Effect of superficial liquid velocity on effective interfacial area,  $a_g$ , in a packed column.

$$\begin{aligned}
 k_L &= 3 \times 10^{-2} \text{ cm/sec.} \\
 [B] &= 4 \times 10^{-4} \text{ gmol/cm}^3 \\
 [A] &= 9.4 \times 10^{-7} \text{ gmol/cm}^3,
 \end{aligned}$$

Then

$$\sqrt{\frac{D_A k_3 [B]^2}{k_L}} = 10.5; \quad \frac{[B]}{Z[A]} = 213$$

Once again the conditions given by expressions (7) and (8) were satisfied. Therefore the equation (18) can be used to determine the effective interfacial area in bubble columns.

Tables 33 and 34 give the values of effective interfacial area in bubble columns of 2.2 cm and 5 cm diameter respectively.

For the continuous runs in bubble columns, oxygen from air was absorbed into aqueous solutions of ammonium sulfite. In this case the value of  $[A] = 2 \times 10^{-7} \text{ gmol/cm}^3$  and  $\frac{[B]}{Z[A]} = 1000$  so that the conditions given by expressions (7) and (8) are satisfied and equation (18) can be used as above.

Table 35 gives the values of effective interfacial area of 5 cm bubble column for the continuous countercurrent operation.

Figure 31 shows the effective interfacial area obtained for bubble column in the present work along with the data reported by Juvekar and Sharma.<sup>66</sup> A close agreement is noted.

TABLE 33

## EFFECTIVE INTERFACIAL AREA IN BUBBLE COLUMNS (BATCH OPERATION)

System = Ammonium sulfite+Oxygen; Temperature = 30°C

Cobaltous sulfate catalyst concentration =  $4.70 \times 10^{-3}$  gmol/l

Inside diameter of column = 2.2 cm

Time of Reaction = 5 minutes

Run No.	Linear velocity cm/sec.	Expanded volume cm <sup>3</sup>	Initial concentration of ammonium sulfite, gmol/l	Final concentration of ammonium sulfite gmol/l	Rate of absorption, $R_a \times 10^7$ gmol/cm <sup>3</sup> sec.	Specific rate of absorption, $R_a \times 10^7$ gmol/cm <sup>3</sup> sec from Fig.13	Effective Interfacial area, cm <sup>2</sup> /cm <sup>3</sup> dispersion
1	4.60	68.0	0.425	0.370	1.62	2.70	0.620
2	9.20	67.5	0.425	0.350	1.90	2.50	0.760
3	12.30	71.5	0.425	0.326	2.36	2.35	1.000

TABLE 34

## EFFECTIVE INTERFACIAL AREA IN BUBBLE COLUMNS (BATCH OPERATION)

System: Ammonium sulfite-oxygen

Temperature = 30°C

Inside diameter of column = 5 cm

Cobaltous sulfate catalyst concentration =  $4.70 \times 10^{-3}$  gmol/l

Time of reaction = 5 min

Run No.	Linear velocity cm/sec	Expanded volume, cm <sup>3</sup>	Initial concentration of ammonium sulfite, gmol/l	Final concentration of sulfite absorption, gmol/l	Rate of absorption, $R_a \times 10^7$ , gmol/cm <sup>3</sup> sec.	Specific rate of absorption, $R \times 10^7$ , gmol/cm <sup>2</sup> sec from Fig. 13	Effective interfacial area, a, cm <sup>2</sup> /cm <sup>3</sup> of dispersion
1	5.0	810	0.425	0.365	1.72	2.65	0.650
2	10.0	790	0.425	0.340	2.18	2.40	0.910
3	20.4	825	0.425	0.300	3.03	2.15	1.400
4	25.4	800	0.425	0.281	3.05	2.00	1.520
5	30.6	830	0.425	0.265	3.25	1.90	1.710



TABLE 35

## EFFECTIVE INTERFACIAL AREA IN BUBBLE COLUMNS (COUNTERCURRENT OPERATION)

Inside diameter of the column = 5 cm

Temperature= 30°C

Expanded volume = 1000 cm<sup>3</sup>

Cobaltous sulfate catalyst concentration =  $4.7 \times 10^{-3}$  gmol/l

Height of dispersion/I.D. of column(L/D) = 10.2

[illegible]

Table 35 (contd)

1	2	3	4	5	6	7	8	9
4	31.0	100 155 210	0.450 0.450 0.450	0.390 0.408 0.418	10.1 10.8 11.2	5.85 6.20 6.30	1.72 1.75 1.78	1.75
5	41.2	105 155 215	0.450 0.450 0.450	0.375 0.394 0.410	13.0 13.50 14.10	5.78 5.90 6.20	2.24 2.25 2.27	2.25

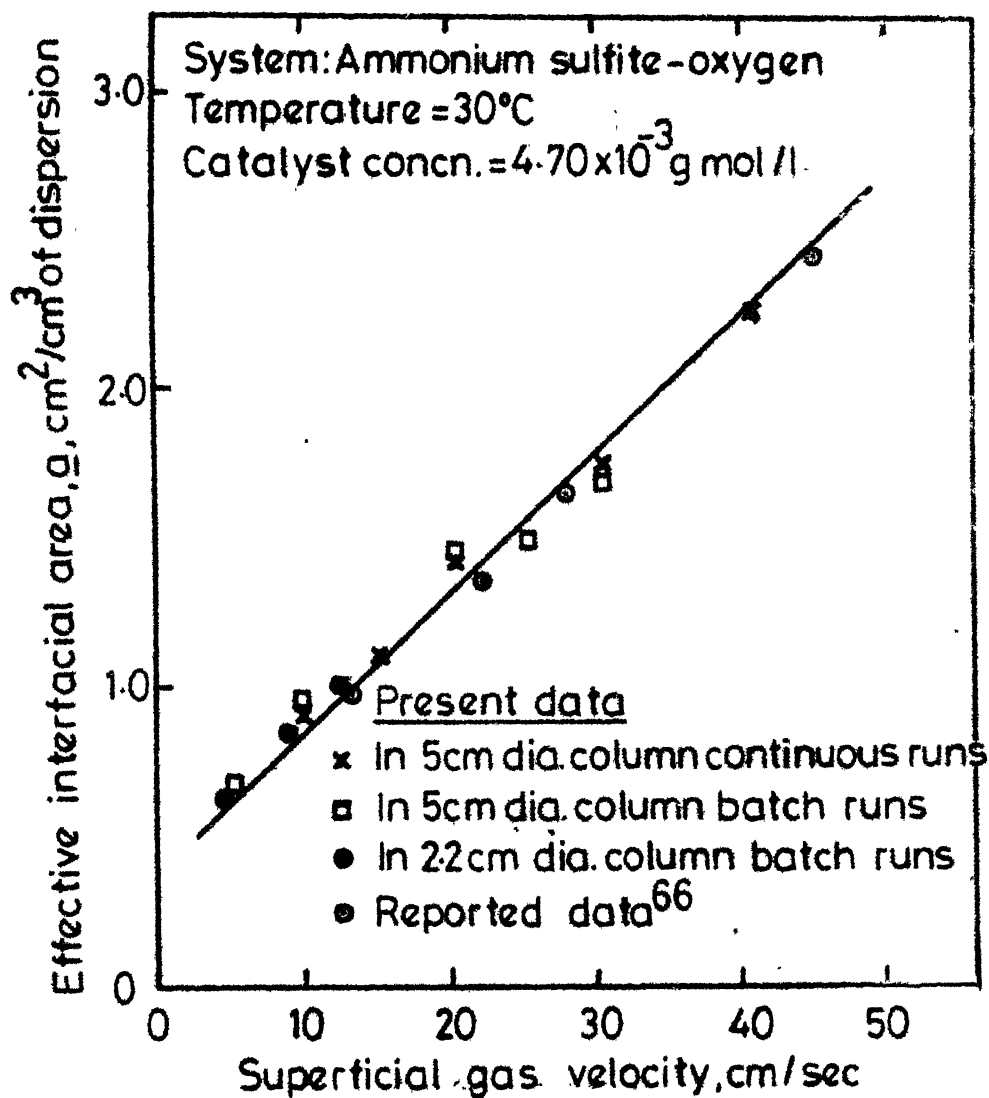
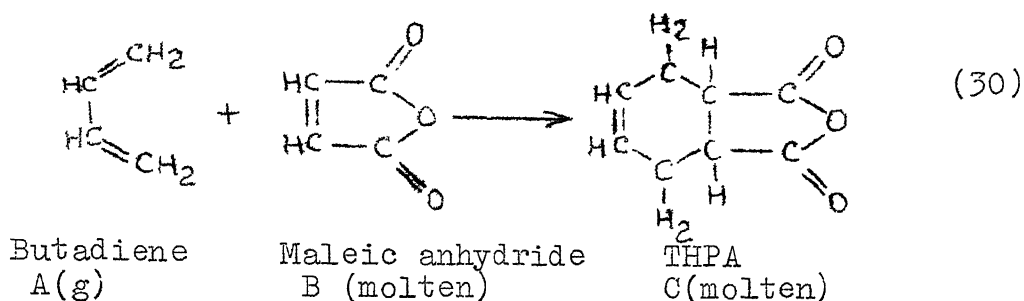


Fig. 31 - Effect of superficial gas velocity on effective interfacial area in a bubble column.

PHYSICAL MASS TRANSFER COEFFICIENTS IN MOLTEN SYSTEMS:

The heterogeneous reaction between gaseous butadiene and molten maleic anhydride to give tetrahydrophthalic anhydride (THPA) may be represented as follows:



The kinetics of this industrially important reaction has been reported by Gehlawat<sup>4</sup>. The reaction is first order in butadiene as well as first order in maleic anhydride. The reaction is relatively slow and in a bubble column the rate of absorption of butadiene in molten maleic anhydride is likely to be given by the equation (4) of Section I.

$$R_a = k_{La} [A] \quad (4)$$

For this system the condition to be satisfied are given by the expression (5) of Section I

$$k_2 [B] > k_{La} \quad (31)$$

It may be noted that the rate of absorption,  $R_a$ , in equation (4) is an experimental observation and hence known.

The values of  $[A]$  are also known.<sup>4</sup> Hence the values of physical mass transfer coefficient,  $k_L a$  can be determined by the use of equation (4).

A typical value of  $k_2[B]$  for the reaction between butadiene and maleic anhydride (where  $k_2 = 10 \text{ cm}^3/\text{gmol sec}$  and  $[B] = 10^{-2} \text{ gmol/cm}^3$ ) works out to be 0.1. The values of physical mass transfer coefficients,  $k_L a$  determined using expression (4) are given in Table 36. They are in the range between  $1.5 \times 10^{-2}$  to  $6 \times 10^{-2} \text{ sec}^{-1}$ . Therefore, the condition given by expression (31), that is,  $k_2[B] > k_L a$  was satisfied.

From the data given in Table 36 it may be noted that the values of  $k_L a$  for different sizes of the bubble column at the same superficial velocity are of comparable order of magnitude. However, the values of  $k_L a$  were appreciably higher in the presence of packings in the bubble column as may be noted from run numbers 3, 9 and 12 of Table 36. Mashelkar and Sharma<sup>64-65</sup> also observed that the presence of packings in bubble columns contributed to an increase in the effective interfacial area.

The typical values of  $k_L a$  reported for aqueous systems are given in Table 37. A comparison of the values given in Tables 36 and 37 would show that the  $k_L a$  values for a molten system as obtained in the present work agree reasonably well with the reported data for aqueous systems. The data are likely to be useful as a design parameter for industrial absorbers.

TABLE 36

EFFECT OF SUPERFICIAL GAS VELOCITY ON PHYSICAL MASS  
TRANSFER COEFFICIENT IN JACKETED BUBBLE COLUMNS

System: Butadiene - maleic anhydride *at 102°C*

No.	Inside dia- meter of column, cm	Superficial gas velocity cm/sec	Physical mass transfer co- efficient $k_{La} \times 10^2 \text{ sec}^{-1}$	Remarks
1	3.5	4.1	1.9	
2	3.5	8.2	3.8	
3	3.5	11.7	5.1	
4	3.5	15.2	5.7	
-----				
5	4.6	4.90	2.2	
6	4.6	10.30	4.6	
7	4.6	15.50	5.9	
-----				
8	4.6	10.30	5.9	9.5 mm i.d. glass Raschig rings were used as column packing
9	4.6	19.40	7.8	
-----				
10	7.5	3.50	1.5	Higher gas flow rates could not be used
11	7.5	7.00	2.5	
-----				
12	7.5	4.30	2.7	9.5 mm i.d. glass Raschig rings were used as column packing

TABLE 37

TYPICAL VALUES OF MASS TRANSFER COEFFICIENT FOR **BUBBLE COLUMN**  
FOR AQUEOUS SYSTEM FROM LITERATURE<sup>6</sup>

Superficial Gas Velocity cm/sec	$k_L a \times 10^2 \text{ sec}^{-1}$
2	1.5
5	2.5
7	4.0
10	5.0
15	6.0
20	6.9

CHAPTER 11

CONCLUSIONS



The theory of absorption accompanied by chemical reaction has been used to study the kinetics of the heterogeneous reaction between oxygen and aqueous solutions of ammonium sulfite. The absorption of oxygen in aqueous solutions of ammonium sulfite in the concentration range of 0.045 to 0.45 gmol/l in the presence of cobaltous sulfate as a soluble catalyst was found to conform to the fast pseudo-nth order mechanism. The overall reaction was found to be third order. It was first order with respect to oxygen and second order with respect to ammonium sulfite. The third order reaction rate constant at 30°C was found to be  $2.70 \times 10^4 (\text{l/gmol})^2 \text{ sec}^{-1}$  and the apparent energy of activation was found to be 14.5 kcal/gmol.

The solubility of butadiene in different organic solvents was found to be sufficiently large to enable the kinetics of the reaction between dissolved butadiene and naphthoquinone to be studied in the homogeneous phase. The reaction was found to be first order both with respect to butadiene and with respect to naphthoquinone. The value of the second order reaction rate constant at 30°C in benzene solution was  $4.21 \times 10^{-6} \text{ l/gmol sec}$ . The activation energy was found to be 22.2 kcal/gmol. The nature of the solvent influenced the reaction rate. A correlation of the rate data with the reciprocal of dielectric constant

of the solvent,  $(1/D)$  gave a straight line. The Diels-Alder addition reaction between butadiene and naphthoquinone appears to occur through a transition state. A reaction mechanism has been proposed which is considered to be consistent with the experimental observations.

The kinetics of two new reactive gas-liquid heterogeneous systems has been used to determine the effective interfacial area and physical mass transfer coefficients in laboratory packed columns and bubble columns. The results obtained in this study are found to agree reasonably well with the reported data. It may be important to note that the values of the mass transfer coefficients for the absorption of butadiene in molten maleic anhydride (a molten system) in bubble columns obtained in this work are found to be comparable with the reported data for the aqueous systems under similar hydrodynamic conditions.

The data on the reaction kinetics, effective interfacial area and mass transfer coefficients obtained in this study are likely to be useful for a rational design of industrial reactors. A worked out design problem for the selective absorption of butadiene from a  $C_4$ -fraction in molten maleic anhydride in a bubble column reactor illustrates the usefulness of the data obtained in the present study. The design details are given in the Appendix.

## R E F E R E N C E S

1. GHARDA, K.H., Chem. Process. Engng (Bombay), 1968, 2(1), 101-104.
2. NEELAKANTAN, K. and GEHLAWAT, J.K., Ind. Engng. Chem. Fundamentals (in press).
3. NEELAKANTAN, K., BHATIA, S., and GEHLAWAT, J.K., J.Chem. Technol. and Biotechnol. (communicated).
4. GEHALWAT, J.K., Indian Chemical Engineer, 1972, 14, 1.
5. NEELAKANTAN, K. and GEHLAWAT, J.K., Ind. Engng. Chem. Process Design and Development (communicated).
6. MASHELKAR, R.A., Br. Chem. Engng. 1970, 15, 1297.
7. HORLACHER, W.R., BARNARD, R.E., TEAGUE, R.K. and HAYDON, P.L., Chem.Eng. Prog., 1972, 68, 43.
8. HORI, S., Kuvagaku Kogyosiryo, 1941, 14, 61-74; Chem. Abstract. 1941, 35, 7663<sup>1</sup>.
9. HORI, S., Rept. Govt. Chem. Ind. Res. Inst. Tokyo 1952, 46, 297, Chem. Abstract, 1952, 46, 8335e.
10. THOMAS, S.B., U.S. Patent 2,869,844 (1959), Chem. Abstract 1959, 53, 6599i.
11. BONNIERE, C. and DELZENEE, A., German Patent 2,355,023 (1974), Chem. Abstract, 1974, 81, 68027s.
12. YAGI, S. and INOUE, H., Chem. Engng. Sc. 1962, 17, 411.
13. BARRON, C.H. and O'HERN, H.A., Chem. Engng. Sc., 1966, 21, 397.

14. de WAAL, K.J.A., and O KESON, J.C., Chem. Engng. Sc. 1966, 21, 559.
- ✓ 15. WESSELNIGH, J.A., and HOOG, A.C. Paper presented at Symp. on Gas Liquid Reactions (1969).
16. LINEK, V. Chem.Engng. Sc. 1971, 26, 1381.
17. LINEK,V. and MYRHOEROVA, J.Chem. Engng. Sc. 1970, 25, 787.
18. YASUNISHI, A., KOGAKU KOGAKU RONBUNSHU, 1977, 3, 62, J. Chem. Eng. Japan, 1977, 1, 80.
19. YOUNG, S.L., J. Am.Chem. Soc., 1902, 24, 297.
20. VORLANDER, D. and LAINAU, A., J. Pr. Chem., 1929, 123, 351. Chem.Abstract, 1930, 24, 1310.
21. GRIGORYAN,G.O., Arm. Khim. Zh. 1968, 21, 711, Chem. Abstract, 1969, 70, 100124j.
22. MATSUURA, R., HARADA, J., AKEHATA, T. and SHIRAI, J., J. Chem. Eng. Japan 1969, 2, 199.
23. MISHRA, G.C. and SRIVASTAVA, R.D., Chem. Engng. Sci. 1975, 30, 1387.
24. MISHRA, G.C. and SRIVASTAVA, R.D., J. Appl. Chem. and Biotechnol., 1976, 26, 401.
25. BRIAN, P.L.T., A.I.Ch.E. J., 1964, 10, 5.
26. DANCKWERTS, P.V., 'Gas Liquid Reactions', 1970, McGraw Hill Book Co., New York.
27. ASTARITA,G., 'Mass Transfer with Chemical Reaction', 1967, Elsevier Scientific Publishing Co., Amsterdam.

28. SHARMA, M.M. and DANCKWERTS, P.V., Chem. Engng. Sci. 1964, 19, 99.
29. GEHLAWAT, J.K. and SHARMA, M.M., Chem. Engng. Sci. 1968, 23, 1173.
30. GEHLAWAT, J.K., Ph.D. Thesis, Bombay University (1969).
31. JHAVERI, A.S. and SHARMA, M.M., Chem. Engng. Sc. 1967, 22, 1.
32. VOGEL, A.I., 'A Text Book of Quantitative Inorganic Analysis' 1951, Longmans Green Co. Ltd., London, page 370.
33. YASUNISHI, A., KOGAKU KOGAKU RONBUSHU, 1977, 3, 154., J. Chem. Eng. Japan 1977, 2, 168.
34. MORRISON, T.J. and BILLET, F., J. Chem. Soc., 1952, 3819.
35. VAN KREVELEN, D.W. and HOFFTIZER, P.J., Chem. Ind. 21st Congress, Int. Chem. Ind. (1948).
- ✓ 36. HIMMELBLAU, D.M., Chem. Rev., 1964, 64, 527.
37. WASSER MANN, A., J. Chem. Soc. 1936, 1028-34.
- ✓ 38. EISLER, B., and WASSERMANN, A., J. Chem. Soc. 1953, 979-82.
39. PRIEMER, JOACHUM, SHAIK, HOBERT, LOSACKER, WULF, SWODEAK WOLF GAS, German Patent, 2532, 422 (1977), Chem. Abstract 1977, 86, 171142.
40. MATSUURA, RYO, R., MAGAOKA, K., MAKINO, KOJI, HATA, K., KEISHRO, K. Japanese Patent 7703,048 (1977), Chem. Abstract. 1977, 87, 39177.
41. MATSUURA, RYO, R. MAGAOKA, K. KAZUYA, A., HATA, K., and KEISHRO, K. Japanese Patent, 7703,048 (1977), Chem. Abstract, 1977, 87, 39179.

42. KENDE, A., ANDREW, S., MILLS, J. and JOHNE., U.S.  
Patent 4,021,457 (1977), Chem. Abstract, 1977, 87, 39185.
43. DAVIS, H.S., CRINDAL, G.S. and HIGBI, W.S., Ind. Engng.  
Chem. (Anal. Edn.) 1931, 3, 108.
44. LUCAS, H.J. and EBERZ, W.F., J. Am. Chem. Soc. 1934, 56, 460.
45. KUMAR, S. and GEHLAWAT, J.K., J. Chem. Technol and  
Biotechnol. (in press).
46. ROBERT, C., WEAST (Editor), Handbook of Chemistry and  
Physics, pages E-56-58, 58th Edition, Chemical Rubber  
Publishing Co., Cleveland (1977-78).
47. WONG, K.F. and RECKER, C.A., Trans. Faraday Soc., 1970,  
66(9), 2313.
48. FROST, A.A. and PEARSON, R.G., 'Kinetics and Mechanism  
(Second Edition), 1961, John Wiley and Sons, New York,  
page 132.
49. COX, E.G., CRUICKSHANK, D.W.J. and SMITH, J.A.S.,  
Proc. Roy. Soc. (Lond) 1958, A247, 1.
50. CALDERBRANK, P.H., Trans. Instn. Engrs. 1959, 37, 173.
51. CALDERBRANK, P.H., Trans. Instn. Engrs. 1958, 36, 443.
52. ABDEL-AAL, H.K., STILES, G.B. and HOLLAND, C.D.,  
A.I.Ch.E. Jl., 1966, 12, 74.
53. QUINGLEY, C.J., JOHNSON, A.I. and HARRIS, B.L.,  
Chem. Engng. Progr. Symposium. Ser. 1955, 51, 31.

54. VOYER, R.D., and MILLER, A.I., Canad JI. of Chem. Engng. 1968, 46, 335.
55. TOWELL, G.D., STRAND, C.P. and ACKERMAN, G.H., A.I.Ch.E. JI. [Ch.E. Symposium Ser] 1965, 10, 97.
56. KAFAROV, V.V. and BABNOV, B.M., J. Appl. Chem.(USSR) 1959, 32, 810.
57. SHARMA, M.M. and DANCKWERTS, P.V., Br. Chem.Engng. 1970, 15, 522.
58. OTTMERS, D.M. and RASE, H.F., Ind. Engng. Chem. Fundamentals, 1964, 3, 106.
59. YOSHIDA, F. and AKITA, K., A.I.Ch.E. JI. 1965, 11, 9.
60. BRAULICK, W.J., FAIR, J.R. and LERNER, B.J., A.I.Ch.E.JI. 1965, 11, 73.
61. COOPER, C.M. FRENSTROM, J.A. and MILLER, S.A., Ind. Engng. Chem., 1944, 36, 504.
62. JHAVERI, A.S. and SHARMA, M.M. Chem. Engng. Sc. 1968, 23, 667.
63. BHARAGAVA, R.K. and SHARMA, M.M. Chem.Engng. Sc. 1978, 33, 525.
64. MASHELKAR, R.A. and SHARMA, M.M., Trans. Instn. Engrs. 1970, 48, T162.
65. MASHELKAR, R.A. and SHARMA, M.M., 'Paper presented at Tripartite Chemical Engineering Conference, Symposium on Mass Transfer with Chemical Reaction, Montreal (1968).
66. JUVEKAR, V.A. and SHARMA, M.M., Chem. Engng.Sc.,1973, 28, 776.



APPENDIX

APPLICATION TO DESIGN

Bubble columns as industrial reactors for gas-liquid reactions have certain basic advantages. These are the absence of moving parts and thus eliminating the need of seals, low maintenance cost and smaller floor space. Also they have large heat transfer area per unit volume of the reactor resulting in higher transfer rates. Low equipment cost, ability to handle solids and high values of effective interfacial area and overall mass transfer coefficients are certain other advantages of the bubble columns. Mashelkar<sup>6</sup> discussed the relevant features of the bubble column reactors.

For relatively small capacities, the recovery of butadiene from a  $C_4$ -fraction may be economically carried out by its selective reaction with maleic anhydride to produce tetrahydrophthalic anhydride which is an industrially important chemical. For lean mixtures of butadiene a bubble column reactor may be the best choice since the gas phase would follow plug flow behaviour and the effective concentration of butadiene may be taken as the logarithmic mean of its partial pressure in the inlet and exit streams. On the other hand, an agitated gas-liquid contactor would be the worst choice since in this case the gas phase will also be completely backmixed and the effective concentration of the solution will correspond to its partial pressure in the exit stream.

### THE PROBLEM:

It is proposed to design a bubble column reactor for the recovery of 1500 tonnes of butadiene per year from an industrial stream by its selective reaction with maleic anhydride. The gaseous stream obtained as a by-product from an industrial unit contains about 35 mole per cent of butadiene. The butadiene content in the outlet stream is to be reduced to 1 mole per cent. The column will operate isothermally at  $105^{\circ}\text{C}$  which is slightly above the melting point of the reaction product.

### Development of the Design Equation:

It will be seen later that the rate of absorption of butadiene in molten maleic anhydride upto a certain concentration of maleic anhydride (4.60 gmol/l) is given by

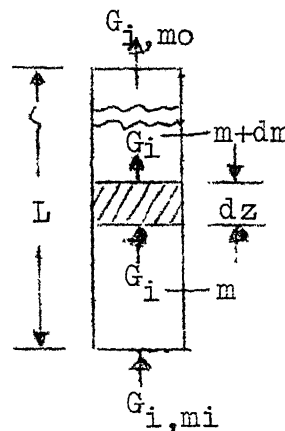
$$R_a = k_L a [A] \quad (4)$$

For a differential height,  $dz$ , of the column the following expression may be written

$$-G_i \frac{dm}{dz} = A k_L a PH\left(\frac{m}{m+1}\right) \quad (32)$$

where  $m$  = mole ratio of the butadiene to inert gas

$A$  = cross-sectional area of the column,  $\text{cm}^2$



$G_i$  = molal flow rate of inerts, gmol/sec

$H$  = Henry's constant, gmol/cm<sup>3</sup> atm

$p$  = pressure, atm

$z$  = distance from the top of the column, cm

This equation may be modified by considering the following:

1. It is assumed that the liquid is completely backmixed.
2. The pressure at any point in the column varies due to the hydrostatic head in the column above that point.

At a point which is at a height  $z$  from the top of the column the pressure will be given by

$$P = P_t + \frac{z \rho_{\text{disp}}}{13.6 \times 76} \quad (33)$$

where  $P_t$  = pressure at the top of the column, atm.

$\rho_{\text{disp}}$  = dispersion density, gm/cm<sup>3</sup>

Assuming that the gas leaves the column at essentially atmospheric pressure the following expression holds.

$$-G_i \frac{dm}{dz} = A k_{La} \left( 1 + \frac{z \rho_{\text{disp}}}{13.6 \times 76} \right) H \left( \frac{m}{m+1} \right) \quad (34)$$

The above expression is integrated to obtain

$$\int_{m_0}^{m_i} \frac{m+1}{m} dm = \frac{A k_L a H}{G_i} \int_0^L \left(1 + \frac{z P_{\text{disp}}}{13.6 \times 76}\right) dz \quad (35)$$

where  $L$  = dispersed height in the column, cm

$m_0$  = mole ratio of butadiene to inert gas in exit stream

$m_i$  = mole ratio of butadiene to inert gas in inlet stream

The integrated expression reduces to

$$m_i - m_0 + \ln \frac{m_i}{m_0} = \frac{A k_L a H}{G_i} \left( L + \frac{L^2 P_{\text{disp}}}{2 \times 13.6 \times 76} \right) \quad (36)$$

Equation (36) would enable the column diameter and height to be calculated.

#### DESIGN PROCEDURE:

Step (1): Assume an average pressure in the column (1.4 atm., in this case based on first trial)

$$\text{Average pressure} = \frac{\text{Pressure at the top} + \text{Pressure at the bottom}}{2}$$

Step (2): Calculate the capacity of the column.

1500 tonnes of butadiene/year of 325 working days

$$= \frac{1500 \times 1000 \times 1000}{325 \times 24 \times 54 \times 3600}$$

1 gmol/sec.

The butadiene content is to be reduced from 35 per cent to 1 per cent, that is,

$$y_i = 0.35, \quad y_o = 0.01$$

The gas phase may be assumed to follow plug flow behaviour which gives an effective butadiene concentration

$$y_{\text{avg}} = \frac{y_i - y_o}{\ln y_i / y_o} = \frac{0.35 - 0.01}{\ln \frac{0.35}{0.01}}$$

$$= 0.096$$

$$\begin{aligned} \text{The gas flow rate through the column} &= \frac{1}{0.096} \\ &= 2.85 \text{ gmol/sec} \\ &= 63100 \text{ cm}^3/\text{sec at } 105^\circ\text{C and } 1.4 \text{ atm.} \end{aligned}$$

In practice a linear gas velocity of 10 cm/sec may be used. Corresponding to this gas velocity the  $k_L a$  value is obtained from Table 36.

$$k_L a = 4.6 \times 10^{-2} \text{ sec}^{-1}$$

$$\begin{aligned} \text{Cross sectional area of the column} &= \frac{\text{Total volumetric flow rate}}{\text{Linear gas velocity}} \\ &= \frac{63100}{10} = 6310 \text{ cm}^2 \end{aligned}$$

wherefrom column diameter = 89.6 cm

A 90 cm diameter column is selected. This gives an area of cross section  $A = 6362 \text{ cm}^2$ .

Step (3): Calculate the height of dispersion, L.

The solubility of pure butadiene in molten maleic anhydride<sup>4</sup>,  $[A]$  at  $105^{\circ}\text{C} = 1.75 \times 10^{-4} \text{ gmol/cm}^3 \text{ atm}$ .

The effective butadiene concentration under column terminal conditions, H, works out as

$$\begin{aligned} H &= 1.40 \times 0.096 \times 1.75 \times 10^{-4} \\ &= 2.34 \times 10^{-5} \text{ gmol/cm}^3 \text{ atm.} \end{aligned}$$

Other conditions and pertinent data are

$$\begin{aligned} y_i &= 0.35 & m_i &= 0.54 \\ y_o &= 0.01 & m_o &= 0.01 \\ y_{\text{avg}} &= 0.096 & k_{La} &= 4.6 \times 10^{-2} \text{ sec}^{-1} \\ & & \rho_{\text{disp}} &= 0.85 \text{ gm/cm}^3 \text{ (assumed)} \end{aligned}$$

Substituting the various values in equation (36).

$$\begin{aligned} 0.54 - 0.01 + \ln \frac{0.54}{0.01} &= \frac{6362 \times 4.6 \times 10^{-2} \times 2.34 \times 10^{-5}}{1.85} \\ & \left[ L + \frac{L^2 \times 0.85}{2 \times 13.6 \times 76} \right] \end{aligned}$$

This simplifies to obtain a quadratic equation gives

$$L^2 + 2430 L - 2.98 \times 10^6 = 0 \quad (37)$$

Solving the above quadratic equation gives

$$L = 895 \text{ cm.}$$

Step (4):

Check the pressure at the bottom of the column

$$\text{Pressure at the bottom of the column} = 1 + \frac{895 \times 0.85}{13.6 \times 76}$$

$$= 1 + 0.740 = 1.740$$

$$\text{Average pressure} = \frac{1 + 1.740}{2} = 1.37 \text{ atm.}$$

Hence the assumption of average pressure as 1.4 atm is nearly correct.

The absorption of butadiene in molten maleic anhydride may be carried out in a semicontinuous reactor, i.e., a given charge of maleic anhydride is taken into the jacketted bubble column to be heated by steam. The gaseous stream containing butadiene is bubbled through the molten mass at the desired flow rate.

Gehlawat<sup>4</sup> has reported reaction rate constant,  $k_2 = 10 \text{ cm}^3/\text{gmol}/\text{sec}$  at  $105^\circ\text{C}$ . The limiting concentration of maleic anhydride for the rate expression (4) to be applicable may be calculated from the inequality expression (31).

$$k_2 [B] > k_{La}$$

$$[B] = 4.60 \text{ gmol/l.}$$

Thus it is interesting to note that for this system the rate controlling step changes from physical rate of



absorption to the true chemical reaction after the reactant concentration has been reduced from an initial value of 10 gmol/l to 4.6 gmol/l.

### CALCULATION OF TIME OF REACTION

#### Physical Absorption Period

A material balance on butadiene is desired.

Rate of absorption of butadiene =  $G_i \times (\text{decrease in butadiene molar content})$

$$= 1.85 (0.54 - 0.01)$$

$$= 0.98 \text{ gmol/sec}$$

Volume of reactant = Column area  $\times$  dispersion height

$$= \frac{6362 \times 895}{1000} = 5693 \text{ l}$$

$$\text{Initial [B]} = 10 \text{ gmol/l}$$

$$\text{Final [B]} = 4.60 \text{ gmol/l}$$

From stoichiometric consideration a material balance on maleic anhydride gives the amount of butadiene to be absorbed.

$$= 5693 (10 - 4.60)$$

$$\text{Hence the time for physical absorption} = \frac{5693 \times 5.4}{0.98 \times 3600}$$

$$t_1 = 8.8 \text{ hrs.}$$

Chemical Reaction Period:

Initial value of  $[B] = 4.60 \text{ gmol/l.}$

Final value of  $[B] = 0.1 \text{ gmol/l}$

(which gives a product purity of 99 per cent).

The operating chemical rate equation is

$R = \frac{d[B]}{dt} = k_2 [A] [B]$ , wherefrom the time of chemical reaction

$$t_2 = \frac{1}{k_2 [A]} \int_{[B_i]}^{[B_o]} \frac{d[B]}{[B]} \quad (38)$$

Substituting the various values in equation (38) and integrating we get

$$t_2 = 6.4 \text{ hrs}$$

$$\begin{aligned} \text{Total time of reaction} &= t_1 + t_2 \\ &= 8.8 + 6.4 = \underline{15.2 \text{ hrs}} \end{aligned}$$

The above estimate of overall time of reaction is a conservative estimate, since it has been implied that the effective solubility of butadiene in molten mass during the chemical reaction period remains constant. However, this is not the true picture. The actual reaction time would be lower than the value estimated above. The error may be of the order of 15 per cent. In practice, a set of two bubble column reactors may be used in series.

During the physical absorption rate period the partial pressure of the exit stream from the first reactor will remain constant at 1 per cent as calculated above. However, this situation would change when the chemical reaction would control after the concentration of maleic anhydride is reduced to lower than 4.6 gmol/l. Then the partial pressure of butadiene in the exit stream from the first reactor would increase gradually. This will, however, mean that the second reactor would receive a richer butadiene stream and the overall rate of absorption in the second reactor would be higher.